ATTENUATION OF RAPID ONSET VASODILATION WITH ADVANCED AGE: ROLES OF ADRENERGIC AND ENDOTHELIAL SIGNALING

A Dissertation

presented to

the Faculty of the Graduate School

at the University of Missouri-Columbia

In Partial Fulfillment

of the Requirements for the Degree

Doctor of Philosophy

---

by

SHENGHUA YUAN SINKLER

Dr. Steven S. Segal, Dissertation Supervisor

MAY 2016

The undersigned, appointed by the dean of the Graduate School, have examined the dissertation entitled

ATTENUATION OF RAPID ONSET VASODILATION WITH ADVANCED AGE: ROLES OF ADRENERGIC AND ENDOTHELIAL SIGNALING

presented by Shenghua Sinkler,

a candidate for the degree of doctor of philosophy,

and hereby certify that, in their opinion, it is worthy of acceptance.

Professor Steven S. Segal

Professor Cheryl M. Heesch

Professor Paul Fadel

Professor Michael Hill

Professor Virginia Huxley

ACKNOWLEDGEMENTS

I would like to acknowledge and thank my dissertation supervisor, Prof. Steven S. Segal, who dedicates a substantial amount of time into my research project and development of my academic skills in writing and presentation, and is always there with great patience to provide his support and walk me through the process of learning. I would like to thank Dr Erika Boerman for teaching me immunostaining and analyzing the perivascular innervations, and for her insightful comments and encouragement for my publications and grant application. I also would like to thank other members of the Segal lab for making the lab a friendly and fun place to work.

TABLE OF CONTENTS

LIST OF FIGURES

Figure Page

LIST OF TABLES

Table Page

LIST OF ABBREVIATIONS

1A ..... 1st Order Arteriole

2A ..... 2nd Order Arteriole

3A ..... 3rd Order Arteriole

ACh ..... Acetylcholine

ARs ..... Adrenergic Receptors

AVD ..... Ascending Vasodilation

DAG ..... Diglyceride

EC ..... Endothelial Cell

EDD ..... Endothelium Dependent Dilation

EDH ..... Endothelium-Derived Hyperpolarization

FA ..... Feed Artery

FITC ..... Fluorescein Isothiocyanate

FMD ..... Flow Mediated Dilation

GM ..... Gluteus Maximus

ID ..... Internal Diameter

IEL ..... Internal Elastic Lamina

IP_3 ..... Inositol Trisphosphate

$K_{Ca}2.3$ ..... Small conductance calcium-activated potassium channels

$K_{Ca}3.1$ ..... Intermediate Conductance Calcium-Activated Potassium Channels

LDT.....Light Dye Treatment

L-NAME..... L-NG-Nitroarginine Methyl Ester

MEJ..... Myoendothelial Junctions

NA.....Noradrenaline

NE ..... Norepinephrine

NO..... Nitric Oxide

NOS..... Nitric Oxide Synthesis

PBS .....Phosphate Buffered Saline

PE..... Phenylephrine

PG .....Prostaglandins

PSS .....Physiologic Salt Solution

PZ.....Prazosin

ROV ..... Rapid Onset Vasodilation

RW .....Rauwolscine

SMC .....Smooth Muscle Cell

SNA.....Sympathetic Nerve Activity

SNP ..... Sodium Nitroprusside

SSV .....Steady-State Vasodilation

TH .....Tyrosine Hydroxylase

UK.....UK14304

ATTENUATION OF RAPID ONSET VASODILATION WITH ADVANCED AGE: ROLES OF ADRENERGIC AND ENDOTHELIAL SIGNALING

Shenghua Yuan Sinkler

Dr. Steven S. Segal, Dissertation Supervisor

ABSTRACT

Rapid onset vasodilation (ROV) initiates hyperemia via relaxation of smooth muscle cells (SMCs) of proximal feed arteries (FAs) and downstream arterioles. SMCs integrate inputs from perivascular sympathetic nerves via α-adrenoceptors (αARs) and from intimal endothelium. Enhanced sympathetic nerve activity and endothelium dysfunction may underlie the deficits muscle blood flow with advanced age. This dissertation explores the roles of adrenergic and endothelial signaling during vasomotor control to understand how aging affects ROV in the resistance vasculature of skeletal muscle network. Using intravital microscopy of the mouse gluteus maximus muscle, contractions were evoked by motor nerve stimulation. In FA and arteriolar networks, αAR subtypes mediating vasoconstriction and endothelium dependent dilation were resolved using selective α_1ARs vs. α_2ARs pharmacological interventions and acetylcholine. Aging altered the functional distribution of αAR subtypes within resistance networks, with α_2ARs most effective in attenuating ROV of FA. An essential role for the endothelium in the conduction of ROV from arterioles in to FA was resolved using light-dye treatment with pharmacological manipulations of autacoid production and ion channel activation. This research provides definitive new insight into signaling pathways underlying the regulation of skeletal muscle blood flow. These findings can be translated into more effective strategies to restore muscle blood flow with aging and improve quality of life.

CHAPTER 1

INTRODUCTION

FUNCTIONAL HYPEREMIA

Skeletal muscle is a unique organ as the blood flow through it can change over a broad range. During physical activities, muscle blood flow can increase 50- to 100-fold (21) in active muscles and is closely matched with metabolic demand (24, 80, 138). Functional hyperemia during exercise is distinct from reactive hyperemia, which is a quick response to restore blood flow following a transient occlusion. Reactive hyperemia involves multiple mechanisms (95) including accumulation of vasodilator metabolites (2, 101), low PO_2 (158), myogenic relaxation during the reduced transmural pressure (4, 59) as well as passive mechanisms due to distention when blood flow is restored from upstream vessels (95). In contrast, functional or exercise hyperemia describes the increase in muscle blood flow in response to contractile activity of skeletal muscle. The earliest study recorded the increase of blood flow responses to muscle contraction was done by Gaskell in 1877 (57), through measuring the effluent blood flow from the vein of dog hindlimb during electrically stimulated contractions.

Vasodilation in contracting muscle is the principal phenomenon driving local blood flow increase to muscular exercise. Traditionally, this has been explained by the production of vasodilator metabolites such as adenosine, ATP, K^+ and CO_2 (13, 60, 80, 149). More recently, an electrical basis has been proposed. Evidence for such regulation was obtained from dog hindlimb muscle, where K^+ infusion blocked the iliac blood flow increase in

response to 1s contraction, by eliminating hyperpolarization of smooth muscle cells (SMCs) as a mechanism of vasodilation (64).

VASODILATION IN RESISTANCE NETWORKS DURING FUNCTIONAL HYPEREMIA

The regulation of local blood flow through vasomotor control of resistance vessels is substantial because small adjustments in their diameters produce robust changes in muscle blood flow according to Poiseuille's law, whereby flow increases with the 4^{th} power of radius. For example, a doubling of vascular diameter predicts a 16-fold increase in blood flow through the vessel at constant perfusion pressure.

Under resting conditions, all branches of resistance vessel networks in skeletal muscle are constricted relative to their maximum diameters. Such intrinsic or spontaneous tone is the integrated effects of multiple stimuli including myogenic, sympathetic, endothelial and local metabolic factors. During exercise, rapid onset vasodilation (ROV) can be evoked in response to a single muscle contraction (1, 29, 30, 102, 105, 161) across all vascular branch orders and initiates rapid hyperemia (28), followed by a steady-state vasodilation (SSV) that sustains the elevation in blood flow (23) during functional hyperemia.

All vascular branch orders in a resistance network are involved (138) in local blood flow regulation; the dilation of proximal feed arteries (FA) and its downstream primary (1A) arterioles contribute to the increased magnitude of total blood flowing into an active muscle, while the distal daughter branches, referred to herein as the second-order (2A) and

third- order (3A) arterioles, dilate in accord with the regional distribution of blood flow. Coordinating vasodilation (87, 138, 141) among branch orders is the key feature of resistance networks in local blood flow regulation. Therefore, effective regulation of reactivity at individual vascular branch orders and the coordination of vasomotor responses among distal and proximal vessels (87, 138, 141) appear integral to functional hyperemia and its local distribution according to the nature of exercise.

VASCULAR REACTIVITY

In respective vascular branch orders, reactivity is manifested through activation or relaxation of vascular SMCs in response to a variety of stimuli. Thus, SMCs receive input from the perivascular sympathetic nerves, which release norepinephrine (NE) to activate α-adrenergic receptors (ARs) (49) and promote vasoconstriction. Concomitant input from the intimal endothelial cells (ECs) promotes vasodilation through release of autacoids [nitric oxide (NO), prostaglandins] and endothelium-derived hyperpolarization (EDH) (56). EDH is initiated by the activation of small (K_{Ca} 2.3)- and intermediate (K_{Ca} 3.1)-conductance Ca^{2+}-activated K^+ channels (17, 26, 51, 72). effected by myoendothelial (SMC: EC) coupling through gap junctions (47). During blood flow regulation in resistance networks, changes in vessel diameter reflect the interaction between signaling events generated in SMCs, endothelial cells and perivascular nerves along with the products of metabolic activity in the surrounding tissue as discussed earlier for functional hyperemia. In addition to the response of microvessels to changes in oxygen availability (45, 77), α-adrenergic vasoconstriction and endothelium dependent vasodilation establish baseline

levels of vasomotor control in respective branch orders. Regional variability in the functional distribution of α_1ARs and α_2ARs has been demonstrated across arteriolar branch orders in rat and mouse cremaster muscles (106, 114) as well as the mouse gluteus maximus muscles (GM) (106). Branch order effects are also manifest in endothelium dependent vasodilation, where autacoid production (e.g., NO and prostaglandins) predominates in some vessel branches (typically larger conduit arteries) while electrical signaling (EDH) predominates in other vessel branches (typically smaller resistance arteries and arterioles) (130, 143). The endothelium may also play a greater role in the dilation of large arterioles than of smaller arterioles (86, 116, 150).

RAPID ONSET VASODILATION

ROV increases blood flow immediately (<1s) (109, 144, 157) at the onset of exercise or transition to more intense activity (133). The magnitude of ROV is proportional to muscle fibers recruitment, muscle contraction intensity and durations (55, 156, 161). Multiple signaling pathways involved in vasomotor control and functional hyperemia have been proposed to mediate ROV (24, 33, 129). These include neurogenic (81, 164), metabolic (13, 60, 67, 125, 127, 149), mechanical (25, 55, 142) and myogenic (4, 104) responses. However, respective vasodilations took 5 seconds or longer to occur, while ROV is initiated much more rapidly (< 1s). The exact stimulus for ROV remains unknown (24, 33, 129). A primary goal of this dissertation research is to push forward our understanding in the initiating and regulatory mechanism(s) of ROV.

ROV occurs in both FA and arterioles (1, 29, 30, 102, 105, 161) across the entire resistance network. In contrast to the arterioles embedded within the muscle fibers, proximal FA are external to muscle fibers and do not receive direct effects from active muscles. Thus, vasodilation in FA following muscle contraction reflects ascending vasodilation (AVD) (141) that originates in downstream arterioles. However, the mechanism of AVD has not been resolved with respect to the time course of its response kinetics nor whether the signaling pathway of AVD may vary with the nature of physical activity. My dissertation explores this relationship using well-defined contraction protocols designed to elicit either ROV in response to brief intense contraction (as in power lifting) or SSV in response to sustained rhythmic contractions (as in walking or cycling).

AGING ATTENUATES MUSCLE BLOOD FLOW AND ROV

Advanced age is a major risk factor for cardiovascular disease (89, 110, 112, 136). Regular physical activity (i.e., muscular exercise) prevents or delays functional aging (15) by promoting a favorable cardiovascular state through preserving endothelial functions (35), and amelioration of impaired blood flow in vascular related disease such as hypertension and diabetes (132). Nevertheless, aging impairs muscle blood flow (20) thus diminishes exercise capacity. ROV initiates the blood flow increase to active muscle fibers and facilitates the transition from rest to physical activity. Remarkably, ROV is blunted in human subjects (22, 38) and in mice (75) during advanced age. Functionally, ROV reflects the near-instantaneous relaxation of SMCs of the resistance vasculature in response to skeletal muscle contraction (28, 102, 157, 161). With aging, enhanced sympathetic nerve

activity (SNA) (22, 38) and endothelium dysfunction (43, 50, 68, 136) may be complementary mechanism(s) underlying the deficit muscle blood flow in advanced age. Thus, insight into the potential roles of α-adrenergic modulation and endothelial signaling in ROV at each branch order of the resistance network, and the respective changes with aging may provide a key towards understanding how aging attenuates ROV and limits muscle blood flow.

FUNCTIONAL SYMPATHOLYSIS AND SYMPATHETIC NERVE ACTIVITY

Sympathetic vasoconstriction restricts muscle blood flow away from inactive skeletal muscles and diverts blood flow from other organs, e.g., renal and splanchnic vascular beds to supply active skeletal muscle. In contracting muscle, the ability of sympathetic nerves to induce vasoconstriction is blunted during muscular activity and this phenomenon has become recognized as "**functional sympatholysis**" (121). Such blunting of sympathetic vasoconstriction in exercising muscles serves to optimize the matching of blood flow with the metabolic needs in active muscle fibers (121, 151). In the resistance vascular network, sympatholysis occurs more readily in distal arterioles when compared with proximal resistance vessels (54, 159), where sympathetic vasoconstriction is preserved to maintain peripheral resistance and arterial blood pressure. Nevertheless, insufficient functional sympatholysis would result in the restriction of blood flow and oxygen delivery to skeletal muscle during exercise (128).

Functional sympatholysis is impaired in humans with advanced age (>60 years) (39) along with the ability to rapidly increase muscle blood flow in response to muscle contraction when compared to younger (~20-30 years) subjects (20, 22). As shown with microneurography in human subjects, SNA increases with exercise intensity and active muscle mass (134, 135). The autonomic nervous system remains active under resting conditions and the background level of SNA increases with advanced age (38, 52). Enhanced SNA during advanced age is also manifest in rodents. For example, release of NE from sympathetic nerves into the circulation was greater at rest and during immobilization stress in aged (24 months) compared to young adult (3 months) male Fischer-344 rats (100). Further, the tyrosine hydroxylase activity, which governs NE synthesis, was ~2-fold higher in adrenal glands of Old (24 months) compared to Young (4 months) male rats and mice (120). How increased SNA with aging affects vascular reactivity in αadrenergic vasoconstriction at respective branch orders remains underappreciated, thus little is known of how or where respective adrenergic signaling pathways are affected by advanced age. Another key goal of this research project is to provide such insight in resistance networks controlling blood flow to skeletal muscle.

ADRENERGIC VASOCONSTRICTION AND AGING

Sympathetic vasoconstriction is mediated through the activation of post-synaptic αARs on vascular SMCs, of which there are 2 major subtypes: α_1 and α_2 (49). Both subtypes are G-protein coupled receptors; however, upon activation, the intracellular signaling pathways leading to vasoconstriction are distinct. The α_1AR pathway is predominantly coupled G_q

protein to activate phospholipase C and result in formation of inositol triphosphate (IP_3) and diacylglycerol (DAG). DAG further stimulates protein kinase C and IP_3 acts on the IP_3 receptor in endoplasmic reticulum to release stored calcium and increase the Ca^{2+} influx to cause SMCs contraction. In contrast, the α_2-AR pathway is negatively couple to G_i protein to inhibit adenylyl cyclase thus decreases the production of cAMP. However, its role in mediating vasoconstriction is not clear and may involve multiple cellular pathways (40). For example, activation of α_2AR can increase IP_3 formation and activate protein kinase C (58, 167) and couple to G_i protein signaling to increase influx of extracellular Ca^{2+} through voltage-operated Ca^{2+} channels (115).

As the functional distributions of α_1ARs and α_2ARs exhibit regional differences along arteriolar networks in rat and mouse cremaster muscles (106, 114) and the mouse GM (106), it is important to understand where these respective signaling pathways are most effective in controlling vascular resistance and tissue blood flow.

Attenuated muscle blood flow with diminished vascular conductance can reflect elevated muscle SNA and the activation of αARs (22, 38). With aging, the sensitivity of neuroeffector signaling pathways may be altered. For example, the attenuated reductions in forearm blood flow in older vs. younger men during tyramine infusion (to evoke release of endogenous norepinephrine) were attributed to reduced responsiveness of α_1ARs (37), while reductions in leg blood flow during tyramine infusion were also attenuated in older (~62 years) vs. younger (~24 years) men and attributed to the attenuation of both α_1AR- and α_2AR-mediated responses with aging (147). Consistent with this interpretation are the effects of αAR inhibition and activation on ROV. Thus, blocking αARs with phentolamine

restored ROV to forearm muscle contractions in old adults (~69 years), whereas increasing SNA (via lower body negative pressure) impaired ROV in younger subjects (~27 years) (22). Remarkably, similar effects of enhanced αAR activation during advanced age on ROV are also manifest in the mouse. Thus, attenuated ROV of distributing arterioles (2A) in the GM of old (20 months) was restored to that of young (3-4 months) male mice by topical phentolamine, while attenuation of ROV could be induced in young mice by topical application of NE at a concentration (1 nM) that is well below what is needed for vasoconstriction (75). In light of the nonuniform distribution of αAR subtypes along arteriolar networks of the mouse GM (106), the role of adrenergic modulation (α_1AR vs α_2AR) in ROV of defined branch orders within resistance network remains to be resolved, particularly from the perspective of aging. Providing this insight is integral to my research as developed in this dissertation.

ENDOTHELIUM DEPENDENT DILATION AND AGING

Impaired endothelium dependent dilation (EDD) has been well-characterized in large arteries of older human subjects (43, 46, 68, 89, 136). In the microcirculation, early studies of the rat cremaster muscle found impaired dilation of 1A and 2A order arterioles to adenosine (27), while constriction to norepinephrine was maintained. However, the cremaster muscle is not a true skeletal muscle because it neither attaches to the skeleton nor is it involved in locomotion. Consistent with reduced blood flow to skeletal muscle with aging in humans (38, 44, 119), the blood flow response to contraction of the plantar flexor (i.e., calf) muscles was impaired in senescent rats (73). Contributing to the restriction

of skeletal muscle blood flow, 1A isolated from rat soleus and gastrocnemius muscles demonstrated impairment in EDD with aging (7, 108) as did FA isolated from the soleus muscle (155, 165). However, little is known of how aging affects EDD in respective branches of resistance networks during their actual control of tissue blood flow in vivo. Again, providing this insight is a key component of my dissertation research.

ASCENDING VASODILATION

In FA, ROV reflects AVD from downstream arterioles. A conceivable cellar pathway of this response entails conduction of a vasodilator signal (e.g., hyperpolarization) along the endothelium (48, 97, 141). This is enabled by gap junctions between neighboring ECs as well as their surrounding SMCs, which readily conduct electrical signals. In such manner, once EDH (56) is initiated, hyperpolarization can travel from cell to cell with high speed (cm/s) over considerable distances (42). As dilation occurs along arterioles, the fall in downstream resistance will increase flow through proximal FA and thereby induce flow mediated dilation (FMD) (117, 146) by releasing of NO and/or prostaglandins from endothelium (84, 101, 117). However, FMD is slower in onset (~8-16s) (83, 87, 146) suggests that the FMD is less likely to initiates rapid hyperemia, but may contribute to sustain the steady-state vasodilation (SSV) that sustains the elevated muscle blood flow during dynamic exercise.

In arterioles located downstream and embedded within the muscle fibers, abundant and redundant vasodilator signals can induce dilation (24). Such changes that occur with

muscle contractions include a fall in pO_2 and pH, a rise in osmolality and CO_2 and the release of vasodilators including adenosine, ATP, K^+ and NO have been proposed as mediators of exercise hyperemia (13, 60, 80, 149). Many of these "classic" vasodilators can also interact with endothelium to evoke EDD by stimulating the release of autacoids (e.g., NO and prostaglandins) or electrical signaling via EDH, best represented by activation of potassium channels, particularly K_{Ca} 2.3 and K_{Ca} 3.1 (17, 26, 51, 72). In such manner, the use of ACh to evoke EDD in resistance vessels provides an established "tool" for evaluating the initiation and conduction of EDH (48, 56) as well as AVD (138). In human subjects, the inhibition of autacoids attenuated SSV only slightly during rhythmic knee extensions (16) but had more pronounced effects in attenuating ROV to single contractions of the forearm (29), suggesting that the nature of contraction my affect underlying signaling events that produce vasodilation. Recent evidence from humans implicates a role for K^+ (29) in rapid ROV, consistent with an underlying electrical signal. Genetic deletion of K_{Ca} 2.3 impaired arteriolar ROV in mouse cremaster muscles (103), implicating a role for ion channels known to cause EC hyperpolarization. Although the exact stimulus of ROV remains unclear, the endothelium has emerged as an important site for vasomotor control in response to muscle contractions (80, 138).

GAPS EXIST IN CURRENT UNDERSTANDINGS

The role of branch order on vascular reactivity and ROV with aging in microvascular resistance networks of skeletal muscle has received little attention in the literature. However, all vascular branch orders dilate to increase local muscle blood flow in response

to increased oxygen demand during muscle contractions and respective branches can differ in signaling pathways that govern their function. The volume of blood flow entering a muscle is governed by proximal vessels upstream, while the distribution of blood flow within a muscle is regulated by the smaller daughter arteriolar branches downstream (138). Due to the inability perform invasive procedures in humans for the purpose of direct observation of the microcirculation, little is known of what happens with aging in vascular reactivity *in vivo*, particularly in smaller 2A and 3A branches. Indeed, such studies have focused on larger arterioles following isolation for in vitro studies (34, 108). When studying blood flow responses to contractile activity in skeletal muscle of human subjects, dynamics of the actual site(s) in resistance vessels cannot be resolved. While the cremaster muscle has been a favored model for intravital microscopy of "skeletal muscle", it neither attaches to the skeleton nor is it involved in locomotion. To address these limitations, we have developed the mouse GM preparation for intravital imaging of the microcirculation. The GM is a powerful hip extensor of mixed fiber type (90, 98) which is typical of human skeletal muscle (93, 127). Earlier studies using mouse GM resolved the attenuated ROV of 2A with aging (75), but did not address other branches of the network. As blood flow regulation requires coordinated activity among upstream and downstream branches, a more comprehensive understanding of respective branch orders is required.

GENERAL METHODS

All experiments are performed using intravital microscopy of the mouse GM (6, 75, 106). Detailed methods including application of reagents and control experiments are described in chapters 2, 3 and 4. The surgical techniques of isolating and stimulating the GM for viable intravital microscopy took several month's practice to acquire, along with the skills required to control superfusion rate, temperature and uniformity over the tissue. Key criteria include being able to maintain and recover the resting diameters and vascular tone within GM networks throughout the 5-6 hours period of experimentation. Before collecting the criterion data presented chapters 2-4 and used for my publications, it was essential to demonstrate consistent results with repeated control experiments. For example, reproducible concentration-response curves to ACh and phenylephrine were obtained with each protocol repeated for 4 times on a given GM preparation with washout and recovery of resting diameters following each protocol. For ROV controls, I ensured that vasomotor responses to single tetanic muscle contractions remained stable throughout 4 series of motor nerve stimulation protocols (4 contraction durations x 4 vessel branches, a total of 64 tetanic contractions with recovery in between each contraction). These controls verified my ability to obtain control responses and to study the effect of 1 or 2 experimental interventions in a given preparation and are included as a supplemental figure in Chapter 3. In addition, to obviate the possibility of order effects, the sequence of treatments and of observation sites (branch orders) was randomized between experiments. The rationale for selected pharmacological treatments and chosen concentrations are described in the methods section of respective chapters in which they are used.

PURPOSE OF DISSERTATION RESEARCH

This dissertation research centers on exploring the role of adrenergic and endothelial signaling in ROV, to gain insight into how aging affects ROV in skeletal muscle network. To provide a foundation for these studies, Chapter 2 centers on determining how aging affect vascular reactivity. I evaluated diameter changes of respective branch orders in the GM during changes in PO_2, selective activation of AR subtypes and during EDD, and determined how aging influences the microcirculation of skeletal muscle *in vivo*. Chapter 3 centers on determining the role of adrenergic modulation on ROV. I characterized ROV in all branch orders in the intact microvascular resistance in vivo in young and old mice along with the effects of selective activation or inhibition of α_1ARs and α_2ARs. The goal of Chapter 4 was to resolve the role(s) of endothelial signaling pathways of ROV in light of potential differences from SSV according to the nature of skeletal muscle contraction (i.e., brief and intense as in power lifting vs. sustained rhythmic activity as in walking or cycling). The role of endothelium in AVD and ROV of FA was tested using light-dye treatment to selectively disrupt intercellular conduction along the vessel wall, while ROV and SSV at all branch orders are evaluated using selective pharmacological interventions focused on endothelial cell signaling pathways. Chapter 5 provides a brief general discussion and a summary of major conclusions from my research findings along with my perspective for future studies.

PEER REVIEWED PUBLICATIONS

This dissertation research encompasses three peer reviewed publication (chapters 2-4). Below listed the title, authorship, journals, and key contents.

1. **Aging alters reactivity of microvascular resistance networks in mouse gluteus maximus muscle**.

   Authors: Shenghua Y. Sinkler and Steven S. Segal.

   Journal: American Journal of Physiology, Heart and Circulatory Physiology (vol. 307: pp. H830-839, 2014).

   This paper (Chapter 2) compared microvascular reactivity in EDD and α_1- vs. α_2-adrenoreceptors mediated vasoconstriction along resistance networks in the GM of old (24 months) and Young (4-6 months) male C57BL/6 mice.

2. **Differential adrenergic modulation of rapid onset vasodilatation along resistance networks of skeletal muscle in old versus young mice**.

   Authors: Shenghua Y. Sinkler and Steven S. Segal.

   Journal: Journal of Physiology (submitted and reviewed, in preparation for resubmission).

   This paper (Chapter 3) encompassed novel analysis of ROV kinetics (magnitude and kinetics) among respective branches of the resistance network with an emphasis on resolving the differential effects of α-adrenergic modulation (i.e., activation vs. inhibition, α_1 vs. α_2) of ROV in the GM of old compared to young mice.

3. **Role of endothelium in conduction and initiation of rapid onset vasodilation in mouse skeletal muscle**.

   Authors: Shenghua Y. Sinkler and Steven S. Segal.

   Journal: Journal of Physiology (in preparation for submission).

   This paper (Chapter 4) investigated the role of endothelium with respect to the initiation and conduction of ROV in light of SSV according to the nature of GM contraction.

CHAPTER 2

AGING ALTERS REACTIVITY OF MICROVASCULAR RESISTANCE NETWORKS IN MOUSE GLUTEUS MAXIMUS MUSCLE

ABSTRACT

Aging occurs with enhanced sympathetic nerve activity and endothelium dysfunction however little is known of how successive branches of microvascular resistance networks are affected *in vivo*. We questioned whether vascular reactivity is altered differentially along resistance networks with advanced age. The left gluteus maximus muscle of anesthetized Young (4 mo) and Old (24 mo) male C57BL/6 mice was exposed for intravital microscopy and superfused with physiological salt solution (3 ml/min; pH 7.4, 34°C). Spontaneous vasomotor tone increased progressively from proximal feed arteries (FA) and first-order (1A) arterioles through distal second- (2A) and third- (3A) order arterioles and was ~15% greater in 2A and 3A of Old vs. Young. Vasoconstriction during elevated superfusion PO_2 increased with branch order and to a greater extent in Young. Peak constrictions to phenylephrine (α_1AR agonist) were similar for FA and 1A of both ages and ~20% greater for 2A and 3A of Young. Across arterioles (but not FA), constrictions to UK 14304 (α_2AR agonist) were depressed ~30% in Old vs. Young. Thus advanced age attenuated vasoconstriction to O_2 throughout networks while blunting vasoconstriction to α_1AR and α_2AR activation in arterioles. With acetylcholine, endothelium-dependent dilation (EDD) was ~20% greater in FA of Young yet was ~two-fold greater for 2A and 3A of Old. Sodium nitroprusside evoked maximal dilations similar to acetylcholine. Thus

while EDD was attenuated with advanced age in FA, EDD was robust in distal arterioles having enhanced vasomotor tone. We conclude that advanced age differentially alters reactivity among branches of microvascular resistance networks.

INTRODUCTION

Advanced age is a major risk factor for cardiovascular disease (89, 110, 112, 136). While impaired endothelium-dependent dilation (EDD) has been well-characterized in large arteries of older human subjects (43, 46, 68, 89, 136), how aging affects reactivity in the microvessels that govern skeletal muscle perfusion is less well-defined. Early studies in the cremaster muscle of male rats found impaired dilation of first- (1A)- and second- (2A) order arterioles to adenosine (27), while constriction to norepinephrine was maintained. However, the cremaster muscle is not a true skeletal muscle because it neither attaches to the skeleton nor is it involved in locomotion. Consistent with reduced blood flow to skeletal muscle with aging in humans (38, 44, 119), the blood flow response to contraction of the plantar flexor muscles was impaired in senescent rats (73). Contributing to the restriction of skeletal muscle blood flow, 1A isolated from rat soleus and gastrocnemius muscles demonstrated impairment in EDD with aging (7, 108) as did feed arteries (FA) isolated from the soleus muscle (155, 165). In the gluteus maximus muscle (GM) of mice, which also has FA that give rise to branching arteriolar networks, impaired dilation and perfusion of 2A in response to muscle contraction was attributed to constitutively enhanced activation of α-adrenoreceptors (αARs) (75). These findings in rodents are consistent with restricted muscle blood flow and enhanced sympathetic nerve activity (SNA) in older

humans (22, 38). Whereas studies in humans have shown impaired α-adrenergic vasoconstriction in the forearm (37) and leg (44, 147), the actual site(s) of such responses within the vascular supply remain obscure.

In response to increased oxygen demand, the volume of blood flow entering a muscle is governed by FAs and proximal (1A) arterioles upstream, while the distribution of blood flow within a muscle is regulated by the smaller daughter 2A and third-order (3A) arteriolar branches downstream (138). A key feature of resistance networks is their ability to coordinate vasomotor responses among vessel branches. For example, ascending vasodilation of FAs arises from signals originating from arterioles embedded within the muscle fibers (141). The wall of arterioles and their proximal FA is comprised primarily of a single layer of smooth muscle cells (SMCs) surrounding the endothelial cell monolayer in contact with the blood. In turn, all branches of the resistance network are surrounded by sympathetic nerve fibers coursing through the adventitia. During blood flow regulation, changes in vessel diameter reflect the interaction between signaling events generated in SMCs, endothelial cells and perivascular nerves. Sympathetic vasoconstriction is mediated through the activation of αARs on vascular SMCs, of which there are 2 major subtypes: α_1 and α_2 (49). Regional variability in the functional distribution of α_1ARs and α_2ARs has been demonstrated along arteriolar networks in rat and mouse cremaster muscles (106, 114) and the mouse GM (106). Remarkably, little is known of how or where respective adrenergic signaling pathways are affected by advanced age. Whereas the effect of aging on EDD has been evaluated in FAs and 1As extensively *in vitro* (7, 108, 165, 166), little is known of what happens *in vivo*, particularly in smaller 2A and 3A branches.

The response of microvessels to changes in oxygen availability can be evaluated by altering PO_2 in the superfusion solution bathing the tissue. The role of α_1ARs and α_2ARs in mediating vasoconstriction and of the endothelium in mediating vasodilation can be evaluated using selective agonists. Thus, α_1AR-mediated responses are evoked by phenylephrine (PE) while α_2AR-mediated responses are evoked by UK 14304 (65, 106). In turn, agonist-mediated EDD is most readily studied with acetylcholine (ACh) via activation of muscarinic receptors on endothelial cells (7, 46, 108, 165). The mouse GM preparation enables direct visualization of respective microvessel branch orders (e.g. FA, 1A, 2A, and 3A) using intravital microscopy (6, 75, 106). Therefore, evaluating diameter changes of respective branch orders in the GM during changes in PO_2, selective activation of AR subtypes and during EDD provides an experimental approach for determining how aging influences the microcirculation of skeletal muscle *in vivo*. In the present study, we tested the hypothesis that advanced age differentially alters reactivity throughout microvascular resistance networks of skeletal muscle using the mouse GM as an experimental model.

METHODS

Animal care and use. All procedures were approved by the Institutional Animal Care-Use Committee of the University of Missouri (Columbia, MO, USA) and were performed in accordance with the *National Research Council's Guide for the Care and Use of Laboratory Animals (2011)*. Male C57BL/6 mice; Young (4-mo, n=5) and Old (24-mo n=5) were obtained from National Institute on Aging colonies (Charles River Laboratories;

Wilmington, MA, USA). These age groups correspond to In humans in their mid-20's and late 60's, respectively (53). Mice were housed in animal care facilities of the University of Missouri maintained at ~24 ^{o}C on a 12h-12h light-dark cycle with food and water available *ad libitum* for at least a week before being studied. On the morning of an experiment, a mouse was anaesthetized by intraperitoneal injection of pentobarbital sodium (60 mg/kg) with supplemental doses (20mg/kg) as needed to maintain a stable plane of anesthesia as confirmed by lack of withdrawal to toe pinch. Throughout surgical preparation and the experimental protocol (Figure 2.1), esophageal temperature was maintained at ~37 ^{o}C by placing the mouse on an aluminum warming plate (5 cm X 11 cm). Upon completion of the experimental protocol (duration, 5-6 h), the mouse was killed by an overdose of pentobarbital sodium (intraperitoneal injection) followed by cervical dislocation.

Intravital microscopy. The GM was prepared as described (6, 75, 106). Briefly, after carefully shaving the surgical area, the mouse was placed in the prone position on the warming plate. While viewing through a stereomicroscope, the overlying skin was removed and the GM was superfused continuously (3 ml/min) thereafter with bicarbonate-buffered physiological salt solution (PSS; 34 °C, pH 7.4) containing (in mM): 131.9 NaCl, 4.7 KCl, 2 $CaCl_2$, 1.17 $MgSO_4$ and 18 $NaHCO_3$ equilibrated with 5% CO_2/95% N_2. Chemicals and reagents were purchased from Sigma-Aldrich (St. Louis, MO, USA). To expose the resistance vasculature, the GM was carefully dissected from the lumbar fascia and iliac crest, spread over a transparent pedestal (Sylgard® 184; Dow Corning, Midland, MI, USA) and the edges were pinned to approximate *in situ* muscle dimensions. The completed preparation was transferred the fixed stage of an intravital microscope (Nikon E600FN; Melville, NY, USA) mounted on an X-Y translational stage (Gibraltar; Burleigh

Instruments, Fishers, NY USA). The image was acquired through a Nikon SLWD 20X (numerical aperture=0.35) objective onto a color camera (KP-D50U CCD; Hitachi-Denshi, Japan) and observed at a final magnification of 1200X on a video monitor; spatial resolution was < 1 μm. The internal diameter (ID) of vessels was measured as the widest distance between luminal edges using a video caliper (Microcirculation Research Institute; Texas A&M University; College Station, TX, USA) calibrated against a stage micrometer (0.01×100=1 mm; Graticules Ltd, Tonbridge Kent, England). The output of the caliper was sampled at 40Hz Hz using a Powerlab/400 system (ADInstruments; Colorado Springs, CO, USA) coupled to a personal computer.

Branch order. The branch order of arterioles and FA were defined as follows. FA: the inferior gluteal artery before it enters the muscle; 1A: continuation of the same vessel embedded within the muscle; 2A: a branch originating from 1A; 3A: a branch originating from 2A. Branch angles were typically ~120°). One vessel from each branch order was studied in each GM; IDs were measured at the same locations (midway along respective branches) throughout experiments. The order in which respective branch orders were observed was varied across experiments as was the age group studied. Three-dimensional mapping with quantitative analyses have shown that the architecture of arteriolar networks supplying the GM of male C57BL/6 mice is conserved during aging (6, 106), substantiating direct comparisons between respective branch orders between Old and Young.

Experimental protocol. Observation sites for each network were defined during a 30-min equilibration following surgery (Figure 2.1) and maintained throughout the experimental protocol. Extensive preliminary experiments defined our protocol and confirmed that

completed GM preparations remained stable with reproducible responses for at least 5 h (106).

Oxygen reactivity. To evaluate the vasomotor response to a rise in PO_2, the O_2 content of the superfusion solution was increased by equilibrating the PSS with 21% O_2, 5% CO_2 and 74% N_2 for ~5 min and ID values were recorded (Figure 2.1). The PSS was then re-equilibrated with 5% CO_2 and 95% N_2 for the remainder of the protocol. Empirically, reactivity to changes in PO_2 is a sensitive index of the viability of a preparation for intravital microscopy (45, 77, 106).

Concentration-response relationships. Respective agonists (PE, UK 14304, ACh) were added ($\leqslant$ 500 µl) to the 50-ml chamber containing PSS in a cumulative fashion to achieve final agonist concentrations that started at 10^{-9} M and increased to 10^{-5} M in 0.5 log increments; steady state IDs were recorded during min 2-8 at each concentration. The order of superfusion with respective agonists was randomized across experiments, with a 30-min equilibration following each agonist to restore resting ID (Figure 2.1). At the end of each protocol, the GM preparation was superfused with 10^{-4} M sodium nitroprusside (SNP) for 5 min to obtain values for maximal internal diameter (ID_{max}) (106). In some cases (irrespective of age) the maximal diameter in response to 10^{-5} M ACh was slightly greater than that evoked by SNP (Table 1). Therefore, the ID_{max} (Figure 2.2) was defined as the maximal value for ID obtained with either 10^{-5} M ACh or 10^{-4} M SNP.

Data analyses and Statistics. For each vessel branch order, spontaneous vasomotor tone was calculated as the difference between resting and maximal ID and expressed relative to maximal ID. Thus, vasomotor tone (%) = $[(ID_{max}-ID_{rest})/ID_{max}] \times 100\%$ where ID_{rest} =

resting baseline (control) ID. The response to elevated O_2 was calculated as the magnitude of vasoconstriction during equilibration of the superfusion solution with 21% O_2 and expressed relative to resting ID. Thus, O_2 response (%) = $[(ID_{rest}-ID_{O2})/ID_{rest}] \times 100\%$, where ID_{O2} = ID during superfusion with 21% O_2. To evaluate reductions in ID from control during AR activation, vasoconstriction was expressed relative to respective resting IDs. Thus, vasoconstriction (%) = $[(ID_{rest}-ID_{ssr})/ID_{rest}] \times 100\%$, where ID_{ssr} = ID of the steady-state response to a given agonist concentration and 100% vasoconstriction indicates closure of the vessel lumen.

To evaluate the sensitivity of EDD for respective vessel branches in response to ACh, vasodilation was normalized to the respective maximal change in ID. Thus, "vasodilator capacity" (%) = $[(ID_{ssr}-ID_{rest})/(ID_{max}-ID_{rest})] \times 100\%$. This definition spans from 0 to 100% for all vessels irrespective of actual diameter values and thereby enables relative differences in sensitivity to be evaluated for a given agonist. Thus EC_{50} values can be determined for each vessel on the same relative scale. However, this normalization does not account for changes in diameter as they pertain to vascular conductance and blood flow regulation. Therefore to evaluate the functional increase in diameter relative to control conditions at rest, vasodilation was normalized to ID_{rest}. Thus, "functional vasodilation" (%) = $[(ID_{ssr}-ID_{rest})/ID_{rest}] \times 100\%$. For example a 100% increase indicates a doubling of ID from the resting baseline and predicts (according Poiseuille's law) a 16-fold increase in blood flow through the vessel at constant perfusion pressure.

Data were analyzed using two-way analysis of variance (GraphPad Prism 5; La Jolla, CA, USA) to evaluate the main effects of age and vessel branch orders. Bonferroni tests were

performed for post-hoc comparisons. Summary data are expressed as means ± standard error (SE). Differences were accepted as statistically significant with $P<0.05$.

RESULTS

All GM preparations included in this study exhibited spontaneous vasomotor tone throughout their resistance networks. Each vessel that was studied underwent constriction during superfusion with elevated O_2, confirming the viability of all preparations for further study.

Diameters, vasomotor tone and O_2 response. At rest under control conditions, ID decreased as branch order increased from proximal FA to distal 3A ($P<0.05$) with no difference between Old and Young for any branch order (Figure 2.2A). During maximal dilation, IDs of Old were slightly but consistently greater than Young across vessel branch orders ($P<0.05$; Figure 2.2B). Spontaneous vasomotor tone was not different for FA or 1A between age groups but was greater ($P<0.05$) in 2A and 3A of Old vs. Young (Figure 2.2C). Vasoconstriction during elevated PO_2 of the superfusion solution increased with branch order from FA to 3A ($P<0.05$) but was reduced in Old compared to Young across vessel branches ($P<0.05$; Figure 2.2D).

Vasoconstriction to PE. Selective activation of α_1ARs with PE induced concentration-dependent vasoconstriction of each branch order (Figure 2.3). From 10^{-9} to 10^{-6} M, PE induced constrictions within each branch order that were similar in Old and Young (Figure 2.3), though an effect of age was apparent. Peak constrictions in Old were less than in

Young, particularly in 2A and 3A where closure occurred in Young (confirmed by absence of red blood cells and disappearance of the lumen) but not in Old (where sluggish movement of red blood cells persisted). The EC_{50} values for PE were similar between Old and Young across branch orders, with differences between age groups consistently within 0.5 log units (Table 2.2).

Vasoconstriction to UK 14304. Selective activation of α_2ARs with UK 14304 induced a concentration-dependent constriction across vessel branches. The efficacy of α_2AR-mediated constrictions increased with branch order from FA to 3A and were greater in Young vs. Old in 1A, 2A and 3A ($P<0.05$; Figure 2.4). The EC_{50} values for UK 14304 were similar between Old and Young across branch orders, with differences between age groups typically within 0.5 log units (Table 2.2).

Effects of selective α_1AR vs. α_2AR activation. Throughout the resistance network of the GM, the magnitude of constriction increased with vessel branch order. Activation of α_1ARs with PE consistently produced ~2-fold greater constriction than did activation of α_2ARs with UK 14304 (Figures 2.3 and 2.4). Whereas α_2AR-mediated constriction was attenuated in all arteriolar branch orders of Old compared to Young (Figure 2.4), α_1AR responses were maintained in Old though 2A and 3A were resistant to closure (Figure 2.3).

Endothelium-dependent dilation. Acetylcholine evoked concentration-dependent vasodilation in all vessel branches of Old and Young GM (Figures 2.5 and 2.6). When expressed relative to vasodilator capacity for respective branches to evaluate sensitivity, FA and 1A responses were not different between Young and Old, while EDD of 2A and 3A in Old were shifted slightly (< 0.5 log unit) but significantly to the left when compared

to Young (Table 2.2 and Figure 2.5). When expressed relative to respective resting control diameters, the magnitude of EDD of FA was less ($P<0.05$) in Old compared to Young (Figure 2.6). In contrast, EDD of 2A and 3A was ~2-fold greater ($P<0.05$) in Old compared to Young (Figure 2.6).

Branch order differences. In addition to differences between Old and Young within individual branch orders, vasomotor responses to respective agonists exhibited differences between branch orders within age groups. In Young, [PE] > 10^{-7} M induced greater α_1AR-mediated constriction in distal vs. proximal branches such that 3A>2A>1A>FA (Figure 2.7). In Old, this effect of branch order was maintained though less robust. For [UK 14304] > 10^{-8} M, α_2AR-mediated constriction also increased with vessel branch order with 3A>2A>1A>FA and this relationship was also maintained (though less robust) in Old (Figure 2.7). For EDD, the trend was reversed from that seen during vasoconstriction such that the sensitivity to ACh was greatest in proximal vessels with FA>1A>2A>3A. As seen with vasoconstriction, differences between branch orders were more robust in Young than in Old (Figure 2.7). For each agonist, there was a significant effect ($P<0.05$) of vessel branch order as well as concentration.

Maximal responses to agonists. To evaluate how advanced age influenced the dynamic range of vasoconstriction and vasodilation in respective vessel branch orders, maximal responses to the activation of α_1ARs (PE), α_2ARs (UK 14304) and muscarinic receptors (ACh) are presented for respective agonists in Figure 2.8. Across vessel branch orders, PE consistently evoked ~2-fold greater vasoconstriction than did UK 14304. Maximal vasoconstriction to the activation of either α_1ARs or α_2ARs was reduced in Old vs. Young

($P<0.05$), particularly in arterioles. EDD increased with branch order in arterioles of Old but not in arterioles of Young. Irrespective of age group, maximal diameters with ACh were similar to those with SNP (Table 1).

DISCUSSION

The present study has defined microvascular reactivity along resistance networks of skeletal muscle in Young (4-mo) and Old (24-mo) male C57BL/6 mice. Using intravital microscopy to study the mouse GM, we evaluated internal vessel diameters, vasomotor tone and responses to defined vasoactive stimuli. Under resting conditions, Young and Old mice exhibited similar diameters for feed arteries and respective arteriolar branches. During maximal dilation, diameters of distal arterioles (i.e., 2A and 3A) tended to be larger in Old compared to Young mice, reflecting greater spontaneous vasomotor tone. Nevertheless, vasoconstriction in response to elevated O_2 was attenuated throughout the networks of Old compared to Young mice. Further, while α_1ARs were twice as effective as α_2ARs in evoking constrictions, advanced age attenuated responses to both AR subtypes, particularly in distal arterioles. Remarkably, with similar resting diameters, vasodilation to ACh (i.e., EDD) was greater in distal arterioles of Old compared to Young. Thus the effect of advanced age on the reactivity of microvessels supplying skeletal muscle varies with branch order and nature of the vasoactive stimulus.

Vessel diameters

In accord with Poiseuilles' law, the IDs of resistance arteries and arterioles are principal determinants of both tissue perfusion and peripheral resistance. Consistent with previous studies of microvascular resistance networks (14, 99, 106), vessel diameter decreased as branch order increased with FA>1A>2A>3A in Young and Old (Figure 2.2). At rest under control conditions, the IDs of respective branch orders were not different between age groups (Figure 2.2A). While these hierarchical relationships were maintained during maximal dilation, arteriolar diameters tended to be larger in Old compared to Young mice as branch order increased (Figure 2.2B). As a consequence, and despite no difference in resting diameters, vasomotor tone increased with vessel branch order, particularly in 2A and 3A of Old when compared to those in Young (Figure 2.2C). This scenario contrasts with hypertension and diabetes, where thickening, narrowing and rarefaction of arterioles (with tissue ischemia) are found (70, 71, 123, 124). Recent findings have shown no difference in systolic blood pressure in male C57BL/6 mice at 3 vs. 24 months (154), thus the present data appear most applicable to "healthy" aging in contrast to conditions associated with vascular disease.

Oxygen response

As O_2 delivery increases relative to demand, resistance vessels constrict as a mechanism of negative feedback. Raising the O_2 content of the superfusion solution provides a source of O_2 in addition to that carried in the bloodstream (45, 94, 158). In turn, constriction of arterioles in response to elevating superfusion PO_2 is an exquisitely sensitive index of the functional integrity of exposed microvessels (45, 77, 106). Typically, O_2 responses are

evaluated in a single arteriole within a preparation prior to beginning experiments to assess viability of the preparation (6, 75, 106). Consistent with such criteria, constriction of each branch of the GM resistance network during equilibration with 21% O_2 confirmed the integrity of our preparations irrespective of age group. As the O_2 "sensor" may be located within the tissue (76), our finding that constriction during elevation of superfusion PO_2 encompassed FAs external to the muscle is consistent with the ability of O_2 to depolarize arteriolar SMCs (163) and evoke conducted vasoconstriction (76). Through evaluating entire resistance networks, we demonstrate that the relative magnitude of constriction in response to elevated PO_2 increased with vessel branch order, from FA to 3A (Figure 2.2D). Consistent with earlier findings focused on 2A of the GM (6, 75), the O_2 response was depressed in all branch orders in Old vs. Young mice (Figure 2.2D). Thus the ability of O_2 to evoke constriction is attenuated throughout the resistance vasculature with aging. Given the similarities in vessel IDs at rest between age groups (Figure 2.2A), greater spontaneous vasomotor tone in 2A and 3A of Old vs. Young mice (Figure 2.2C) suggests that the role of PO_2 in governing SMC activation is reduced in advanced age. In light of tissue oxygenation being integral to capillary perfusion and blood flow regulation (45, 94, 158), attenuated O_2 responses in Old mice (Figure 2.2D) imply alterations in the regulation of muscle blood flow during advanced age; e.g., as manifested through a greater role for reactive oxygen species (9, 107, 136).

Adrenergic reactivity

In human subjects, femoral arterial blood flow and vascular conductance were 30-40% lower in older (~63 years) compared to young (~28 years) males in association with tonic

elevation of muscle SNA and the activation of αARs (22, 38). Though comparable recordings of SNA with aging are lacking in mice, the activities of key enzymes governing catecholamine synthesis (e.g., tyrosine hydroxylase) were ~2-fold higher in the adrenal glands of Old (28 mo) compared to Young (4 mo) male mice and rats (120). Independent studies found norepinephrine release from sympathetic nerves to be greater at rest and during stress in Old (24 mo) vs. Young (3 mo) male Fischer-344 rats (100). In light of enhanced constitutive αAR activation in GM of Old (6, 75, 106), findings collectively suggest a greater level of SNA in Old vs. Young mice. Adrenergic vasoconstriction is mediated postsynaptically by two AR subtypes on vascular SMCs, α_1ARs and α_2ARs (49, 106). The selectivity of PE and UK 14304 on respective αAR subtypes has been confirmed in the mouse GM (106). In both Young and Old mice studied here, the activation of α_1ARs with PE constricted all vessel branches to a greater extent than did activation of α_2ARs with UK 14304 (Figures 2.3 and 2.4). Thus while both receptor subtypes mediate vasoconstriction in the GM microcirculation, α_1ARs consistently displayed ~2-fold greater efficacy when compared to α_2ARs. Further, while the ability of α_1ARs and of α_2ARs to evoke constriction increased with vessel branch order (Figure 2.8), there were no consistent differences between age groups in their sensitivity (i.e., EC_{50} values) to respective agonists (Table 2.2).

In humans, reductions in forearm blood flow during α_1AR activation (via intra-arterial infusion of PE) were blunted in older (~65 yr) compared to younger (~26 yr) males while blood flow reductions to α_2AR activation with clonidine infusion were similar between age groups (37). Thus attenuated reductions in forearm blood flow in older vs. younger men during tyramine infusion (to evoke release of endogenous norepinephrine) were attributed

to reduced responsiveness of α_1ARs (37). During exposure to PE, our finding that 2A and 3A of Old mice were unable to constrict to the same extent observed in Young mice (Figure 2.3). This new finding illustrates an important functional limitation that may help to explain the reduced response to activation of α_1ARs in the human forearm with aging. In turn, the inability to fully constrict 2A and 3A of Old during maximal activation of α_1ARs (Figure 2.3) may reflect tissue remodeling with aging (169). For example, an increase in the amount, orientation and/or stiffness of the extracellular matrix (88, 92) may resist lumen closure of smaller arterioles in Old mice that are otherwise able to do so in younger animals. Further studies at the ultrastructural level are required to provide greater insight into the nature of this adaptation to aging.

During tyramine infusion into the femoral artery, reductions in leg blood flow were also attenuated in older (~62 yr) vs. younger (~24 yr) men and attributed to the attenuation of both α_1AR- and α_2AR-mediated responses with aging (147). The effect of aging on reducing maximal constriction was greater for α_2AR vs. α_1AR activation in the mouse GM (Figure 2.8). α_1ARs were more efficacious than α_2ARs in evoking vasoconstriction and were relatively less affected by advanced age, particularly in FA and 1A (Figure 2.8). Thus, AR activation is still able to restrict muscle blood flow. Indeed, relative to attenuated α_2AR-mediated constriction of arterioles with aging, α_1AR-mediated constriction was maintained at all but the highest PE concentrations (Figure 2.3) which may help to ensure the maintenance of peripheral resistance and arterial blood pressure during exercise (152).

Endothelium dependent dilation

As demonstrated in humans (43, 68, 136) and in resistance vessels isolated from rats (7, 108, 165, 166), advanced aging is associated with attenuated EDD, typically characterized by activating muscarinic receptors on the endothelium. Nevertheless, intravital studies of the mouse GM had indicated no difference in the ability of ACh to dilate 2A of Young vs. Old mice *in vivo* (6). To investigate the effect of advanced age on EDD along resistance networks, we quantified responses to ACh in two ways. First, to address the sensitivity of EDD, changes in ID at each ACh concentration were normalized to the corresponding maximal change in ID. These data indicate that the "vasodilator capacity" of FA and of arterioles in Old mice was not different from that of Young mice (Figure 2.5). Further, there was a trend for greater sensitivity to ACh in 2A and 3A of Old mice compared to Young mice (Figure 2.5). Finding that the maximal ID of each branch order to ACh was similar to that evoked by the nitric oxide donor SNP (Table 2.1) indicates that the endothelium lining resistance networks of Old mice were fully able to drive vascular smooth muscle relaxation. In contrast, as an index for the dynamic range of blood flow control, normalizing ID changes to respective resting diameters (i.e., "functional vasodilation") revealed that EDD was depressed significantly in FA of Old mice while enhanced in 2A and 3A of the same networks (Figure 2.6). Whereas reduced EDD in FA of Old vs. Young is consistent with impaired EDD of conduit and resistance arteries with advanced age (46, 136, 162), enhanced EDD of the smaller downstream arterioles in Old mice suggests that the effect of advanced age on EDD varies with microvessel branch order *in vivo*. Such regional differences within the microcirculation have not been documented previously. In part this is attributable to the focus on FA and 1A in previous studies (7,

108, 155, 165). Further, *in vivo* studies evaluating ACh-induced EDD in human skeletal muscle with aging were based on changes in limb blood flow (43, 44, 68). In such cases, specific branch orders within the microcirculation as emphasized here could not be accounted for.

SUMMARY AND PERSPECTIVE

Studies in humans have illustrated that skeletal muscle blood flow is reduced with advanced age in association with augmented SNA (38, 52) along with impaired EDD (43, 136). However, such studies are based primarily upon evaluating diameter and velocity in conduit (e.g., brachial and femoral) arteries, where changes in blood flow reflect regulatory events occurring further downstream; i.e., in the microcirculation. Such measurements in humans are thereby limited by the inability to directly observe those vessels actually responsible for controlling tissue perfusion and peripheral resistance. Thus, using rodents as a model system provides an opportunity to extend direct observations of blood flow control into the mammalian microcirculation. The effect of aging on resistance microvessels of rats has focused on FAs (155, 165, 166) and the large arterioles (e.g., 1A) (7, 108). These proximal microvessels are most readily isolated and studied *in vitro* because they are of sufficient diameter and length to enable microdissection and cannulation for evaluation using pressure myography. Where the effect of aging on arterioles has been studied *in vivo*, observations have focused on 1A and 2A in muscles of rats and mice (6, 27). In contrast, this study is the first to examine the effects of aging on vascular reactivity

throughout microvascular resistance networks of skeletal muscle *in vivo*, from proximal feed arteries through third-order arterioles.

Using the GM preparation in male C57BL/6 mice, we report that advanced age (i.e., 24 vs. 4 mo) blunted the sensitivity to O_2 throughout networks with the greatest effect in distal (2A, 3A) arterioles. Aging also prevented closure 2A and 3A arterioles during maximal activation of α_1ARs, which may be explained by associated changes in the extracellular matrix. Nearly all constrictions to α_2AR activation were attenuated throughout arteriolar networks but not in FAs, highlighting regional differences in microvascular adaptations to aging. We speculate that the loss of arteriolar α_2AR reactivity with aging may result from a tonic increase in receptor activation (75, 120), consistent with findings in humans (22, 38). Remarkably, whereas constriction of the smaller (2A, 3A) arterioles was impaired consistently in Old vs. Young mice, these same arteriolar branches in Old mice exhibited enhanced EDD and greater spontaneous vasomotor tone. Thus distal arterioles exhibiting the greatest attenuation of constrictor responses simultaneously exhibited the greatest dilator responses. Nevertheless, maintained constriction (or impaired EDD) of proximal FA can restrict muscle blood flow even when distal arterioles are dilated maximally (75, 160). Unlike studies in humans, which have relied on indirect measurements of limb blood flow, intravital studies in mice enable direct observations of respective microvessels that control flow magnitude (FA, 1A) as well as its distribution within the tissue (2A, 3A).

The consistency of our present findings in the mouse GM with those from earlier studies of human subjects suggests that the GM is a viable model for investigating how aging affects the microcirculation of skeletal muscle. As typical of human skeletal muscles (93,

127), the mouse GM is of mixed fiber type (90, 98). Thus the insight gained from understanding where and how advanced age affects adrenergic vasoconstriction, EDD and blood flow control in respective microvascular branch orders of the mouse GM *in vivo* may well be applied towards developing selective therapeutic strategies for promoting muscle blood flow in aging humans.

ACKNOWLEDGEMENTS

This research was supported by NIH grant R01-HL086483. The content is solely the responsibility of the authors and does not necessarily represent the official views of the National Institutes of Health. Drs. Erika Boerman and Matthew Socha provided a critical review of this work.

AUTHOR CONTRIBUTIONS

SYS and SSS designed these experiments. SYS performed these experiments in the laboratory of SSS in the Department of Medical Pharmacology and Physiology at the University of Missouri. SYS and SSS analyzed and interpreted the data. SYS prepared the initial figures and drafted the manuscript. SSS edited the figures and text. SYS and SSS reviewed and edited successive versions of the manuscript. SYS and SSS read and approved the final version of this work to be submitted for publication.

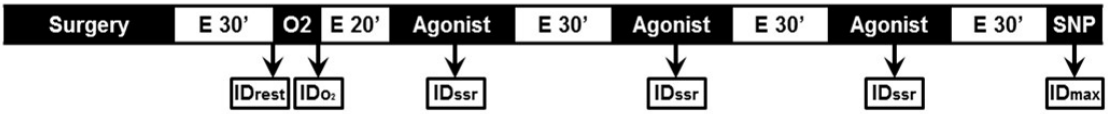

Figure 2.1. Experimental protocol for evaluating diameters and reactivity in microvascular resistance networks of mouse gluteus maximus muscle. Once anesthesia was induced, surgery required ~1 h. Evaluation of vasoconstriction in respective vessel branch orders (FA, 1A, 2A, 3A) during equilibration with 21% oxygen (O_2) in the superfusion solution required ~15 min. The superfusion was then re-equilibrated with 0% O_2 for another 20 min before proceeding (E 20'). Cumulative concentration-response relationships (10^{-9} to 10^{-5} M) required ~40 min to evaluate each agonist (PE, UK14304, ACh) across vessel branch orders followed by 30 min washout and equilibration (E 30') with control PSS to restore spontaneous vasomotor tone. Each preparation experienced all stimuli with the order of agonist treatment and the sequence in which vessel branch orders were studied randomized across preparations. An entire experiment required 5-6 h to complete. ID, internal diameter; ssr, steady state response at each [agonist]; max, maximal; SNP, sodium nitroprusside.

Vessel branch	Young		Old	
	SNP	ACh	SNP	ACh
FA	57 ± 2	60 ± 2*	61 ± 4	62 ± 5
1A	50 ± 2	51 ± 2	55 ± 5	56 ± 5
2A	35 ± 3	35 ± 2	44 ± 3	44 ± 4
3A	23 ± 2	23 ± 1	32 ± 3	31 ± 4

Table 2.1. Maximal internal diameters (μm) for FA and arterioles in Young and Old mice. One vessel from each branch order was studied in each GM preparation. Maximal IDs were obtained during superfusion with 10-4 M SNP and with 10-5 M ACh. Summary data are means ± SE, n=5 per group. *P<0.05, ACh vs. SNP.

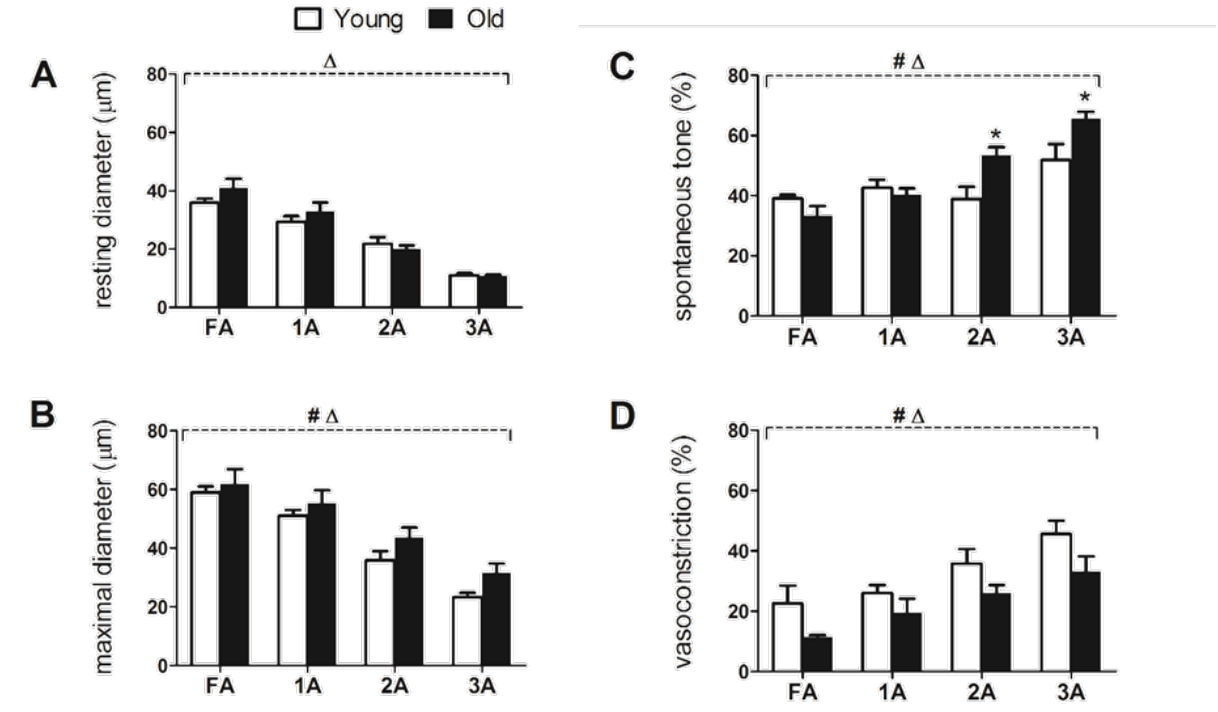

Figure 2.2. Diameters, vasomotor tone and O_2 response in feed artery and arterioles of Young and Old mice. A. Resting diameters decreased from proximal to distal vessels as branch order increased from FA to 3A in both age groups. **B**. Maximal diameters decreased as in **A** and were slightly but consistently greater in Old vs. Young. **C**. Spontaneous vasomotor tone (%, calculated as $[(ID_{max}-ID_{rest})/ID_{max}] \times 100\%$) of 2A and 3A was greater in Old vs. Young. ID_{rest} = resting ID and ID_{max} = maximal ID to 10^{-4} M SNP or 10^{-5} M ACh. **D**. Vasoconstriction (%) to 21% O_2 in the superfusion solution (calculated as $[(ID_{rest}-ID_{O2})/ID_{rest}] \times 100\%$) was reduced throughout network branches in Old compared to Young. ID_{rest} = as in **B**, ID_{O2} = ID during 21% O_2. Summary data are means ± SE, n=5 per group. $^{\#}P<0.05$, main effect of age; $^{\Delta}P<0.05$, main effect of vessel branch order; *P < 0.05, Old vs. Young.

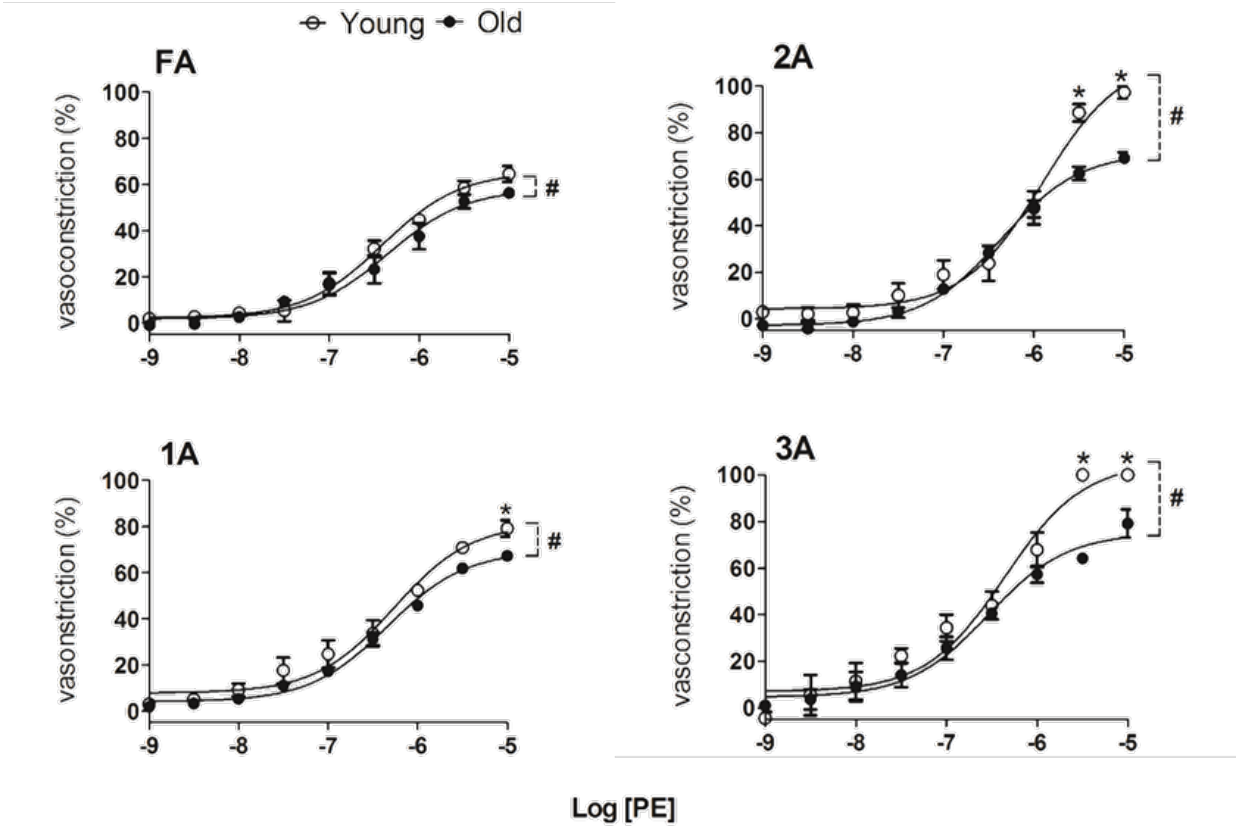

Figure 2.3. Response curves to phenylephrine in feed artery and arterioles of Young and Old mice. Advanced age attenuated peak vasoconstriction to α_1AR activation and this effect increased with vessel branch order. Vasoconstriction (%) calculated for each branch order as: $[(ID_{rest}-ID_{ssr}) / ID_{rest}] \times 100\%$, where ID_{rest} = resting ID and ID_{ssr} = steady-state response ID. Summary data are means ± SE, n=5 per group. $^{\#}P<0.05$, main effect of age group. *P<0.05, Old vs. Young.

Vessel branch	PE		UK 14304		ACh	
	Young	Old	Young	Old	Young	Old
FA	-6.4 ± 0.1	-6.4 ± 0.1	-6.2 ± 0.2	-6.4 ± 0.3	-7.5 ± 0.1	-7.4 ± 0.1
1A	-6.3 ± 0.1	-6.3 ± 0.1	-6.5 ± 0.2	-6.3 ± 0.2	-7.0 ± 0.1	-6.9 ± 0.1
2A	-5.9 ± 0.1	-6.4 ± 0.1	-6.7 ± 0.1	-6.5 ± 0.2	-6.4 ± 0.1	-6.9 ± 0.1
3A	-6.4 ± 0.1	-6.5 ± 0.1	-7.2 ± 0.2	-6.5 ± 0.2	-6.2 ± 0.1	-6.7 ± 0.1

Table 2. 2. Log EC50 values for PE, UK 14304 and ACh for FA and arterioles in Young and Old mice. One vessel from each branch order was studied in each GM preparation. With EC_{50} values as an index, vascular sensitivity to PE, UK and ACh was not significantly different between age groups as determined using 2-way ANOVA. Summary data are means ± SE, n=5 per group.

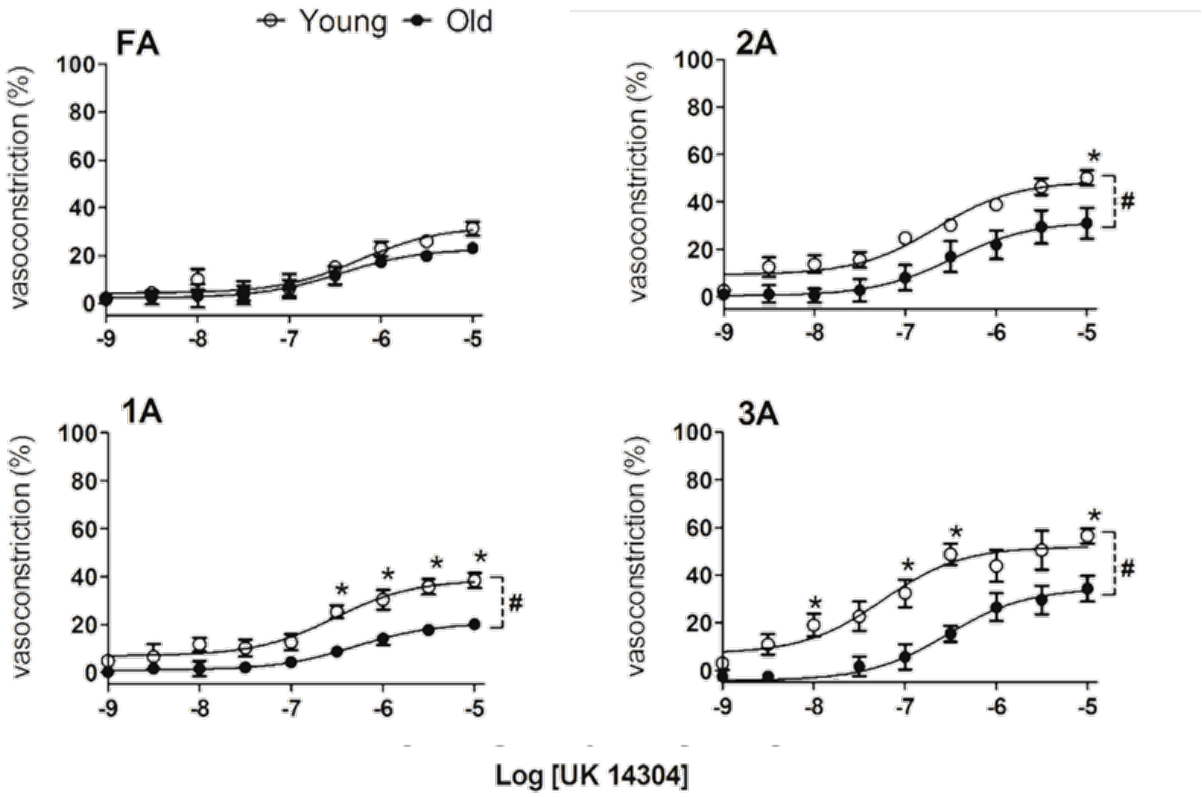

Figure 2.4. Response curves to UK 14304 in feed artery and arterioles of Young and Old mice. Advanced age attenuated vasoconstriction to α_2AR activation throughout the arteriolar network despite negligible effect in FA. Vasoconstriction (%) calculated as in Figure 2.3. Summary data are means ± SE, n=5 per group. $^{\#}P<0.05$, main effect of age. *P<0.05, Old vs. Young.

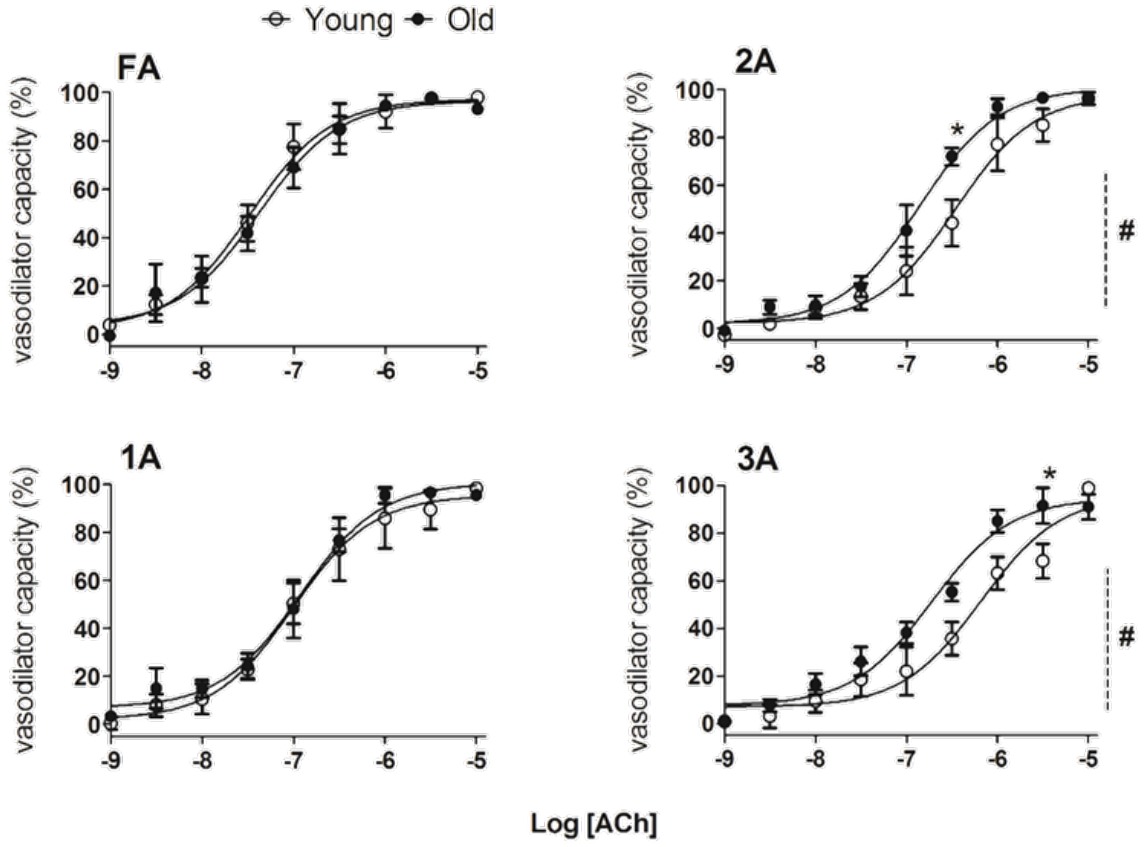

Figure 2.5. Response curves to ACh in feed artery and arterioles of Young and Old mice relative to maximal changes in diameter. Vasodilator capacity (%) was calculated as: $[(ID_{ssr}-ID_{rest})/(ID_{max}-ID_{rest})] \times 100\%$ and was preserved with advanced age across vessel branches with greater potency for Old vs. Young in 2A and 3A. ID_{rest} = resting ID, ID_{ssr} = steady-state response ID, ID_{max} = maximum ID with 10^{-5} M ACh or 10^{-4} M SNP, whichever was greater. Summary data are means ± SE, n=5 per group. $^{\#}P<0.05$, main effect of age. *P<0.05, Old vs. Young.

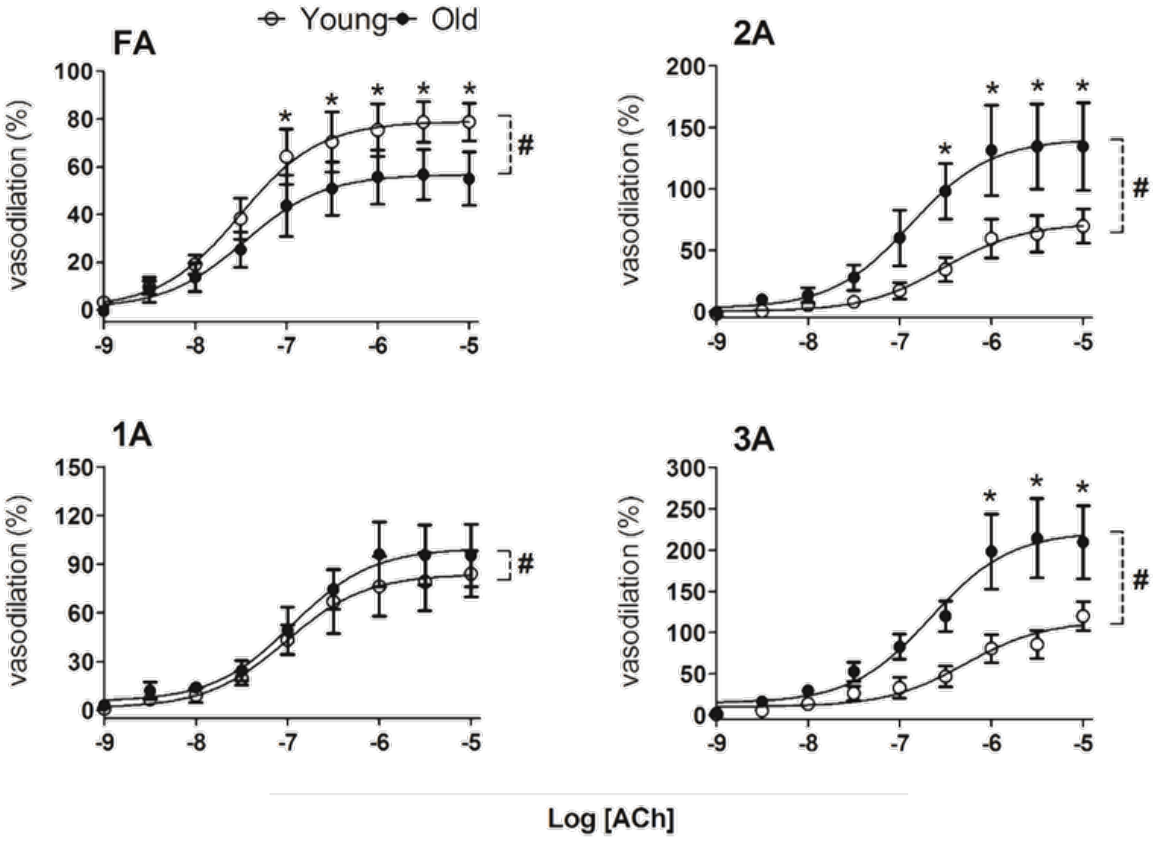

Figure 2.6. **Response curves to ACh in feed artery and arterioles of Young and Old mice relative to resting diameters.** "Functional vasodilation" (%) was calculated as: $[(ID_{ssr}-ID_{rest})/ID_{rest}] \times 100\%$ and increased with branch order from FA to 3A (note difference in ordinate scales). ID_{rest} and $ID_{ssr,}$ as in Figure 2.5. Whereas EDD of FA was attenuated in Old vs. Young, EDD in arterioles was enhanced with advanced age, particularly in 2A and 3A. Summary data are means ± SE**,** n=5 per group. $^{\#}P<0.05$, main effect of age. *P<0.05, Old vs. Young.

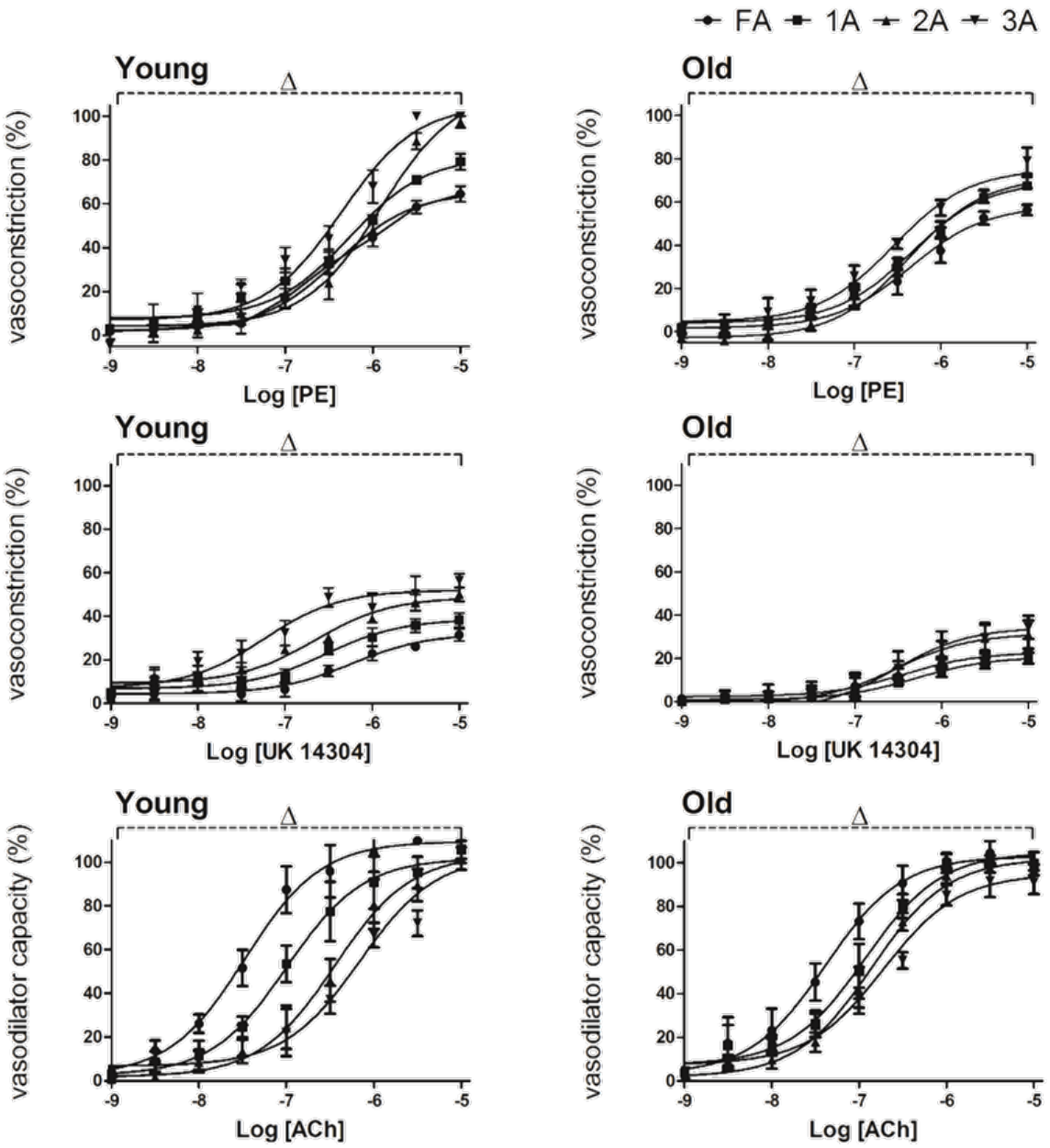

Figure 2.7. Branch order differences in reactivity to agonists in Young and Old mice. In Young (left), α_1AR mediated constriction increased with PE $>10^{-7}$ M and was greater in distal vs. proximal branches (3A>2A>1A>FA). With lower efficacy, a similar trend resulted from α_2AR-mediated constriction in response to [UK 14304]. In contrast, proximal vessels exhibited greater sensitivity during EDD with [ACh] such that FA>1A>2A>3A. In Old (right), respective patterns of branch order differences persisted but encompassed a smaller range. Summary data are means ± SE, n=5 per group. $^{\Delta}P<0.05$, main effect of branch order. Data from Figures 3-5 are re-plotted here to facilitate comparisons across branch orders for respective age groups and agonists. Respective EC_{50} values are given in Table 2.2.

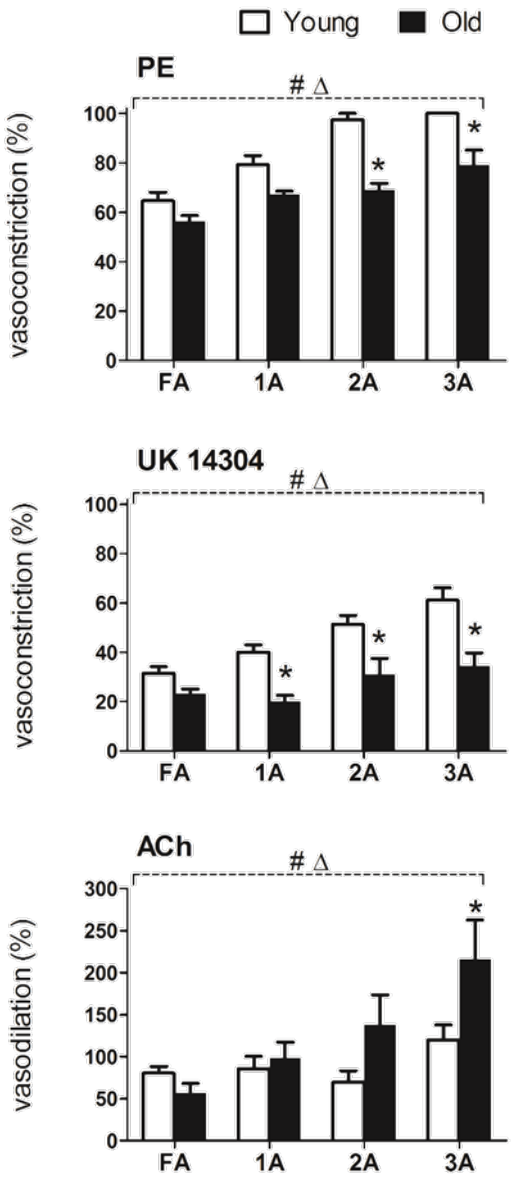

Figure 2.8. Maximal responses to agonists in feed arteries and arterioles of Young and Old mice. Maximal vasoconstrictions to PE (from Figure 2.3) and to UK 14304 (from Figure 2.4) were attenuated throughout the resistance network of GM in Old vs. Young; this effect increased with arteriolar branch order. Maximal dilation to ACh (from Figure 2.6) was depressed in FA of Old vs. Young; in arterioles, maximal vasodilation increased with branch order with Old progressively greater than Young. Summary data are means ± SE, n=5 per group. $^{\Delta}P<0.05$, main effect of branch order; *P<0.05, Old vs. Young.

CHAPTER 3

DIFFERENTIAL ADRENERGIC MODULATION OF RAPID ONSET VASODILATATION ALONG RESISTANCE NETWORKS OF SKELETAL MUSCLE IN OLD VERSUS YOUNG MICE

KEY POINTS

- Rapid onset vasodilatation (ROV) initiates functional hyperemia upon skeletal muscle contraction and is attenuated during ageing via α-adrenoreceptor (αAR) stimulation. However it is unknown where this effect predominates in resistance networks.
- In the gluteus maximus muscle of young (4 months) and old (24 months) male C57BL/6 mice, a brief tetanic contraction initiated ROV while observing feed arteries and arterioles. ROV increased with contraction duration, peaked later in upstream versus downstream branches and was attenuated throughout networks with advanced age.
- Inhibiting αARs improved ROV in old mice while activating αARs attenuated ROV in young mice. Modulating ROV through αAR activation was greater in upstream feed arteries and arterioles compared to downstream arterioles, with α_2ARs more effective than α_1ARs.
- ROV is coordinated along resistance networks supplying skeletal muscle and modulated differentially between young and old mice via αARs. With advanced age, attenuated dilatation of upstream branches will restrict muscle blood flow.

ABSTRACT

Rapid onset vasodilatation (ROV) in skeletal muscle is attenuated during advanced age via α-adrenergic receptor (αAR) activation however it is unknown where such effects predominate in the resistance vasculature. Studying the gluteus maximus muscle (GM) of anesthetized young (4 months) and old (24 months) male C57BL/6 mice (n=6/group), we tested the hypothesis that attenuation of ROV during advanced age is most effective in proximal branches of microvascular resistance networks. Diameters of a feed artery (FA), first (1A), second (2A) and third (3A) - order arteriole were studied in response to single tetanic contractions (100Hz, 100-1000ms). ROV began within 1s and peaked sooner in 2A and 3A (2-3s) than in 1A or FA (3-4s). Relative amplitudes of dilatation increased with contraction duration and with vessel branch order (FA<1A<2A<3A). In old mice, attenuation of ROV was greater in FA and 1A compared to 2A and 3A. Inhibiting αARs (phentolamine; 10^{-6}M) improved ROV of FA and 1A in old mice while subliminally stimulating αARs in young mice (noradrenaline; 10^{-9}M) depressed ROV of FA and 1A more than for 2A and 3A. In young mice, stimulating α_1ARs (phenylephrine; 10^{-7}M) and α_2ARs (UK 14304; 10-7M) attenuated ROV primarily in FA. In Old mice, inhibiting α_2ARs (rauwolscine; 10^{-7}M) restored ROV more effectively for FA and 1A than did inhibiting α_1ARs (prazosin; 10^{-8}M). With temporal and spatial coordination along resistance networks, attenuation of ROV with advanced age is most effective in proximal branches via constitutive activation of α_2ARs.

INTRODUCTION

Rapid onset vasodilatation (ROV) reflects the near-instantaneous relaxation of smooth muscle cells (SMCs) of the resistance vasculature in response to skeletal muscle contraction (28, 102, 157, 161). Through initiating the increase in blood flow to active muscle fibers, ROV facilitates the transition from rest to physical activity. These same vessels are surrounded by sympathetic nerves which release noradrenaline (NA) to evoke vasoconstriction that increases with the level of α-adrenoreceptor (αAR) activation (49, 99). As shown with microneurography in human subjects, sympathetic nerve activity (SNA) increases with exercise intensity and active muscle mass (134, 135).The autonomic nervous system remains active under resting conditions and the background level of SNA increases with advanced age (38, 52). Enhanced SNA during advanced age is also manifest in rodents. For example, release of NA from sympathetic nerves into the circulation was greater at rest and during immobilization stress in aged (24 months) compared to young adult (3 months) male Fischer-344 rats (100). Further, the tyrosine hydroxylase activity, which governs NA synthesis, was ~2-fold higher in adrenal glands of Old (24 months) compared to Young (4 months) male rats and mice (120). Such similarities support these species as a model to understand how advanced age affects the role of SNA in modulating muscle blood flow.

Functional sympatholysis describes the inhibition of sympathetic vasoconstriction during muscular activity (121) and is impaired in humans with advanced age (39). Further, the ability to rapidly increase muscle blood flow in response to muscle contraction is attenuated in older (>60 years) compared to younger (~20-30 years) humans (20, 22). Attenuated

muscle blood flow with diminished vascular conductance can reflect elevated muscle SNA and the activation of αARs (22, 38). Thus, blocking αARs with phentolamine restored ROV to forearm muscle contractions in old adults (~69 years), whereas increasing SNA (via lower body negative pressure) impaired ROV in younger subjects (~27 years) (22). The effect of enhanced αAR activation during advanced age on ROV is also manifest in the mouse. Thus, attenuated ROV of distributing arterioles in the gluteus maximus muscle (GM) of old (20 months) was restored to that of young (3-4 months) male mice by topical phentolamine (75). However, these initial studies did not address other branches of the network and blood flow regulation requires coordinated activity among upstream and downstream branches (138). In such manner, volume flow into the muscle is governed by proximal feed arteries (FAs) and first-order (1A) arterioles with regional distribution governed by second- (2A) and third-order (3A) arteriolar branches; the latter give rise to terminal arterioles and capillaries. Whilst sympathetic vasoconstriction reflects the activation of αARs on SMCs, the functional distribution of α_1AR and α_2AR subtypes vary with vessel branch order along microvascular resistance networks (14, 41, 49, 106). With advanced age (24 versus 4 months) in the mouse GM, response curves to progressive α_1AR activation were maintained in FAs and 1As while being attenuated in 2A and 3A branches. During α_2AR activation, the efficacy of constriction decreased as vessel branch order increased (145). Such regional differences in adrenergic reactivity suggest that modulation of ROV by α_1AR versus α_2AR activation may vary among upstream and downstream branches. However, it is unknown how the activation or inhibition of αARs may affect ROV in respective branch orders, nor how these relationships are affected by advanced age.

A limitation when studying blood flow responses to contractile activity in skeletal muscle of human subjects is the inability to resolve the dynamics of the actual site(s) of vascular resistance. To elucidate such behaviour requires invasive methods, for which the mouse GM is well-suited (6, 145). The GM is a powerful hip extensor of mixed fiber type (90, 98) which is typical of human skeletal muscle (93, 127). Using the GM, the goal of this study was to evaluate ROV in proximal FA and 1A as well as distal 2A and, 3A of intact microvascular resistance networks controlling blood flow to skeletal muscle fibres in vivo. Diameter responses of respective branch orders to graded single tetanic contractions were recorded in young and old mice before and during selective activation or inhibition of α_1ARs and α_2ARs. We tested the hypothesis that ROV is attenuated most effectively in proximal branches of the resistance network during advanced age.

METHODS

Animal care and use

Experimental protocols were approved by the Animal Care and Use Committee of University of Missouri and were performed in accordance with the National Research Council's *Guide for the Care and Use of Laboratory Animals* (2011). Young (4 months; n =12, 30.9 ± 0.5 g) and old (24 months; n=12, 32.3 ± 0.7g) C57BL/6 male mice were obtained from National Institute on Aging colonies (Charles River Laboratories, Wilmington, MA). Respective age groups in mice correspond to humans in their middle 20's and late 60's (53). For the data presented in this study, a total of 12 mice of each age

group were acclimated in animal care facilities of the University of Missouri for at least one week before being studied. Room temperature was maintained at ~24°C on a 12h: 12h light: dark cycle with food and water available *ad libitum*. On the morning of an experiment, a mouse was anaesthetized by intraperitoneal injection of pentobarbital sodium (60 mg kg^{-1}) which was supplemented as needed (20 mg kg^{-1}) to maintain anesthesia as confirmed by lack of withdrawal to toe pinch (monitored every 15 min during surgery and throughout experimental protocols). Esophageal temperature was maintained at ~37°C by placing the mouse on an aluminum warming plate (5 cm × 11 cm). Upon completion of the experimental protocol (duration, ~5-6 h), the mouse was euthanized by an overdose of pentobarbital sodium (intraperitoneal injection) followed by cervical dislocation.

Gluteus maximus muscle preparation for intravital microscopy

The GM was prepared by shaving the left hindquarter then placing the mouse in the prone position on the warming plate. The skin and connective tissue overlying the left GM was removed and exposed tissue was superfused continuously at 3 ml/min with bicarbonate buffered physiological salt solution (PSS) that contained (in mM): 131.9 NaCl, 4.7 KCl, 2 $CaCl_2$, 1.17 $MgSO_4$, 18 $NaHCO_3$ and equilibrated with 5% CO_2/95% N_2 (34-35°C, pH 7.4). Viewing through a stereomicroscope, the left GM was carefully dissected away from its the lumbar fascia and iliac crest, reflected away from the hindquarter onto a transparent rubber pedestal (Sylgard 184; Dow Corning, Midland, MI) and the edges pinned to approximate its dimensions *in situ*. Superficial connective tissue and fat were carefully removed to expose the resistance network including the FA (i.e., the inferior gluteal artery

before it enters the muscle), which becomes the 1A upon entering the muscle, and the downstream 2A and 3A branches. The inferior gluteal motor nerve bundle was cut proximally and the free end aspirated into an insulated borosilicate glass microelectrode filled with PSS (105). To minimize stray current, the interface between the nerve and suction electrode was insulated with Kwik-Cast Sealant (World Precision Instruments, Inc. USA). The completed preparation was transferred to the fixed stage of an intravital microscope (Nikon E600FN; Melville, NY) mounted on an X-Y translational stage (Gibraltar; Burleigh Instruments, Fishers, NY). Images were acquired through a Nikon SLWD 20X objective (numerical aperture = 0.35) focused onto a FireWire color charge-coupled device camera (DFK 21AF04; The Imaging Source, Charlotte, NC). Spatial resolution on the video monitor was ~1 μm. Digital images were recorded at 30 frames per second (fps) using LabView software (National Instruments, Austin, TX) provided by Dr. Michael J. Davis (University of Missouri). The internal diameter (ID) of each vessel studied was measured frame-by-frame during playback using a video caliper integrated into the software. Each GM preparation was equilibrated for 30 min before evaluating ROV. Data were acquired only from preparations exhibiting robust vasomotor tone under resting conditions (145). At the end of each experiment, maximal vasodilatation was recorded during superfusion with sodium nitroprusside (SNP; 10^{-4} M).

Motor nerve stimulation

Single tetanic contractions of the inferior GM were induced by electrical stimulation of the motor nerve (30V, 100Hz, 0.1 ms pulse) for durations of 100, 250, 500 and 1000 ms; stimulation at 100 Hz evokes maximal tetanic contraction (6). One vessel (FA, 1A, 2A, or

3A) was observed for each set of 4 contractions, with the order of respective branches randomized across experiments. Each vessel was allowed to recover to its resting baseline diameter following a given contraction. Thus, evaluating ROV to 4 contraction durations in 4 branch orders during a given condition required a series of 16 contractions and 3 series of contractions (control + 2 experimental treatments) were studied in each GM preparation. Preliminary control experiments performed when designing this study confirmed that vasomotor tone and ROV remained stable throughout 4 series of contractions performed in this manner (**Supplemental Figure 3.1**).

Pharmacology

All pharmacological treatments were added to the superfusion solution for topical application at the designated concentration (145). Nonselective activation of αARs used 10^{-9} M NA, this concentration of NA activates αARs at a subthreshold level; i.e., without eliciting obvious vasomotor response (75). Nonselective inhibition of αARs used 10^{-6} M phentolamine, this concentration of phentolamine has been verified to effectively block αARs response on the same GM preparation in previous studies in our laboratory (75, 106). The effects of selective inhibition of α_1ARs or α_2ARs on ROV was investigated using 10^{-8} M prazosin (PZ) or 10^{-7} M rauwolscine (RW) (106); the respective concentration has been verified in a previous study from our laboratory using the same GM preparation studied here (106). The effects of selective activation of α_1ARs and α_2ARs on ROV was investigated using 10^{-7} M phenylephrine (PE) and 10^{-7} M UK 14304 (UK) respectively. To ensure that PE and UK were exerting effects, each was applied at a concentration (10^{-7} M) that I found to just begin to elicit vasoconstriction (145). The order of respective treatments

varied across experiments. Reagents were obtained from Sigma Chemical Co. (St. Louis, MO) unless indicated otherwise.

Immunofluorescence

To confirm the presence of perivascular sympathetic innervation, individual FAs were dissected and pinned in a Sylgard-coated Petri dish, fixed in 4% paraformaldehyde for 20 min, blocked with 10% normal goat serum and incubated overnight at 4°C with primary antibodies for tyrosine hydroxylase (TH; dilution, 1:250; #T2928, Sigma) to identify sympathetic nerves (96) and for protein gene product 9.5 (PGP 9.5; dilution, 1:400; UltraClone Ltd., Isle of Wight, England) to identify all perivascular nerves (153). Vessels were incubated with secondary antibodies for 90 min at room temperature (Alexa Fluor-488 or -546; Molecular Probes/Life Technologies; Carlsbad, CA; USA) each at 1:500 dilution then transferred to a glass slide and mounted with ProLong Gold (Invitrogen). Cover slips were applied and sealed with clear nail polish. Between each step, vessels were rinsed 3 times in phosphate-buffered saline (PBS; #P5368, Sigma). Primary and secondary antibodies were diluted in PBS + 0.2% Triton X-100. Labeled vessels were imaged on a Leica SP5 confocal microscope using a HCX PL APO 40X oil immersion objective (numerical aperture, 1.25) with a 2X optical zoom and 1 μm Z-slices.

Data analysis

Diameter responses of FA, 1A, 2A, and 3A during ROV were obtained using frame by frame measurements of internal diameter (ID, defined as the widest distance between edges of the lumen) during offline analyses of video recordings. “Peak” vasodilatation refers to

the largest ID recorded in response to a contraction and is used to express the amplitude of ROV. Thus, diameter change = $ID_{peak} - ID_{rest}$, where ID_{rest} = baseline resting ID. To facilitate comparison of responses across vessel branch orders, vasodilatation is expressed as % of respective maximal IDs during superfusion with 10^{-4} M SNP and calculated as: vasodilatation (% max) = $[(ID_{response}-ID_{rest})/(ID_{max}-ID_{rest})] \times 100\%$, where $ID_{response}$ = ID at designated time point(s) following contraction and ID_{max} = maximal ID during SNP. Temporal aspects of ROV are defined by the onset of dilatation and the time required to attain peak diameter upon cessation a given contraction. Due to tissue displacement during contraction, "onset" was evaluated at 1 s post-contraction, as this was the earliest time we were able to consistently refocus vessel images. Time to peak was defined as the interval between the end of contraction and peak ID.

Statistics

Data were analyzed with two-way analysis of variance (ANOVA) and linear regression to evaluate the effect of vessel branch order and age on ROV. Two-way repeated measures ANOVA was used to evaluate main effects of pharmacological interventions with respect to vessel branch order. Post-hoc comparisons were performed using Bonferroni tests. Summary data are expressed as means ± SE. Differences were considered statistically significant with $P<0.05$.

RESULTS

Resting and maximal diameters are similar for GM of young and old mice

Internal diameters were similar between young and old mice across all branch orders at rest and during maximal dilatation with 10^{-4} M SNP (**Figure 3.1**). Spontaneous vasomotor tone at rest was similar between age groups; however slightly larger resting diameters for 1A of old mice was reflected in significantly lower spontaneous tone in this branch order (Figure 3.1C). Nonselective inhibition of αARs with 1 μM phentolamine had no effect on resting diameters, nor did subliminal activation of αARs with 1 nM NA (**Table 3.1**).

ROV is blunted during advanced age throughout resistance networks

Single tetanic contractions evoked ROV in all vessel branch orders of both young and old mice (**Figure 3.2**). Expressed relative to respective maximal vasodilatations with SNP, peak ROV tended to increase with branch order, with FA<1A<2A<3A. Within each branch order, ROV increased with contraction duration, such that 100<250<500<1000 ms. While the effects of branch order and contraction duration were similar between age groups, respective ROV responses in old mice were generally depressed relative to those in young mice. Maximal force produced by the GM (e.g., at 100 Hz) is not different between young and old C57BL/6 mice (6).

Because of tissue movement and vessel displacement during muscle contraction, it was not possible to precisely determine the time of dilatation onset. As an alternative approach, the initial response was evaluated at 1 s post-contraction, i.e. immediately upon refocusing the vessel image. At this first time point, the increase in diameter was greatest in the smaller

downstream branches compared to larger upstream branches, with 3A>2A>1A>FA (**Figure 3.3**). The initial response also increased with the duration of muscle contraction and these relationships were maintained with responses expressed in either absolute or relative terms (**Figure 3.3**, left and right panels, respectively). Despite maintaining graded responses to contraction duration, dilatations were attenuated by ~half in arterioles of old mice compared to young mice, with the inhibitory effect of advanced age most apparent in FA (**Figure 3.3**).

Expressed in absolute values, peak dilatations were greater in arterioles than in FA and were similar across branch orders for 1A, 2A and 3A within each age group (**Figure 3.4**, *left panels*). However responses in old mice were consistently lower by ~half when compared to responses in young mice. Relative to maximal diameters with SNP, peak dilatations during ROV increased with vessel branch order from FA to 3A and with the duration of tetanic contraction yet were attenuated consistently in old mice compared to young mice (**Figure 3.4**, *right panels*). These differences in ROV between age groups were manifest despite similar resting and maximal diameters between age groups (**Figure 3.1**). The depression of peak ROV with advanced age was greatest in FA, which control the total volume of blood flow into arteriolar networks. In 3A of young mice, peak vasodilatation to 1000 ms contraction approximated maximal diameter with SNP.

Temporal dynamics of ROV are not affected by ageing

Peak ROV was attained within ~4 s across branch orders (**Figure 3.5**). Within respective branch orders, the time-to-peak for ROV was remarkably consistent across contraction durations. However, the time-to-peak ROV was longer in FA (~4 s) and 1A (~3.5 s)

compared to 2A and 3A (~3 s) and this temporal delay for proximal versus distal branches was manifest across durations of muscle contraction. Respective time-to-peak values for ROV was not different between age groups (**Figure 3.5**).

Sympathetic innervation

Sympathetic innervation was tested by labeling with a nonspecific neural marker (PGP9.5) and with a selective marker of sympathetic nerves (TH), which overlapped with each other for FAs (**Figure 3.6**). It was impossible to obtain definitive staining of arterioles embedded within the GM however our findings are confirmatory in nature as perivascular sympathetic nerves are known to course along arteriolar networks of skeletal muscle (14, 99).

Differential modulation of ROV by αARs in Young versus Old mice

To investigate the role of subtle αAR activation, 10^{-9} M NA was added to the superfusion solution; alternatively, to investigate the role of constitutively activated αARs, 10^{-6} M phentolamine was added (75). Neither treatment affected resting diameter in either age group (**Table 3.1**). Further, neither treatment affected the onset of ROV in either age group (i.e., not different from Figure 3.3. Nevertheless, peak ROV was affected differentially in the GM of young versus old mice, respectively.

Activation of αARs attenuates peak ROV in Young mice. Across vessel branch orders and contraction durations, subthreshold stimulation with NA attenuated peak ROV in resistance networks of Young mice (**Figure 3.7**, *left panels*), particularly in proximal FAs and 1As compared to 2A and 3A further downstream. In contrast, there was little effect

of NA on peak ROV in respective vessels of old mice (**Figure 3.7**, *right panels*), which was attenuated (compared to young mice) under control conditions.

Inhibition of αARs improves peak ROV in Old mice. Across vessel branch orders and contraction durations, nonselective inhibition of αARs with phentolamine enhanced peak ROV in old mice (**Figure 3.8**, *right panels*). However, phentolamine had negligible effect in young mice (**Figure 3.7**, *left panels*).

The functional distribution of α_1ARs and α_2ARs varies with branch order in arteriolar networks of the GM (106). With NA having the greatest effect in young mice and phentolamine having the greatest effect in Old mice, we used differential approach to investigate the role of αAR subtypes under respective conditions.

Selective stimulation of α_1ARs or α_2ARs attenuates peak ROV of Young mice. In the GM of young mice, selective stimulation of α_1ARs with 10^{-7} M PE or of α_2ARs with 10^{-7} M UK [i.e. using concentrations slightly above respective thresholds for vasoconstriction (145)], attenuated peak ROV across contraction durations, particularly in proximal branches (**Figure 3.8**). Nevertheless, this effect of αAR stimulation diminished as contraction duration increased (**Figure 3.8**). In downstream 3A, peak ROV in 3A "escaped" attenuation during activation of either αAR subtype. Thus, activation of either α_1ARs or α_2ARs can blunt peak ROV of proximal branches in GM resistance networks of young mice.

Selective inhibition of α_1ARs or α_2ARs enhances peak ROV of Old mice. In the GM of old mice, selective inhibition of α_1ARs with 10^{-8} M PZ or of α_2ARs with 10^{-7} M RW

(106) increased peak ROV of FA across contraction durations (**Figure 3.9**). Further downstream, α_2AR inhibition with RW increased peak ROV in 1A but not in 2A or 3A, while α_1AR inhibition with PZ had no effect on peak ROV in any arteriolar branch order. Thus, constitutive activation of respective αAR subtypes exerts the greatest inhibitory effect on peak ROV in FA, with the effect of α_2ARs extending into 1A. In contrast, peak ROV in 2A and 3A were unaffected by selective inhibition of either αAR subtype.

DISCUSSION

Dilatations of the resistance vasculature to single brief muscle contractions illustrate the regulatory events at exercise onset that facilitate transitioning from rest to physical activity; i.e., the rapidity with which blood flow and oxygen delivery can be increased to active skeletal muscle fibres and promote ATP generation through oxidative phosphorylation. Advanced age is known to restrict muscle blood flow, in part through the activation of αARs. This study has defined the kinetics and magnitude of ROV along microvascular resistance networks controlling blood flow to the mouse GM. Further, we have resolved differential modulation of ROV through αARs in young versus old male mice. In response to single tetanic contractions, ROV typically began within 1 s of muscle contraction and reached peak dilatation within 4 s post-contraction throughout the networks of young and old mice. The relative magnitude of ROV increased from proximal to distal branches (FA<1A<2A<3A) and increased with contraction duration (100-1000 ms) in all branch orders. Nevertheless, ROV was depressed in all vessel branches of old compared to young mice. Whereas subthreshold stimulation of αARs with NA depressed ROV only in young

mice, inhibition of αARs with phentolamine improved ROV only in old mice yet neither intervention affected resting diameters. Thus, subtle manipulation of αARs has significant physiological consequences that vary with age. With pharmacological interventions selective for α_1ARs versus α_2ARs, activating either AR subtype attenuated ROV in young mice while inhibiting α_2ARs was most effective (versus α_1ARs) in restoring ROV for old mice. Integration of these findings uniquely illustrates differential modulation of ROV by ARs in young versus old skeletal muscle. While manifest throughout resistance networks, the modulation of ROV through αARs is most effective in upstream branches (FA, 1A) that govern the volume of blood flowing into arteriolar networks. In contrast, the downstream 2A and 3A, which control regional distribution of flow to capillary beds, are less susceptible to modulation through αARs, particularly as contraction duration increases.

ROV across branch orders

With peak ROV quantified as the actual change in vessel ID, dilatations increased with contraction duration but were similar in magnitude across arteriolar branch orders for each contraction duration (**Figure 3.4**). For a given change in diameter, the net effect on blood flow increases with resting ID. In branching networks, the number of segments increases with each branch order, thus the increase in flow through a parent vessel is distributed among its smaller daughter branches. In contrast, expressing ROV as a percentage of maximal vasodilatation within each branch order (i.e. relative to the dynamic range between resting ID and maximal ID) enables comparison of reactivity across vessels that differ in size and branch order. With such perspective, the present data illustrate the trend

for ROV to increase with branch order (FA<1A<2A<3A) for each contraction duration and with the duration of contraction across branch orders. Thus, 2A and 3A approach maximal ID in response to our longest contraction duration (**Figure 3.2**). Consistent with findings in hamsters (161) and rats (113) these findings confirm that ROV is more robust in distal compared to proximal branches of the resistance network (54, 61). Nevertheless, ROV was attenuated throughout networks of old mice compared to those of young mice (**Figure 3.2**). While consistent with initial studies focused on distributing (2A) arterioles (75), the present data demonstrate that the effect of advanced age encompasses the entire resistance network but does so in a graded manner. Thus, FA dilatations are consistently less than observed in arterioles, underscoring the importance of maintaining resistance to blood flow external to the muscle even as intramuscular arterioles approach maximum dilatation. As functional sympatholysis is most effective in distal branches of the resistance vasculature (54, 159), restricting muscle blood flow by inhibiting ascending vasodilatation through αAR activation (66) effectively maintains peripheral resistance and arterial perfusion pressure when intramuscular arterioles dilate. This role for αAR activation becomes especially important when the energy requirements of aerobic activity become limited by cardiac output (126).

Initiation of ROV in downstream microvessels ascends into proximal feed arteries

Recording individual branches at 30 fps throughout each response to GM contraction enabled temporal resolution of vasomotor responses with high fidelity (**Figure 3.2**). With tissue displacement during contraction and time required to refocus, 1 s post-contraction was the first time point in which ID was resolved effectively across all durations (**Figure**

3.3). These data illustrate that the initiation of ROV occurs in the distal branches, i.e. the 3A and 2A or their dependent terminal arterioles and capillaries even further downstream. Indeed, only the most distal branches began dilating at 1 s post-contraction in response to the shortest (100 ms) contraction. As contraction duration increased, proximal branches were "recruited" in this initial response, albeit to a lesser extent as compared to distal branches. Nevertheless, with almost negligible differences in IDs or vasomotor tone (**Figure 3.1**), respective branches of networks supplying the GM of old mice were consistently less responsive than those of young mice (**Figure 3.3**). Although this distal-to-proximal evolution of ROV is more subtle during peak dilatation (**Figure 3.4**), the inhibitory effect of advanced age is manifest throughout. The present data reveal a temporal gradient along the network, with peak ROV occurring progressively later in more proximal branches (**Figure 3.5**). This coordinated behavior documents ascending vasodilation within arteriolar networks leading up to the parent FA , which has otherwise been presented as originating within the muscle and ascending into the proximal arterial supply (54, 69, 141, 161). A key finding here is the consistency of time-to-peak ROV within each branch order across contraction durations (**Figure 3.5**), even while response amplitude increases with contraction duration (**Figures 3.2 and 3.4**) [(75, 113, 161)]. As this temporal relationship is maintained during advanced age, we suggest that the signal(s) mediating the onset and time course of ROV are unaffected by ageing even while response amplitude is attenuated.

When the kinetics of ROV in the mouse GM (**Figure 3.2**) are compared to ROV kinetics recorded in human subjects performing single contractions of the forearm (20, 22, 29) or knee extensors (30), respective time courses are remarkably similar, peaking in ~4-5 s post-

contraction across respective ranges of contraction intensities. While the temporal correspondence of these integrated responses is apparent, the distal-to-proximal gradient in time-to-peak ROV along the resistance network is resolved here for the first time (**Figure 3.5**). If such a gradient occurs along resistance networks in humans, it is masked by evaluating ROV based upon blood flow responses in the principal artery (e.g., brachial or femoral) supplying musculature in the active limb. Nevertheless, the overall correspondence of ROV kinetics between mice and humans supports the mouse as a model to gain mechanistic insight into how advanced age attenuates ROV. A key feature and unique advantage of observing the microcirculation directly is the ability to determine what happens where and when along the resistance networks that control muscle blood flow.

Attenuated ROV with advanced age and the effect of vessel branch order

Resting conditions. Our improved surgical approach enabled exposure of the inferior gluteal artery (the FA studied here) along with arteriolar networks embedded within the GM. Because FAs are external to the tissue, they are not directly affected by active (i.e. contracting) muscle fibers. Thus ROV in FA reflects ascending vasodilation initiated within the muscle fibers in response to muscle contraction. The ~1 s delay between peak ROV in proximal FAs (~4 s) compared to peak ROV in distal 3As (~3 s) strengthens this interpretation. Further, ROV occurs first in the smallest arterioles located furthest downstream (**Figures 3.2 and 3.5**), which in turn may reflect signals originating from terminal arterioles and capillaries (5, 12, 137, 148) most intimately associated with skeletal muscle fibers. Thus, dilatation of distal arterioles will promptly increase capillary perfusion while total flow increases as dilatation ascends the resistance network (139). The rapid

onset of vasodilation and its ability to ascend into FA are reminiscent of conducted vasodilation initiated via hyperpolarization of the endothelium (48, 141). Thus, ROV may entail activation of membrane ion channels in microvessels responding to muscle fiber contraction. Indeed, on likely signal for the initiation of ROV is membrane hyperpolarization of the microvessel wall through activation of K^+ channels (1, 29). At the earliest time point we resolved (1 s post-contraction), vasodilatation was blunted throughout networks of old mice compared to young mice. This effect of advanced age was most pronounced in FA (**Figure 3.3**). These data illustrate that advanced age delays ROV, particularly in proximal branches and lower contraction duration. Thus, the coupling between contractile activity and the rapid onset of vasodilation loses sensitivity with ageing, which points to a defect in the underlying signaling events. Supporting this conclusion are the reductions in peak ROV for each branch order at each contraction duration in old compared to young mice (**Figures 3.2 and 3.4**). Recent findings show that activation of K_{Ca} channels in the endothelium of old mice dissipated electrical signals through "leaky" membranes more effectively when compared to young (4 months) mice (9). In light of the present data, such an effect on electrical signaling would blunt the initiation of hyperpolarization and restrict conducted vasodilatation [as shown in the GM (6)] as well as ascending dilatation of FA. Further studies are required to resolve the role of the endothelium and of particular K^+ channels in the initiation of ROV and ascending vasodilation of FAs.

Nonselective manipulation of αARs. In the GM of young mice, stimulation of ARs with NA attenuated peak ROV across all branch orders and did so at a concentration (10^{-9} M) that had no effect on resting diameters (**Table 3.1**). This effect of "subliminal" stimulation

was greatest in proximal FA and 1A branches while nearly absent in distal 3A branches (**Figure 3.7**, *left panels*). This behaviour is consistent with the ability of distal branches to more readily escape from sympathetic vasoconstriction during muscle contraction when compared to proximal arterioles or FAs (54, 159) likely due to their being more intimately associated with active muscle fibers and vasodilator metabolites. In contrast, 10^{-9} M NA had no effect on ROV of vessels in the GM of Old mice under control conditions, suggesting that the attenuation of ROV (compared to young mice) was due to a preexisting level of αAR activation no less than that of 1 nM NA (**Figures 3.4 and 3.7**). However, nonselective inhibition of ARs with phentolamine improved peak ROV in old (but not young) mice and this effect was greater in proximal versus distal branches (**Figure 3.7**, *right panels*).

Previous studies implicating a role for αAR stimulation in the attenuation of ROV with advanced age (22, 75). The present data uniquely illustrate that ROV is inhibited to the greatest extent in proximal FA and 1A branches. Thus, restoration of ROV during αAR inhibition was greatest in FAs, which are positioned to control the total volume of blood flowing into the arteriolar networks regulating blood flow within the tissue. That FAs are a key site for restricting ROV during advanced age is consistent with blood flow in 2A branches remaining significantly lower in old compared to young mice despite no difference in 2A diameters or levels of dilatation during rhythmic contractions (75). The activation of αARs inhibits conducted (ascending) vasodilation of FAs (66, 160) and may well explain the attenuation of conducted vasodilation along arterioles in old mice (6). Such a conclusion is supported by the inability of vasodilation to spread from the active (inferior) to inactive (superior) region of the GM until αARs were inhibited by

phentolamine (105). In turn we suggest that constitutively enhanced SNA (38) and αAR stimulation (22, 75) during advanced age effectively restrict muscle blood flow by attenuating ascending dilatation and ROV of FAs.

Roles of α_1ARs and α_2ARs. In light of the nonuniform distribution of αAR subtypes along arteriolar networks of the mouse GM (106), finding that stimulation of αARs attenuated ROV in young mice while inhibiting αARs restored ROV in old mice led us to resolve the contribution of αAR subtypes for respective age groups. Thus, by addition to the superfusion solution, agents selective for stimulating α_1ARs (PE) versus α_2ARs (UK) were tested in young mice while agents selective for inhibiting α_1ARs (PZ) versus α_2ARs (RW) were tested in old mice, with the efficacy and selectivity of respective agents confirmed in previous studies (106, 145). To ensure that PE and UK were exerting effects, each was applied at a concentration (10^{-7} M) that just begins to elicit vasoconstriction (145). In young mice, stimulating either α_1ARs with PE or α_2ARs with UK attenuated ROV similarly. Across contraction durations, this effect was greatest in FAs and decreased as branch order increased, with negligible effect in 3A (**Figure 3.8**). In old mice, the inhibition of either α_1ARs or α_2ARs had similar effects on restoring ROV in FAs. However, in 1A branches only the inhibition of α_2ARs improved ROV, which is consistent with constriction to NA (i.e., the nonselective physiological agonist) being dominated by α_2ARs in this branch order of the GM (106). Unlike the ability of phentolamine to improve ROV in nearly all branch orders of the GM in old mice (**Figure 3.7**, *right panels*), neither of the selective αAR antagonists affected ROV in 2A or 3A branches (**Figure 3.9**). Thus, constitutive activation of either αAR subtype alone can attenuate ROV in these distal branches of GM networks in old mice.

SUMMARY AND PERSPECTIVE

The present findings illustrate that advanced age depressed ROV in all branch orders of resistance networks controlling blood flow to the mouse GM. In old mice, this effect was attenuated by the inhibition of αARs and recapitulated in young mice by stimulating αARs. The concentrations of αAR agonists and antagonists used in our experiments were based on finding them to have little or no effect on vessel diameters (106, 145). Our data thereby illustrate a subtle yet physiologically significant role for αARs in modulating ROV. While consistent with earlier findings of attenuated ROV with ageing in animals (75) and human subjects (22), this is the first study to identify where the effects of α_1ARs and α_2ARs predominate among branches of microvascular resistance networks. By stimulating the inferior gluteal nerve in anesthetized mice, contractions were restricted to the inferior region of the GM and thus avoided potentially confounding effects of central command (74). Further, our manipulations of αAR stimulation and inhibition were constrained to the GM by the addition of respective agents to the superfusion, thereby avoiding systemic effects and the possibility of evoking systemic cardiovascular reflexes. In such manner, our experimental paradigms emulate local infusion of αAR agonists and antagonists into the human forearm performing contractions of a relatively small muscle group (22, 37).

Unlike the human forearm, where αAR stimulation contributes to vasomotor tone in a manner that decreases with ageing (37), the level vasomotor tone in the mouse GM at rest is independent of αAR activation, nor were there consistent differences in resting or maximal diameters between age groups. Prior studies in humans have implied that functional sympatholysis is impaired during advanced age (39, 82). Consisted with this

interpretation, the present findings suggest that inhibition of ROV by αAR stimulation are exerted throughout the resistance network and vary with vessel branch order. Thus, attenuation of ROV is greatest in FAs due to constitutive activation of both αAR subtypes. Because FA are external to the muscle, these proximal vessels avoid the direct effects of active muscle fibers on promoting vasodilatation (i.e. functional sympatholysis) and thereby maintain peripheral resistance upstream from arteriole networks embedded within the muscle. In young mice, ROV of 2A and 3A branches is robust and these vessels readily escape the inhibitory effect of exogenous (1 nM) NA. In old mice, ROV in the same branches is attenuated due to constitutive stimulation of αARs. While this attenuation can be reversed pharmacologically, both αAR subtypes must be inhibited for the greatest effect. We conclude that a subtle level of αAR stimulation attenuates the ability of the resistance vasculature to respond rapidly to the onset of muscle contraction. In proximal branches, this effect will restrict the volume of blood entering the muscle, while in distal branches the attenuation of ROV can adversely affect blood flow distribution and capillary perfusion. These concerted effects help to explain the impairment in functional sympatholysis that is manifest during advancing age, which contributes to the difficulty in transitioning from rest to physical activity or to increase from moderate to more intense levels of exercise.

COMPETING INTERESTS

The authors declare no competing interests. The content of this article is solely the responsibility of the authors and does not necessarily represent the official views of the National Institutes of Health or the American Heart Association.

AUTHOR CONTRIBUTIONS

S.Y.S. and S.S.S conceived and designed the experiments. S.Y.S. performed the experiments in the laboratory of S.S.S. Both authors analyzed and interpreted the data. S.Y.S. prepared the figures and drafted the manuscript. S.S.S. edited the manuscript and figures. Both authors reviewed and approved the final version of the article for publication.

FUNDING SOURCES

S.Y.S. was supported by Predoctoral Fellowship 15PRE22840000 from the Midwest Affiliate of the American Heart Association. S.S.S. was supported by National Institutes of Health grants R01-HL086483 and R37-HL041026.

ACKNOWLEDGEMENTS

Dr. Michael J. Davis (University of Missouri) provided the software used for recording and analyzing the vasomotor responses in these experiments. Dr. Erika M. Boerman (University of Missouri) assisted in the analysis of perivascular innervation density.

	Young			Old		
	Control	Phentol	NA	Control	Phentol	NA
FA	38 ± 2	36 ± 3	38 ± 1	43 ± 3	42 ± 3	43 ± 3
1A	30 ± 2	29 ± 1	29 ± 1	34 ± 2	33 ± 2	34 ± 2
2A	20 ± 1	19 ± 1	2 0 ± 1	21 ± 1	20 ± 1	21 ± 1
3A	10 ± 1	9 ± 1	10 ± 1	9 ± 1	9 ± 1	9 ± 1

Table 3.1. Resting diameters are maintained during manipulation of αARs. Compared to Control, phentolamine (Phentol, 10^{-6} M) or noradrenaline (NA, 10^{-9} M) had no significant effect on resting diameters of any branch order in the GM of either young or old mice. Summary data are means ± S.E., n=6 per age group.

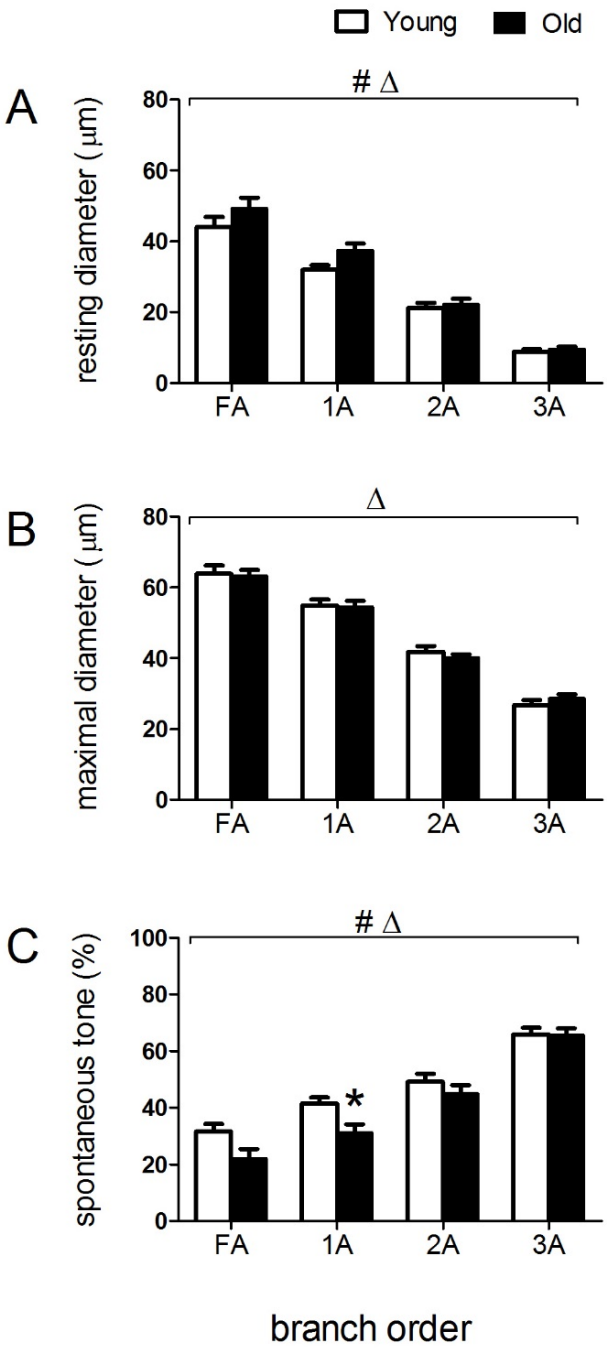

Figure 3.1. Internal diameters and spontaneous tone in GM feed arteries and arterioles are similar for young and old mice. Resting diameter (**A**) and maximal diameter (**B**) decreased as vessel branch order increased for both age groups (FA>1A>2A.3A). Spontaneous tone (**C**; see Methods) increased with vessel branch order. Summary data are means ± S.E., n=6 per age group. $^{\#}P<0.05$, main effect of age. $^{\Delta}P<0.05$, main effect of vessel branch order; $^{*}P<0.05$, old vs. young mice for designated branch order.

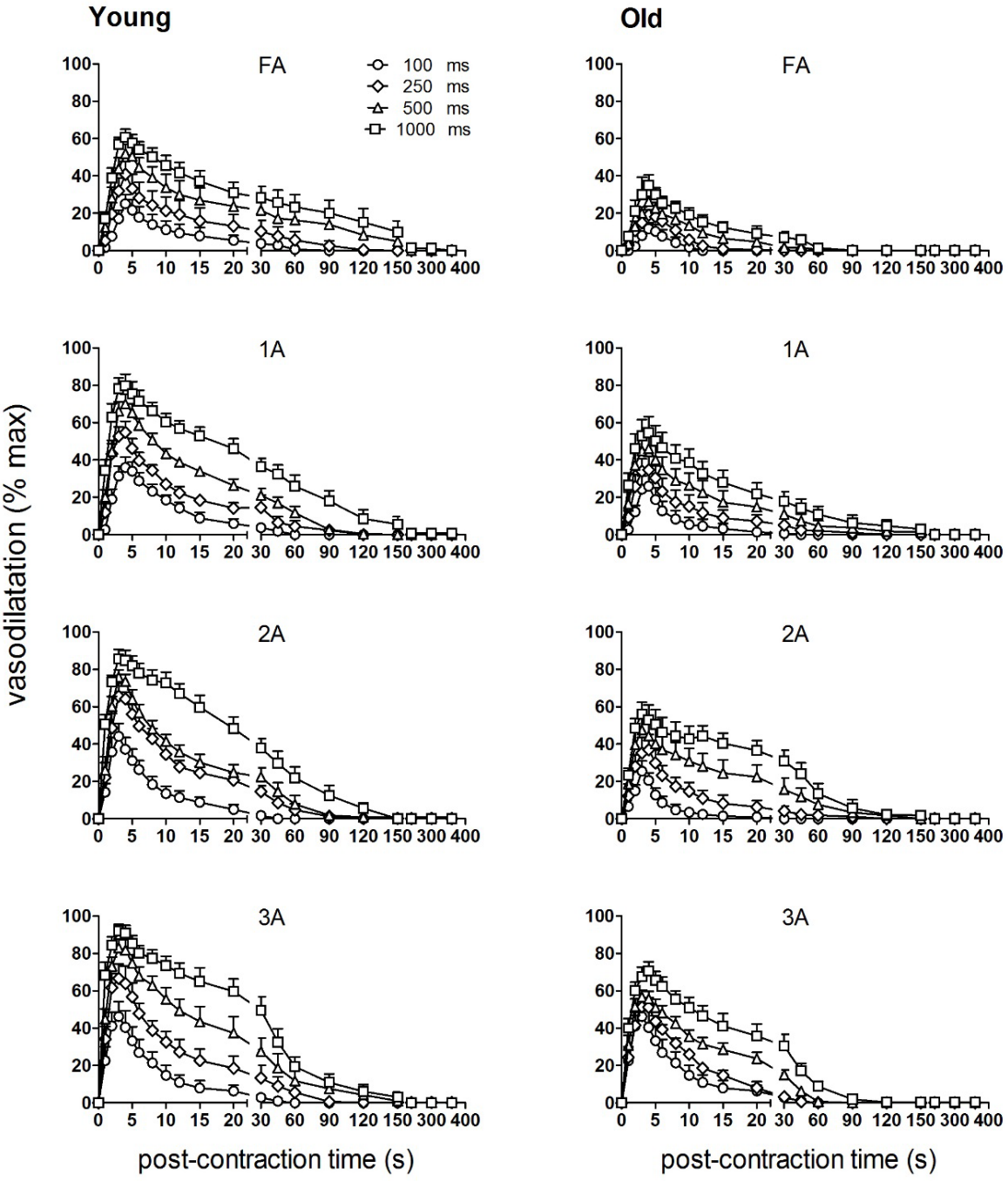

Figure 3.2. With similar time course, ROV is depressed throughout resistance networks of old versus young mice. For single tetanic contractions of 100, 250, 500, or 1000 ms duration (key applies to all panels), vasodilatation (expressed in relative terms as % max; see Methods) tended to increase with vessel branch order (FA<1A<2A<3A) and with contraction duration (100<250<500<1000 ms). Across branch orders, ROV was lower for GM in old compared to young mice. Summary data are means ± S.E., n=6 per age group.

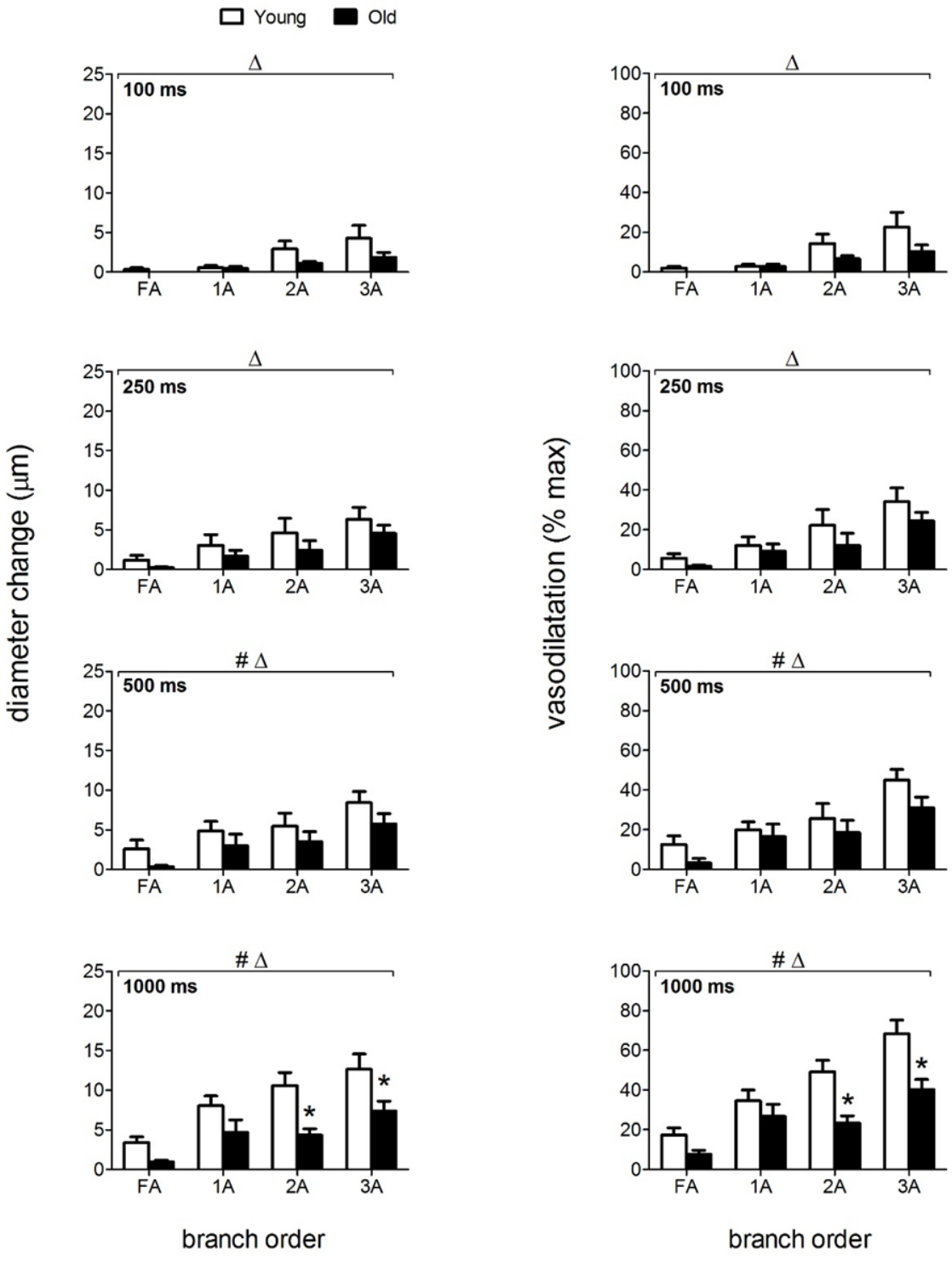

Figure 3.3. Initiation of ROV at 1 s post-contraction increases with contraction duration and branch order but is diminished with advanced age. Following each contraction duration, vasodilatation increased with branch order (FA<1A<2A<3A), whether expressed as absolute diameter change (μm, *left panels*) or relative responses (% max, *right panels*) at 1 s post-contraction. These initial responses were attenuated for all branch orders in GM of old mice compared to young mice. $^{\Delta}P< 0.05$, main effect of branch order; $\#P< 0.05$, main effect of age. $*P< 0.05$, old vs. young mice within respective branch order. Summary data are means ± S.E., n=6 per age group.

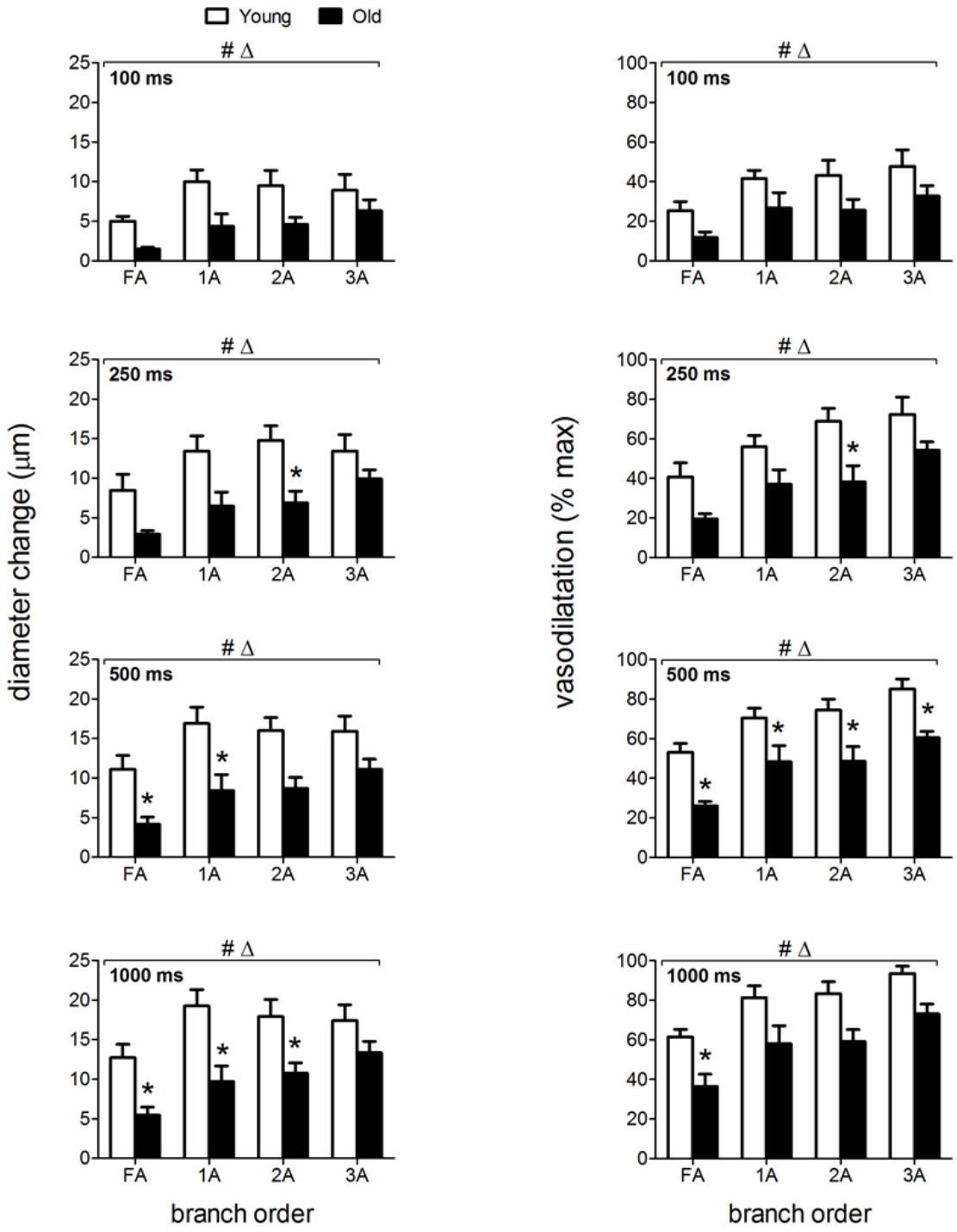

Figure 3.4. Peak ROV increases with contraction duration and branch order but is diminished with advanced age. Following each contraction duration, peak vasodilatation expressed as absolute diameter change (μm, *left panels*) was similar across branch orders while relative responses (% max, *right panels*) increased with branch order (FA<1A<2A<3A). Both absolute and relative peak ROV increased with contraction duration for all branch orders in both age groups, however Peak ROV was diminished consistently in all branch orders for old mice compared to young mice with the greatest effect in FA. $^{\Delta}P<$ 0.05, main effect of branch order; $^{\#}P<$ 0.05, main effect of age, $^{*}P<$ 0.05, old vs. young within respective branch order. Summary data are means ± S.E., n=6 per age group.

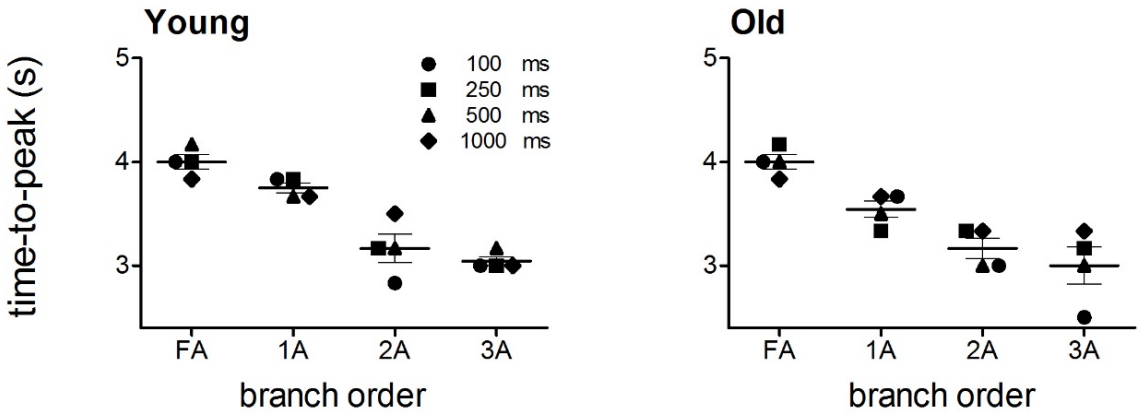

Figure 3.5. ROV peaks earlier in downstream branches of the resistance network. The time-to-peak for ROV decreased as branch order increased (FA>1A>2A>3A) in GM of both young mice (R^2=0.950) and old mice (R^2=0.986). For each branch order, the time-to-peak ROV was consistent across contraction durations for both age groups. Note lag between downstream 3A and upstream FA, particularly in old mice for 100 ms contraction. Each data point represents the mean value for given duration from n=6 mice; horizontal bar for each branch indicates mean time-to-peak across respective contraction durations.

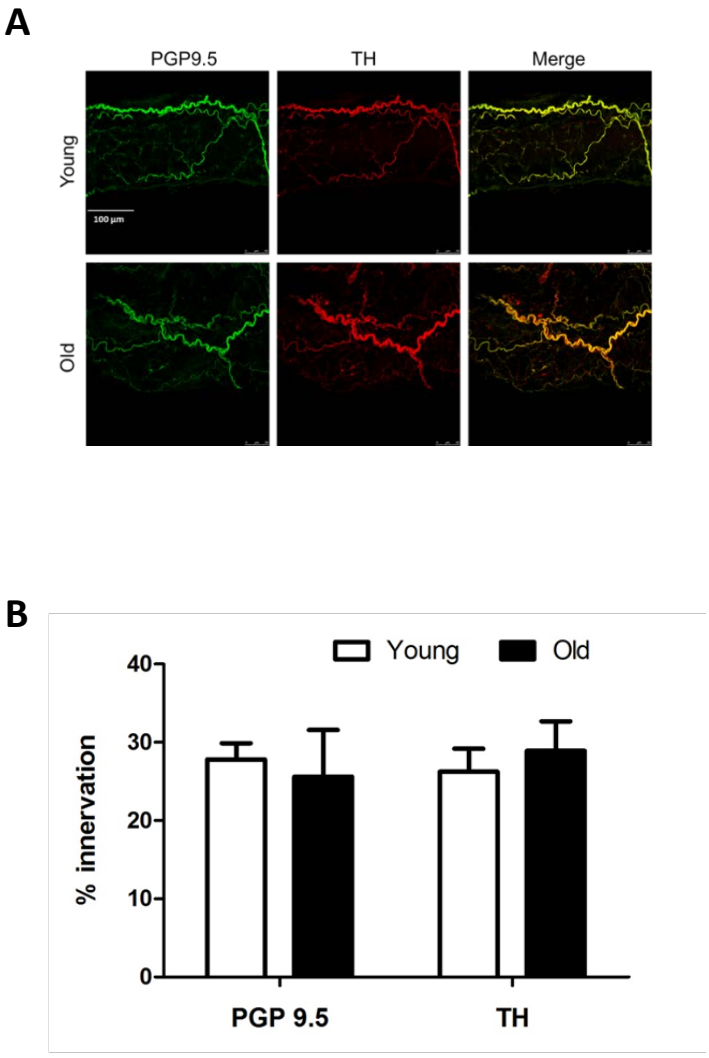

Figure 3.6. Sympathetic innervation of GM feed arteries for young and old mice. **A**. Representative immunofluorescent staining of all perivascular nerves (protein gene product 9.5, PGP9.5) and of sympathetic nerves (tyrosine hydroxylase, TH) in GM feed arteries of young and old mice. **B**. Innervation per vessel surface area (% innervation) for PGP9.5 and TH was not different between FA of young and old mice. Summary data are means ± S.E., n=4 per age group.

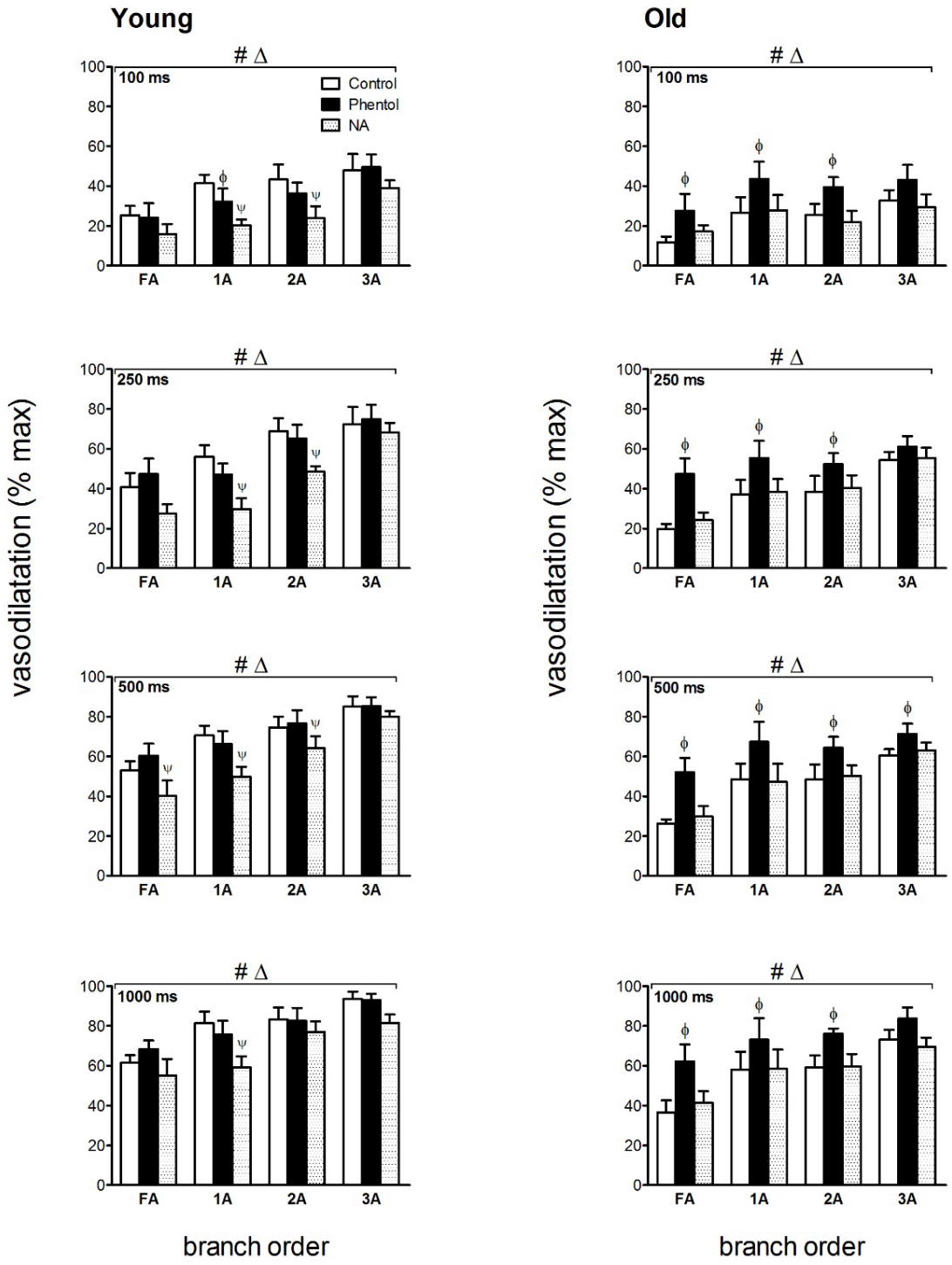

Figure 3.7. Differential modulation of ROV in GM branch orders by αARs in young versus old mice. Peak ROV (% max) in FA, 1A, 2A and 3A following 100, 250, 500 and 1000 ms contraction in the GM of young and old mice. Peak ROV increased as GM contraction duration increased in both age groups. Stimulation of αARs with NA (10^{-9} M) attenuated peak ROV in young but not in old. In contrast, inhibition of αARs with phentolamine (Phentol, 10^{-6} M) enhanced peak ROV in old but not in young. The effect of αAR modulation on peak ROV tended to be greater in FA and 1A than in 2A and 3A. $^{\Delta}P<0.05$, main effect of branch order. $^{\#}P< 0.05$, main effect of Phentol or NA. $^{\Psi}P< 0.05$, NA vs. Control in designated branch order. $^{\Phi}P< 0.05$, Phentol vs. Control in designated branch order. Summary data are means ± S.E., n=6 per age group.

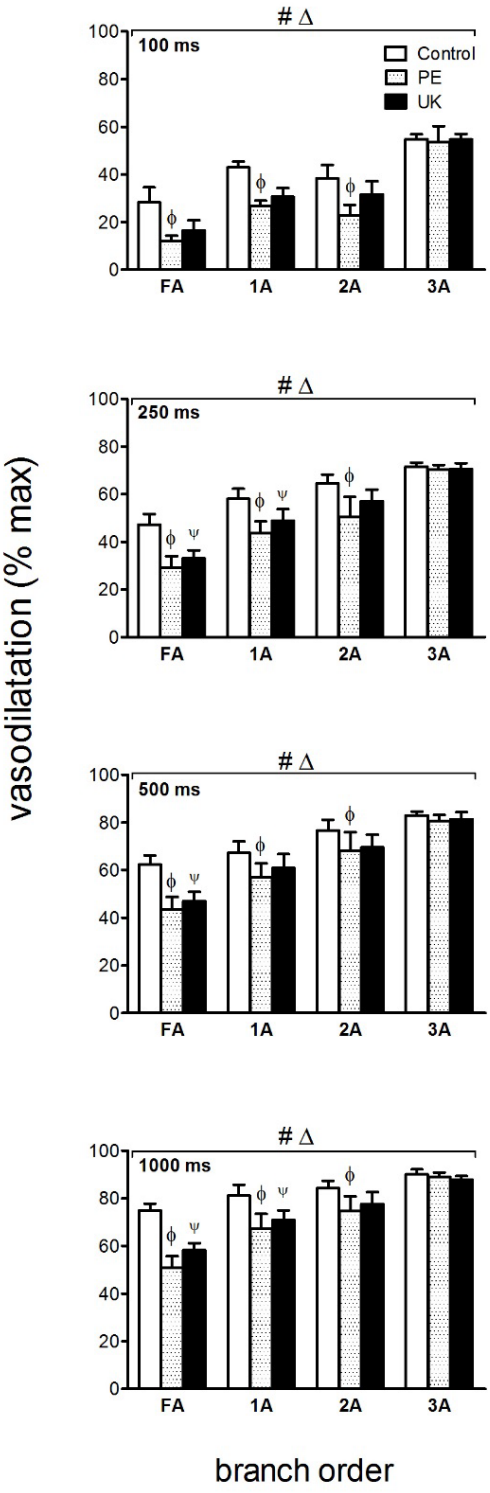

Figure 3.8. Selective activation of α_1ARs or α_2ARs attenuates ROV in upstream branches of GM in young mice. Peak ROV (% max) in FA, 1A, 2A and 3A following 100, 250, 500 and 1000 ms contraction in the GM of young mice. Across contraction durations, selective activation of α_1ARs (PE, 10^{-7} M) or of α_2ARs (UK, 10^{-7} M) attenuated ROV (% max) in FA, 1A and 2A but had no effect on ROV in 3A. $^{\Delta}P< 0.05$ main effect of branch order; $^{\#}P< 0.05$ main effect of treatment; $^{\Phi}P< 0.05$, PE vs. Control, $^{\Psi}P< 0.05$, UK vs. Control. Summary data are mean ± S.E. for n=6 young mice.

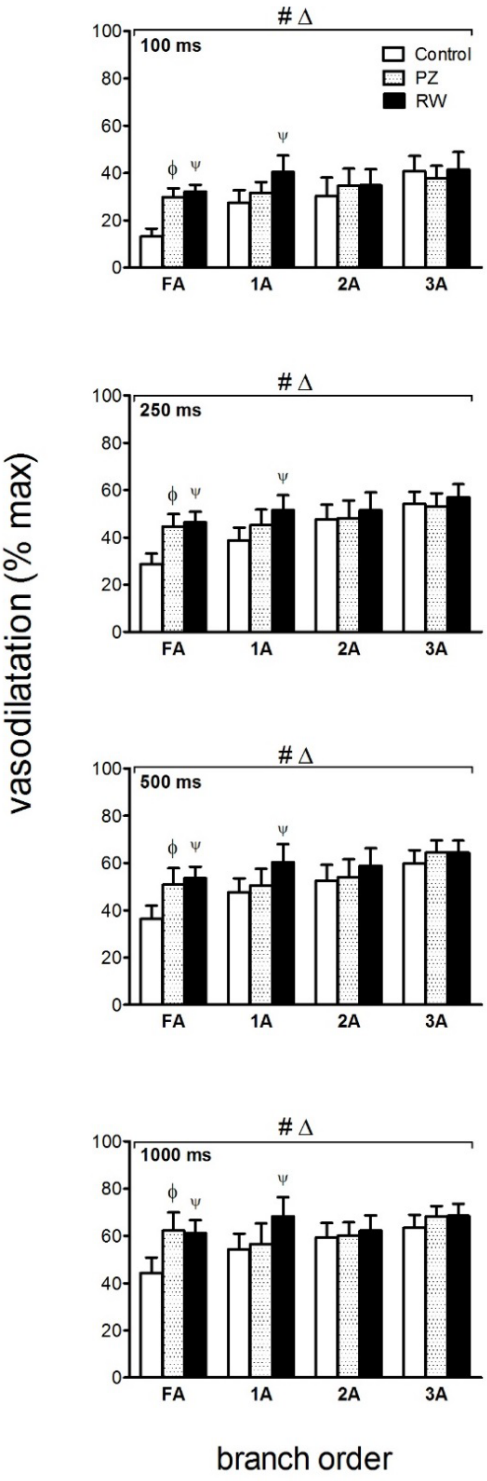

Figure 3.9. Selective inhibition of α_1ARs or α_2ARs improves ROV in upstream branch orders of GM in Old mice. Peak ROV (% max) in FA, 1A, 2A and 3A following 100, 250, 500 and 1000 ms contraction in the GM of old mice. Across contraction durations, selective inhibition of α_1ARs (PZ, 10^{-8} M) or of α_2ARs (RW, 10^{-7} M) improved ROV in FA while inhibition of α_2ARs improved ROV in 1A. However, selective inhibition of either αAR subtype alone had no effect in 2A or 3A. $^{\Delta}P< 0.05$ main effect of branch order; $^{\#}P< 0.05$, main effect of treatment; $^{\Phi}P< 0.05$, PZ vs. Control, $^{\Psi}P< 0.05$, RW vs. Control. Summary data are mean ± S.E. for n=6 old mice.

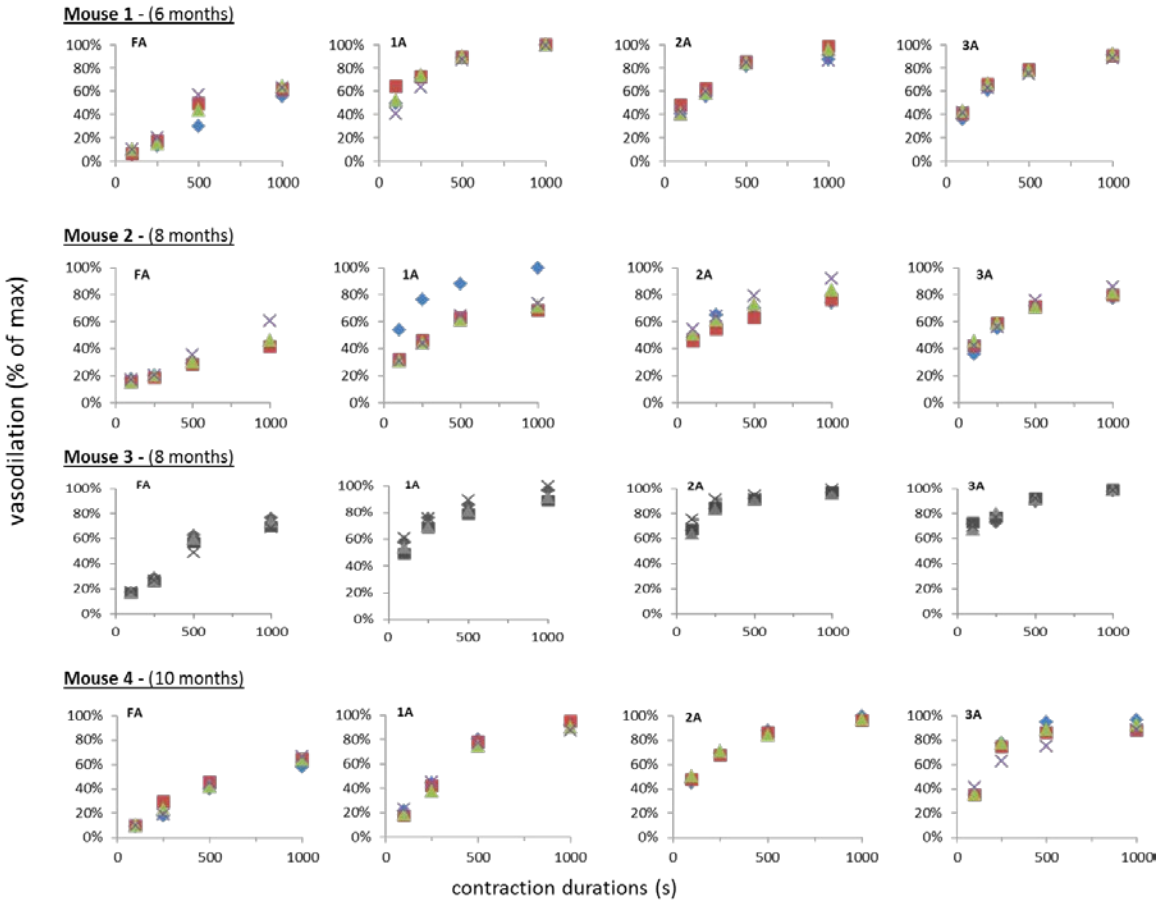

Supplemental figure 3.1 Time control study of ROV in GM. In 4 female C57BL/6 mice (6-10 months), electrical stimulation of motor nerves was applied and the peak ROV of all 4 vessel branch orders for 4 complete sets of stimulation protocols was recorded. Each panel represents the repeated vascular response from an animal; In each panel, each data point represent a ROV following a tetanic muscle contraction at a given branch order. With the sequence of contraction durations (100, 250, 500, 1000 ms) and observation sites (FA, 1A, 2A, 3A) randomized, the ROV response was highly reproducible and remained stable throughout the protocols.

CHAPTER 4

ROLE OF ENDOTHELIUM IN CONDUCTION AND INITIATION OF RAPID ONSET VASODILATION IN MOUSE SKELETAL MUSCLE

ABSTRACT

In response to contractile activity, ascending vasodilation (AVD) of proximal feed arteries (FAs) reflects signals initiated from arterioles embedded within active muscle fibers. We tested the hypothesis that the mechanism of AVD differs with the nature of skeletal muscle contraction. The resistance microvasculature supplying the gluteus maximus muscle (GM) of anesthetized male C57BL/6J mice (3-4 months old) was studied using intravital microscopy. Under control conditions, single maximal tetanic contraction (100Hz, 500ms) evoked rapid onset vasodilation (ROV) in FAs and primary (1A) arterioles (< 1s onset, $\leqslant$ 4s peak response). In contrast, during 4 Hz twitch contractions, FA and 1A dilations began after 10-15s and plateaued by 30s. Microiontophoresis of acetylcholine onto a 1A increased diameter locally and evoked conducted vasodilation of upstream FA. Light-Dye Treatment (LDT) disrupted the endothelium between 1A and FA and eliminated ROV in FA but not 1A. Nevertheless, FA dilated during rhythmic contractions until nitric oxide synthesis was inhibited (L-NAME; 10^{-4}M). In intact GM preparations, superfusion of UCL1684 (10^{-6}M) and TRAM34 (10^{-5}M) to block $K_{Ca}2.3$ and $K_{Ca}3.1$ channels attenuated ROV by ~half in proximal FA and 1A with negligible effects on arteriolar dilations downstream. Superfusion of L-NAME (10^{-4}M) and indomethacin (10^{-5}M) to inhibit NO and prostacyclin had little effect on ROV across branch orders. We conclude that ROV of FAs reflects

hyperpolarization initiated from endothelium in downstream arterioles and conducted along the endothelium. During rhythmic contractions, AVD reflects NO release from elevated shear stress during functional dilation of downstream arterioles, where metabolic vasodilator signaling prevails.

INTRODUCTION

Muscle blood flow increases immediately (<1s) at the onset of exercise (109, 144, 157) and plateaus at a steady state according to the level of sustained contractile activity (24). Rapid onset vasodilation (ROV) can be evoked in response to a single muscle contraction (1, 29, 30, 102, 105, 161) and initiates hyperemia, followed by a steady-state vasodilation (SSV) that sustains the elevation in blood flow (23). Coordinated vasodilation among all branch orders of the microvascular resistance network, including proximal feed arteries (FA) and primary arterioles (1A) along with downstream [e.g., second (2A)- and third (3A)-order] arterioles is essential for muscle blood flow to increase in accord with local metabolic demands (24, 138). Because they are located external to muscle fibers, feed arteries (FAs) do not receive direct stimulation from active muscle fibers. Instead, dilation of FA reflects “ascending vasodilation” (AVD) that originates in the downstream arterioles embedded within the active muscle fibers (141). The mechanism(s) underlying AVD during ROV and SSV remain unclear, as do the respective vasodilator signals initiating these responses in downstream arterioles.

The endothelium has come to be recognized as an integral mediator of vasomotor control in response to muscle contractions (80). For example, rapid electrical signaling in response to endothelium-derived hyperpolarization (56)] is attributable to the conduction of the signal from cell to cell along the endothelium (8, 10). Thus, the endothelium is the apparent pathway for conduction of vasodilation induced by acetylcholine (ACh) (48, 140) and AVD in response to skeletal muscle contraction (141). In downstream arterioles embedded within the muscle, there are redundant stimuli for vasodilation that include substances released during muscle contractions. These substances include vasodilator metabolites such as adenosine, ATP and K^+ (13, 24) as well as changes in pO_2, pCO_2 and pH associated with exercise hyperemia (60, 80, 149). Many of these "classic" vasodilators can exert their effects through endothelium dependent vasodilation through stimulating the release of autacoids [e.g., nitric oxide (NO) and prostaglandins (mainly PGI_2)] or electrical signaling via EDH initiated by the activation of small ($K_{Ca}2.3$,)- and intermediate ($K_{Ca}3.1$)-conductance Ca^{2+}-activated K^+ channels (17, 26, 51, 72). While the inhibition of autacoids in humans performing rhythmic knee extensions attenuated hyperemia reflecting SSV (16), such interventions did attenuate ROV to single contractions of the forearm (29). Thus, distinct signaling pathways are apparent that may vary with the nature of muscle contraction. Recent evidence implicates a role for K^+ (29) in ROV and the genetic deletion of $K_{Ca}2.3$ impaired arteriolar ROV in mouse cremaster muscles (103). Collectively, these findings from studies of humans and animals support an integral role for the endothelium in exercise hyperemia.

In the current study, we utilized intravital microscopy to study intact microvascular resistance networks of the mouse gluteus maximus muscle (GM). By manipulating

electrical stimulation of the inferior gluteal motor nerve to evoke single tetanic maximal contractions (75, 105) or moderate rhythmic twitch contractions (6, 75), we were able to elicit either ROV or SSV, respectively. Our surgical approach enabled exposure of the inferior gluteal FA (145) and to thereby evaluate AVD as well as dilation in downstream arterioles of the same GM preparations *in vivo*. Conduction of vasodilator signals along the endothelium was tested using light-dye treatment (LDT) to selectively damage the endothelium (3, 18, 141) at an anatomically defined site located midway between a FA and 1A. Selective pharmacological interventions were performed to resolve the role of EDH and ion channel activation ($K_{Ca}2.3$ + $K_{Ca}3.1$) vs. autacoids (NO and prostaglandins). To gain insight into signals governing muscle blood flow regulation at the onset of exercise vs. sustained activity from the perspective of regional differences in vasomotor control within the resistance network (138), we tested the hypothesis that the mechanism of vasodilation differs with the nature of skeletal muscle contraction.

METHODS

Animals: Experimental protocols were approved by the Animal Care and Use Committee of University of Missouri. C57BL/6 male mice from Jackson Laboratory were anaesthetized by intraperitoneal injection of pentobarbital sodium (60mg/kg), and supplemented as needed (20mg/kg) by checking the toe withdraw and pupil reflex every 15 min to maintain anesthesia for the duration of each experiment.

Intravital gluteus maximus muscle preparation: After shaving the skin of surgical area overlying the left GM, the mouse was placed in a prone position on a heating plate with body temperature maintained at 37°C. Viewing through a stereomicroscope, the skin overlying the left GM was carefully removed. With the exposed tissue superfused continuously with bicarbonate-buffered physiological salt solution (PSS, 3 ml/min, 35°C, pH 7.4, equilibrated with 5% CO_2 and 95% N_2), the left GM was carefully dissected away from its the lumbar fascia and iliac crest. The muscle was reflected away from the hindquarter and spread over a transparent rubber pedestal (Sylgard 184, Dow-Corning; Midland, MI, USA) with the edges pinned to approximate *in situ* dimensions. The entire microvascular resistance network was thereby exposed (145), including the FA (i.e., the inferior gluteal artery before it enters the muscle), which becomes the 1A upon entering the muscle, and the downstream 2A and 3A branches **(Figure 4.1)**. The inferior gluteal motor nerve bundle was then carefully isolated and cut proximally to leave a stump that was aspirated into an insulated borosilicate glass microelectrode filled with PSS (105). The interface between the electrode and surrounding tissues was sealed with Kwik-Cast Sealant (World Precision Instruments Inc, Sarasota, FL, USA).

Imaging: The completed GM preparation was transferred to the fixed stage of an intravital microscope (Nikon E600FN; Melville, NY) mounted on an X-Y translational stage (Gibraltar; Burleigh Instruments, Fishers, NY). A FireWire color charge-coupled device camera (DFK 21AF04; The Imaging Source, Charlotte, NC) acquired the image at 30 frames/s through a Nikon SLWD X20 objective (numerical aperture =0.35). The image was displayed onto a personal computer monitor with spatial resolution of ~1 µm calibrated with a stage micrometer. Digital images were recorded at 30 frames per second (fps) using

LabView software (National Instruments, Austin, TX) provided by Dr. Michael J. Davis (University of Missouri). The preparation was equilibrated for 30 min before beginning data acquisition. Respective vessel branch orders were studied in each GM preparation as described below. Prior to beginning motor nerve stimulation, a map of the resistance network was drawn and observation sites were identified for each vessel branch with reference to anatomical landmarks.

Motor nerve stimulation: The motor nerve was stimulated (30V, 0.1ms pulses) at 10-fold greater voltage than the threshold determined for evoking a muscle twitch to evoke GM contractions. The nature of muscle contraction was controlled as follows. A stimulus train of 100Hz for 250 or 500 ms duration induced single tetanic contractions that evoked ROV. For SSV, rhythmic twitch contractions were evoked at 4Hz for 30s. For each stimulation, recording was initiated prior to the onset of contraction and maintained throughout recovery to resting diameter. The order in which respective branches were studied was randomized across experiments. In preliminary time controls (n=4; **Supplemental Figure 3.1**), we performed electrical stimulations and recorded vasomotor responses of all 4 vessel branch orders for 4 complete sets of stimulation protocols to confirm that vasomotor tone recovered and remained stable throughout criterion protocols.

Light-dye treatment: Fluorescein isothiocyanate conjugated to dextran (FITC-Dextran, 70 kDa) was injected retro-orbitally (168) into the systemic circulation to reach a final plasma concentration of ~2 mg/ml by estimating blood volume as ~10% of body weight (122). This concentration has been used in previous studies, and was verified with the in vitro studies of erythrocytes photohemolysis. The hemolysis was completed within 7 min

which is a reasonable time frame for our purpose of selective damage of endothelium in vivo (Supplemental Figure 4.1). The site where FA enters into muscle fibers and becomes the 1A **(Figure 4.2)** was illuminated (excitation, 460-500 nm) using a mercury arc lamp through a Nikon SLWD X20 objective (numerical aperture =0.35), thereby restricting damage to a ~300 µm segment. Photon intensity was ~0.3 mW (PM100D, Thorlabs Inc., Newton, NJ, USA). Preliminary experiments established that a 7-9 min period of illumination damaged ECs within the site of illumination while preserving the integrity of surrounding smooth muscle cells (SMCs).

Microiontophoresis: For each experiment, successful disruption of ECs was tested through by local delivery of the endothelium-dependent vasodilator ACh or the SMCs agonist phenylephrine (PE) using micoiontophoresis at the site of LDT. Loss of dilation to ACh confirmed disruption of the endothelium, while maintenance of constriction to (PE) confirmed the integrity of SMCs (3). A borosilicate glass micropipette (~1 µm tip ID) was filled with 1M ACh or 1M PE and secured in a holder mounted in a micromanipulator. A silver wire (diameter, 0.010”) inserted into the micropipette was connected to the positive terminal of a microiontophoresis programmer (Model 260, World Precision Instruments (WPI); Sarasota, FL, USA), where a retain current of 400 nA prevented leakage of ACh. For the reference electrode, a second silver wire was secured at the edge of the GM and immersed in the superfusion solution. With the tip of the micropipette positioned adjacent to the site of LDT, the criterion stimulus was delivered using positive current (1000 nA, 1s pulse) to eject ACh or PE; respective agents are positively charged in solution.

Pharmacological treatment: All pharmacological agents were dissolved in PSS and superfused over the entire GM preparation. Indomethacin (10^{-5}M) and L-NAME (10^{-4}M) were applied to inhibit release of prostaglandins and nitric oxide, respectively. The synthetic ion channel antagonists UCL1684 (10^{-6}M) and TRAM 34 (10^{-5}M) were applied to block $K_{Ca}3.1$ and $K_{Ca}2.3$ channels, respectively. The order of treatments was rotated across experiments. To evaluate the impact of NO during SSV, L-NAME (10^{-4}M) was also applied following LDT. At the end of each experiment, maximal vasodilation was induced by 10^{-4}M sodium nitroprusside (SNP) superfusion.

Experimental Protocols

Light Dye Treatment: Vasodilation to GM contractions and ACh microiontophoresis were observed downstream in the 1A and upstream in the FA before and following LDT at a site midway between respective segments; i.e., where the FA enters the GM to become a 1A (**Figure 4.2**). First, ROV and SSV were evaluated in respective branches under control conditions. Next, ACh was delivered onto the 1A at ~500 µm downstream from where LDT was to be performed. The response to ACh was observed locally at the site of stimulation and in the FA ~500 µm upstream from the site of LDT (i.e., 1000 µm upstream from the ACh micropipette; **Figure 4.3**). The FITC-dextran was then injected and the ACh micropipette was repositioned to the site of LDT. The local response to ACh was evaluated then LDT was performed. The local response to ACh was re-evaluated to confirm endothelial damage and the ACh micropipette was replaced with a PE micropipette to evaluate the response of SMCs at the LDT site. Responses of the 1A and FA to tetanic (ROV) and rhythmic (SSV) contractions were re-evaluated, as were local and conducted

responses to ACh delivered at the 1A downstream. In separate experiments, L-NAME was added after determining the effect of LDT to evaluate any contribution of NO (**Figure 4.4**).

Pharmacological combinations: In each branch of the network (FA, 1A, 2A, and 3A; **Figure 4.1**) ROV and SSV in were recorded under control conditions. The combination of indomethacin (10^{-5}M) + L-NAME (10^{-4}M) was then superfused to inhibit the synthesis of autacoids (NO and prostaglandins) or the combination of UCL1684 (10^{-6}M) + TRAM 34 (10^{-5}M) were superfused to block electrical signaling (EDH) through $K_{Ca}2.3$ and $K_{Ca}3.1$ channels (i.e., "K_{Ca}") (19, 56). Respective concentrations of UCL and TRAM were confirmed to inhibit hyperpolarization to ACh in endothelial tubes isolated from skeletal muscle feed arteries (E. Behringer, unpublished). Following 20 min equilibration, ROV and SSV were re-evaluated in each vessel branch during continuous superfusion of respective antagonists. The complementary pair of inhibitors was then added to the superfusion solution so that all 4 agents were present and equilibrated for 20 min then ROV and SSV were evaluated a final time throughout the network. Thus, each pair of inhibitors was studied alone and in combination with the second pair of inhibitors (**Figure 4.6**). The same protocol was also used to evaluate its effects on concentration-response curves to ACh (**Figure 4.7**). The order of respective treatment combinations was varied across experiments. At the end of the day's experiments, the preparation was superfused with 10^{-4} M sodium nitroprusside (SNP) to obtain maximal internal diameter (IDmax) at each site of observation.

Data acquisition: Following the 30 min equilibration, resting internal diameter (IDrest) was recorded for FA, 1A, 2A and 3A using a video caliper integrated with the software.

Vasomotor responses were recorded under each of the conditions described respective protocols and the IDresponse of each vessel branch was measured at designated time points during playback of the video recordings. To facilitate comparisons among respective branch orders having different resting and maximal diameters, vasodilation was normalized to maximal change in diameter during superfusion with 10^{-4}M SNP. Thus, vasodilation (% maximal response) = (IDresponse-IDrest)/(IDmax-IDrest) X 100% (145). The magnitude of ROV was quantified as the peak vasodilation attained following a given tetanic contraction. The magnitude of SSV was quantified during the plateau of the steady-state response during rhythmic muscle contractions. Only preparations with robust spontaneous vasomotor tone were included in data analysis (145).

Statistics: The effects of LDT at the site of illumination were analyzed using repeated 1-way ANOVA with Tukey tests performed for post-hoc comparisons. Differences in vasodilation among vascular branch orders with respect to the effects of LDT or pharmacological treatments were analyzed using 2-way ANOVA with Bonferroni tests for post-hoc comparisons. Summary data are presented as means ± S.E. Differences were accepted as statistically significant with $P < 0.05$.

RESULTS

Selective disruption of endothelium. In GM resistance network, the FA is external to the muscle while arterioles are embedded within the muscle fibers (**Figure 4.1**). Microiontophoresis of ACh at the site where a FA enters the GM and becomes the 1A

(**Figure 4.2A**) evoked an instant vasodilation. After performing LDT to disrupt the endothelium, an identical ACh stimulus no longer evoked a response. Nevertheless, microiontophoresis of PE at the same site constricted the FA by ~40% while superfusion of SNP dilated the FA by similar amount, confirming the integrity of surrounding SMCs (**Figure 4.2B**).

Conducted vasodilation to ACh is blocked by LDT. Microiontophoresis of ACh onto the 1A at ~500 µm downstream from the site of LDT (**Figure 4.3A**) evoked vasodilation at the site of stimulation and this response conducted upstream into the FA recorded ~500 upstream from the site of LDT. After LDT, local vasodilation of the 1A in response to ACh was maintained; however conducted vasodilation no longer occurred in the FA upstream from the site of endothelial damage (**Figure 4.3B**). Nevertheless, superfusion with SNP evoked maximal dilation at respective sites.

Rapid onset vasodilation in FA is blocked by LDT. Stimulation of the GM motor nerve to evoke a tetanic contraction (100 Hz, 500 ms) resulted in ROV of 1A and FA (**Figure 4.4A**). After LDT, ROV was maintained in 1A but was abolished in FA. Nevertheless, both sites dilated maximally in response to SNP.

Steady state vasodilation of FA remained intact following LDT until inhibition of NO production. In contrast to ROV, dilation of FA in response to 4Hz contractions was not affected by LDT. As observed under conditions, SSV began within 10-15s after initiating contractile activity and plateaued by 30s in all branches. However, when L-NAME was added following LDT, vasodilation was maintained in 1A but abolished in FA.

Vasomotor tone and the effect of pharmacological interventions. Resting IDs decreased as branch order increased from proximal FA to distal 3A, as did maximal diameters (**Figure 4.5**). All branch orders exhibited robust spontaneous vasomotor tone that increased with branch order (from 40% in FA to 60% in 3A). Equilibration with either I+L (to inhibit autacoids) or T+U (to inhibit K_{Ca}) constricted FA significantly, as did the combination of I+L+T+U (**Table 4.1**). For 1A, only the combination of all 4 agents produced a significant constriction. In contrast, resting diameters of 2A and 3A were relatively unaffected by any of these agents. Thus, resting tone was enhanced only in proximal vessels during inhibition of respective signaling pathways.

Effects of pharmacological interventions on endothelium dependent vasodilation. To evaluate the contribution of endothelium-derived autacoids (NO + prostaglandins) or K_{Ca} in mediating vasodilation to ACh, concentration-response curves were evaluated in the presence of respective inhibitors relative to control (**Figure 4.6**). In FA, inhibiting either autacoids (with I+L) and/or K_{Ca} channels (with T+U) shifted the ACh concentration-response curves 1-2 log units to the right and their combined inhibition had the greatest effect. In downstream arterioles, inhibition of autacoids also shifted the ACh response curves to the right though K_{Ca} inhibition had negligible effect. The ~100% efficacy of vasodilation with 10^{-5}M ACh was attenuated only in 3A when all 4 inhibitors were present (**Figure 4.6**). Under these conditions, 10^{-4}M ACh was able to evoke 100% dilation of 3A in the presence all inhibitors (data not shown).

Effects of pharmacological interventions on ROV. A single tetanic contraction evoked ROV in all branch orders (**Figure 4.7**). Under control conditions, ROV was manifest within

1s post-contraction and attained peak values within 4s in all vessel branches; response amplitude increased with branch order and was ~10% greater following 500 ms compared to 250 ms contraction duration. In proximal FA and 1A, inhibition of K_{Ca} (with T+U) attenuated ROV to a greater extent than did autacoid inhibition (with I+L) while the combination of all 4 inhibitors had the greatest effect. In distal 2A and 3A, respective treatments produced more subtle attenuation and delay of ROV (**Figure 4.7**). For either contraction duration, evaluating ROV at 1s post-contraction illustrates the trend for a diminished initial response in the presence of respective inhibitor combinations, particularly in proximal FA and 1A (**Figure 4.8**). The time-to-peak for ROV decreased as branch order increased (FA>1A>2A>3A, $P<0.05$) for both contraction durations, indicating that vasodilation occurred earlier in more distal branches. In the presence of all inhibitors, ROV was delayed such that the time-to-peak nearly doubled (**Figure 4.9**).

To evaluate the role of autacoids and K_{Ca} on the amplitude of ROV, we compared peak ROV across vessel branch orders before and during respective pharmacological interventions. Peak ROV increased with contraction duration ($P<0.05$). **Figure 4.10,** *left vs. right panels*). With either contraction duration, peak vasodilation increased with branch order from FA to 3A. Superfusion of T+U attenuated peak ROV in proximal FA and 1A following both 250 ms and 500 ms tetanic contractions, whereas I+L had no significant effect. The combination of I+L+T+U had the greatest effect in FA, with ~65% attenuation following 250 ms contractions. In downstream 2A and 3A, peak ROV was unaffected by respective pharmacological treatments.

Subtle effect of pharmacological interventions on SSV. Following LDT, L-NAME superfusion abolished SSV in FA during rhythmic contractions (**Figure 4.4B**). For intact resistance networks, superfusion of I+L or T+U had no effect on SSV in any branch order (**Figure 4.11**). The combination of I+L+T+U tended to decrease SSV in FA and 1A but this effect was not significant.

DISCUSSION

In response to contraction of the mouse GM skeletal muscle, all branch orders of resistance vessels dilated coordinately to enable the increase in blood flow and fulfill muscle metabolic needs. By evoking contractions that differ in nature in mouse GM (e.g., single tetanic contraction vs. rhythmic twitch contractions), the ensuing ROV and SSV represent the vasodilator events that occur at exercise onset and during sustained activity, respectively. Application of LDT to selectively disrupt the endothelium segment between FA and 1A blocked conducted vasodilation of FA initiated by local stimulation of the downstream 1A with ACh microiontophoresis. In contrast, SSV of the FA during twitch contractions was not affected by LDT however the inhibition of NO synthase following LDT was effective in preventing FA dilation during rhythmic contractions. In the intact resistance network of the GM, inhibition of EDH through selective $K_{Ca}2.3$ and $K_{Ca}3.1$ blockers significantly attenuated peak ROV in upstream FA and 1A yet had only subtle effects in downstream 2A and 3A; blockade of autacoids (NO and prostacyclin) had little effect on peak ROV across all vascular branch orders. Remarkably, simultaneous inhibition of NO, prostacyclin and EDH significantly attenuated the onset of ROV and delayed the

peak response across all vascular branch orders. In contrast, neither EDH nor autacoid inhibition attenuated SSV, though the combination of blocking EDH, NO synthase and prostacyclin production tended to decrease SSV in proximal vessels. The present findings thereby resolve distinct mechanisms of AVD for ROV compared to SSV for brief tetani compared to sustained rhythmic contractions. Thus, ROV in FA following tetanic contraction reflects conducted vasodilation along the endothelium initiated by EDH in downstream arterioles, while SSV of FA during continuous rhythmic contraction is mediated by NO release. Consistent with classic findings, additional vasodilator signaling prevails in downstream arterioles to ensure that muscle oxygen supply meets the metabolic needs of active muscle fibers.

Role of the endothelium in conducted vasodilation

Endothelial cells are oriented longitudinally along the axis of FA and arterioles, with abundant homocellular gap junctions expressed between neighboring cells (62, 97, 131). These structural properties explain why the endothelium is the favored pathway for conducting vasodilation along resistance vessels and, in turn, to relax surrounding SMCs rapidly through myoendothelial coupling via heterocellular gap junctions (47). In contrast, SMCs have circumferential orientation and lack effective SMC: SMC coupling through gap junctions (36, 63, 97). In FAs from hamster retractor muscle (48) and arterioles of mouse cremaster muscle (97), selective disruption of endothelium with LDT blocked conducted vasodilation to ACh beyond the site of damage, while the effect of selective SMC damage on conducted vasodilation was negligible (48). In the current study, LDT was used to interrupt the endothelium as a conduction pathway between the FA external to

muscle fibers and downstream arterioles embedded within muscle fibers (**Figure 4.2**). For this purpose, LDT could be performed anywhere along the FA. For example, in hamster retractor muscle with relatively long FA segments (several mm) located external to muscle fibers (141). However, applying LDT *in vivo* with the mouse GM preparation was more difficult anatomically due to the much shorter segment of FA that could be exposed (⩽1 mm) . Thus, LDT was performed at the transition of the FA into the 1A to ensure that a long enough segment of FA (>500 μm) was visible for vasomotor studies *in vivo*. Following selective disruption of the endothelium at the designated site, there was no longer vasodilation in response to local delivery of ACh, while SMCs remained able to contract and relax to PE and SNP, respectively (**Figure 4.3**). Consistent with earlier observations, the present data confirm that conducted vasodilation along the wall of FA in skeletal muscle relies on integrity of endothelium, but not SMCs (48, 141).

Conduction of ROV along endothelium

Light-dye treatment enables disruption of the endothelium within a defined segment of a vessel as determined by the presence of fluorescein within the vessel lumen (constrained to the vascular compartment by conjugation to 70-kDa dextran) and the optics of illumination (3, 48). In the present experiments, disruption of the endothelium within a ~300 um segment located midway proximal FA was confirmed to be selective for ECs (**Figure 4.2**) and to inhibit conducted vasodilation to ACh (Figure 4.3), which requires integrity along the entire vessel to provide cellular pathway for conducting hyperpolarization and, thereby, vasodilation (48). As substantiated by these controls, the selective elimination of ROV in proximal FA shown here (Figure 4.4) is the first

demonstrate that ROV of FA reflects conduction of an electrical signal along the endothelium in response to skeletal muscle contraction. However, this is not the first study to address the coupling of endothelium conducted vasodilation and muscle contraction. An earlier study in hamster retractor muscle found that LDT prevented vasodilation evoked by muscle contractions in response longer periods (60-100s) of stimulus trains (400–800 ms @ 40–70 Hz, 0.5 Hz) quite different from those used here (141). Moreover, these previous experiments did not resolve AVD from SSV, which was a key goal of the present study. Nevertheless, respective findings are consistent in supporting a key role for conduction along the endothelium in coordinating vasodilation among proximal and distal branches of the resistance network – particularly at the onset of contractile activity. In such manner, the increase in blood flow is able to peak rapidly (within 4s, **Figure7**). It is reassuring to note that these temporal dynamics are remarkably similar to those recorded in human subjects performing single contractions of the forearm (Carlson et al., 2008; Casey & Joyner, 2012; Crecelius et al., 2013) or knee extensors (Credeur et al., 2015).

In our preceding experiments (Sinkler and Segal, 2016; *Chapter 3*), we resolved the temporal pattern of ROV across respective vascular branch orders in GM and found that only the most distal branches initiated ROV with the shortest contraction duration (100 ms) and that with longer durations (e.g, 500 ms as used here), peak ROV was attained more rapidly (2-3 s) in 2A and 3A than in proximal 1A and FA (3-4s). A similar distal-to-proximal gradient in onset was observed in the present study as well (**Figure 4.9**). Taken together, these data illustrate that ROV is initiated in downstream arterioles and then conducted into proximal vessels. A corollary to this finding is that ROV is not initiated at the level of FA, which is located external to muscle fibers and thereby avoids direct

exposure to vasodilator signals from active muscle fibers. Because SMCs remained intact following LDT while ROV of FA was abolished, the present data further exclude SMCs as an effective pathway for AVD in response to brief tetanic contractions of skeletal muscle. Whether the endothelium initiates ROV within the intramuscular arteriolar networks is addressed below.

Endothelial signaling and vasodilation in GM resistance networks

Endothelium dependent vasodilation with ACh. Relaxation of SMCs during endothelium dependent vasodilation is mediated by 2 primary signaling pathways: release of autacoids [NO and prostaglandins (particularly prostacyclin, PGI_2)] and electrical coupling through gap junctions (17, 26, 51, 72), with EDH initiated through activation of $K_{Ca}2.3$ and/or $K_{Ca}3.1$ (19, 56). In cannulated mouse cremaster arterioles concentration-response curves to ACh showed a modest shift to the right following superfusion of indomethacin (10^{-5}M) + L-NAME (10^{-4}M), however maximal vasodilation was maintained until K_{Ca} inhibitors (apamin and charybdotoxin) were added to the superfusate (118). Thus, EDH appeared to be the predominant mechanism of endothelium dependent vasodilation in cremaster arterioles. In the current study, we chose the synthetic inhibitors [UCL1684 and TRAM 34] instead of apamin and charybdotoxin because of their smaller size and greater lipophilicity, thereby facilitating access to microvessels imbedded within the striated muscle fibers of the GM. Combined superfusion of indomethacin (10^{-5}M) + L-NAME (10^{-4}M) as well as combined superfusion of UCL1684 (10^{-6}M) + TRAM 34 (10^{-5}M) over the entire *in vivo* GM network, caused a significant shift to the right of concentration-response curves to ACh in FA and 1A and this effect of indomethacin + L-NAME extended into

distal 2A and 3A. Nevertheless, maximal dilation to the highest concentration of ACh was attained at each branch irrespective of pharmacological inhibitions (**Figure 4.6**). This was the case even when the concentrations of UCL1684 and TRAM 34 were increased 3-fold (data not shown). The difference in response to ACh and inhibitors of GM arterioles studied here compared to cremaster arterioles studied by others (118) here may be explained by differences in experimental approach (cannulated vs. in vivo), regional differences in vascular networks (GM vs. cremaster muscle) and the activation of additional signaling pathways [e.g., cytochrome P450 metabolites (32)]. Nevertheless, the rightward shift in response to defined concentrations of ACh in the presence of our pharmacological inhibitors indicated that NO, prostaglandins and K_{Ca} effectively contribute to endothelium dependent vasodilation in the resistance network controlling blood flow to the mouse GM.

Role for endothelium dependent hyperpolarization in ROV. In the human forearm, combined inhibition of NO and prostaglandins attenuated ROV in response to single handgrip contractions (29), while in the mouse cremaster muscle, genetic deletion of $K_{Ca}2.3$ impaired ROV of arterioles (resting diameter, 10-15 μm) in response to muscle contraction (103). In FA and 1A, we quantified ROV as the actual change in diameter to compare responses before vs. after LDT (**Figure 4.4**). In contrast, to enable comparison of vasodilation across vessel branches that differ in diameter (**Figure 4.5**), ROV was expressed as the percentage of maximal vasodilatation within each branch order (i.e. relative to the difference between resting and maximal IDs). Under control conditions, the kinetics of ROV from initiation through recovery (**Figure 4.7**) exhibited the distal-to-proximal gradient as described above. When the inhibitors of autacoids and EDH were present, ROV had slower onset in FA and 1A (**Figure 4.7**) and the initiation of ROV (e.g.

at 1s post-contraction) was depressed (**Figure 4.8**), while the time-to-peak nearly doubled (**Figure 4.9**). While these findings implicate a role for autacoids as well as EDH in ROV, the ~50% attenuation in peak ROV of FA with EDH inhibition (T+U; **Figure 4.10**) but not autacoid inhibition (I+L, **Figure 4.10**) points to a key role for EDH in the initiation AVD with tetanic contraction. Inhibiting EDH was similarly effecting in attenuating peak ROV of 1A which, unlike FA, is embedded within muscle fibers. Thus 1A may initiate ROV as well as receive signals from downstream branches.

Initiation of ROV in distal arterioles. In downstream 2A and 3A, inhibition of autacoids and EDH had little effect on the magnitude of ROV (**Figures 4.7 & 4.10)**. However, under these conditions all branches experienced similar delays in their time-to-peak (**Figure 4.9**), as illustrated by data obtained at 1s post-contraction, the earliest time point that could be accurately resolved for analysis (due to the time required to refocus the image following contraction). Attenuation of vasodilation at this early time point in the distal arterioles is thereby associated with the signaling that initiates ROV. Although the fastest component of ROV was disrupted, finding that the amplitude of ROV was maintained implies that additional vasodilator signaling prevails in distal arterioles. For example, the activation of inward rectifying K^+ channels (K_{ir}) (29) in either ECs or SMCs (the latter via myoendothelial coupling) would contribute outward K^+ current (hyperpolarization) to initiate or augment the spread of hyperpolarization (78, 111). With the exact stimulus that initiates ROV still to be resolved, ROV may well involve redundant mechanisms (24, 33, 129, 161). In such a manner, when one or more key stimuli are ineffective, other vasodilators [e.g., metabolites produced by contracting muscle fibers (80)] could initiate ROV to increase muscle blood flow.

SSV and NO mediated vasodilation

During rhythmic muscle twitch contractions, SSV was observed in all branches of the resistance networks studied here. With data normalized to account for differences in diameter, SSV increased with vessel branch order from FA to 3A (**Figure 4.11**). A key finding was that, in contrast to ROV (**Figure 4.4A**), SSV in FA was not affected by LDT (**Figure 4.4B**) that otherwise eliminated conducted responses along the endothelium. Thus, SSV appears to occur independent of signals conducted from downstream branches. When NO availability was then eliminated with L-NAME, SSV in FA no longer occurred, thereby indicating critical role for NO in mediating AVD of FA during SSV (**Figure 4.4B**). In light of increased blood flow through FA as downstream arterioles undergo dilation, the increase in shear stress on FA endothelium thereby stimulate NO synthase via flow mediated vasodilation (31, 79, 83). Nevertheless, superfusion of indomethacin + L-NAME onto intact networks of the GM failed to inhibit SSV in FA (**Figure 4.11**). Thus, rather than identifying NO as the mediator of FA dilation during rhythmic contractions, we suggest either endothelium-derived autacoids or the conduction of EDH can mediate SSV as complementary signaling pathways that may fully compensate for each other. In support of this interpretation is the tendency for SSV to be attenuated in FA when autacoids and EDH were inhibited simultaneously (**Figure 4.11**). Because the inhibition of these same signaling pathways had no apparent effect on SSV in downstream arterioles, and SSV reflects a much slower (10-15s) onset and plateau (25-30s) during continuous rhythmic muscle contractions, many other vasodilators directly associated with metabolic activity may contribute (e.g., adenosine, ATP and CO_2), consistent with redundancy in mediators

of functional vasodilation during muscular exercise (24, 80). Under such conditions, when the efficacy of one vasodilator is compromised, another is ready to take over.

SUMMARY AND PERSPECTIVES

Using intravital microscopy of mouse skeletal muscle, two type of muscle contractions, tetanic maximal contractions (simulating brief intense activity, e.g. sprinting and powerlifting) vs. rhythmic twitch contractions (simulating moderate rhythmic activity, e.g. walking and cycling) were induced via motor nerve stimulation. Using LDT to selectively disrupt the endothelium and pharmacological interventions to inhibit different components of endothelium dependent vasodilation, we resolved distinct vascular signaling pathway involved in exercise hyperemia. Our findings illustrate that the ROV following tetanic contraction initiates rapid rise of muscle blood flow at the onset of exercise to facilitate the transition from sedentary to active, while SSV that develops during the rhythmic contraction contributes to the sustained blood flow elevation during steady-state exercise. Resolving these respective components of functional vasodilation underscores differences in the nature of vasodilation required to fulfill different needs of muscle fibers in accord with the nature of contractile activity. In turn, the time course of vasodilation and regulation of muscle blood flow should be considered with respect to how muscles may be recruited during different types of activity.

The temporal resolution of ROV is fundamental to identifying the most rapid (i.e., initiating) vasodilator signals from the redundancy in vasodilator substances mediating

SSV. Such temporal resolution of respective aspects of vasodilation along microvascular resistance network is a unique feature of the present study. In addition to the effects of LDT on ROV, the distal-to-proximal temporal gradient in attaining peak ROV (occurring sooner in distal compared to proximal branches) and the effect of K_{Ca} inhibition provide strong evidence supporting the initiation and conduction of ROV from small arterioles located downstream to larger vessels located upstream. Furthermore, combined inhibition of endothelium derived autacoids and EDH depressed the initial response and delayed peak of ROV at all vascular branch orders, further supporting an integral role for the endothelium in the initiation as well as the conduction of ROV.

In skeletal muscle network, the magnitude of blood flowing into a muscle is controlled by FA and 1A (138), ROV of these proximal vessels is integral to increasing blood flow at exercise onset while ROV of distal branches ensures greater perfusion of dependent capillary networks surrounding active muscle fibers. Thus, impairment of endothelium function limits effective regulation of muscle flow by attenuating both the initiation of ROV in small arterioles and the conduction of ROV into proximal vessels. Our present findings are consistent with evidence that the dysfunction of the endothelium with aging (20), obesity (11, 85) and diabetes (91) are associated with impaired muscle blood flow and exercise capacity. Thus, from a translational perspective, the present findings shed new light towards understanding key aspects of endothelial signaling and how it may be affected under different (patho)physiological conditions.

We conclude that ROV of feed arteries in response to a tetanic contraction reflects AVD initiated by endothelium in downstream arterioles that is conducted rapidly as EDH along

the endothelium. AVD of feed arteries during rhythmic twitch contractions can also be mediated by NO release, consistent with elevated luminal shear stress during functional hyperemia and dilation of downstream arterioles. For arterioles embedded within the muscle, additional vasodilator signaling prevails.

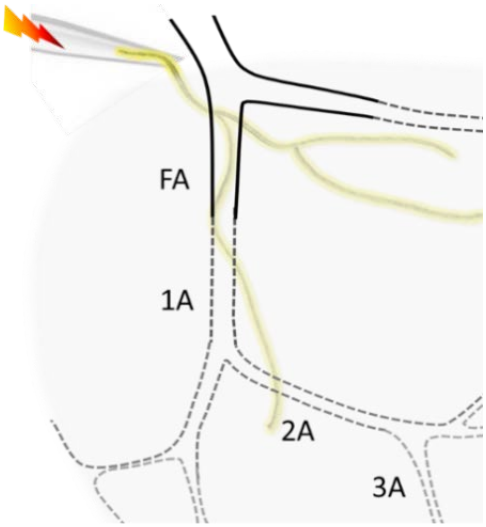

Figure 4.1. Experimental preparation of the mouse GM.
The resistance vessel network supplying inferior GM includes feed artery (FA) external to the muscle (solid lines) and downstream arterioles (1A, 2A, 3A) embedded within muscle fibers (dotted lines). Following muscle contraction evoked by stimulating the motor nerve using a suction electrode, vascular response were recorded in vessel each branch order.

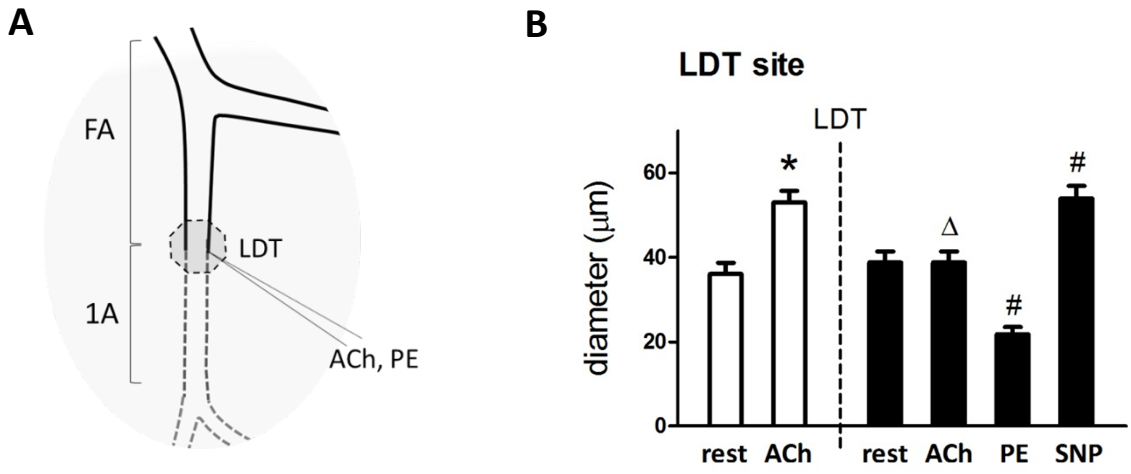

Figure 4.2. Light-Dye Treatment selectively disrupted the endothelium.
A. The site of LDT was located where a FA enters the GM and becomes the 1A. LDT was restricted to a ~300 μm segment. Damage was verified through local delivery of ACh and PE at the site of LDT using microiontophoresis.
B. Selective damage of the endothelium was confirmed when ACh no longer increased diameter. The reduction in diameter in response to PE and dilation to SNP confirmed integrity of smooth muscle cells. Summary data are means ± SE, n=6. *P<0.05 vs rest before LDT, $^{\Delta}$P<0.05 vs. ACh before LDT; $^{\#}P<$ 0.05 vs. rest after LDT.

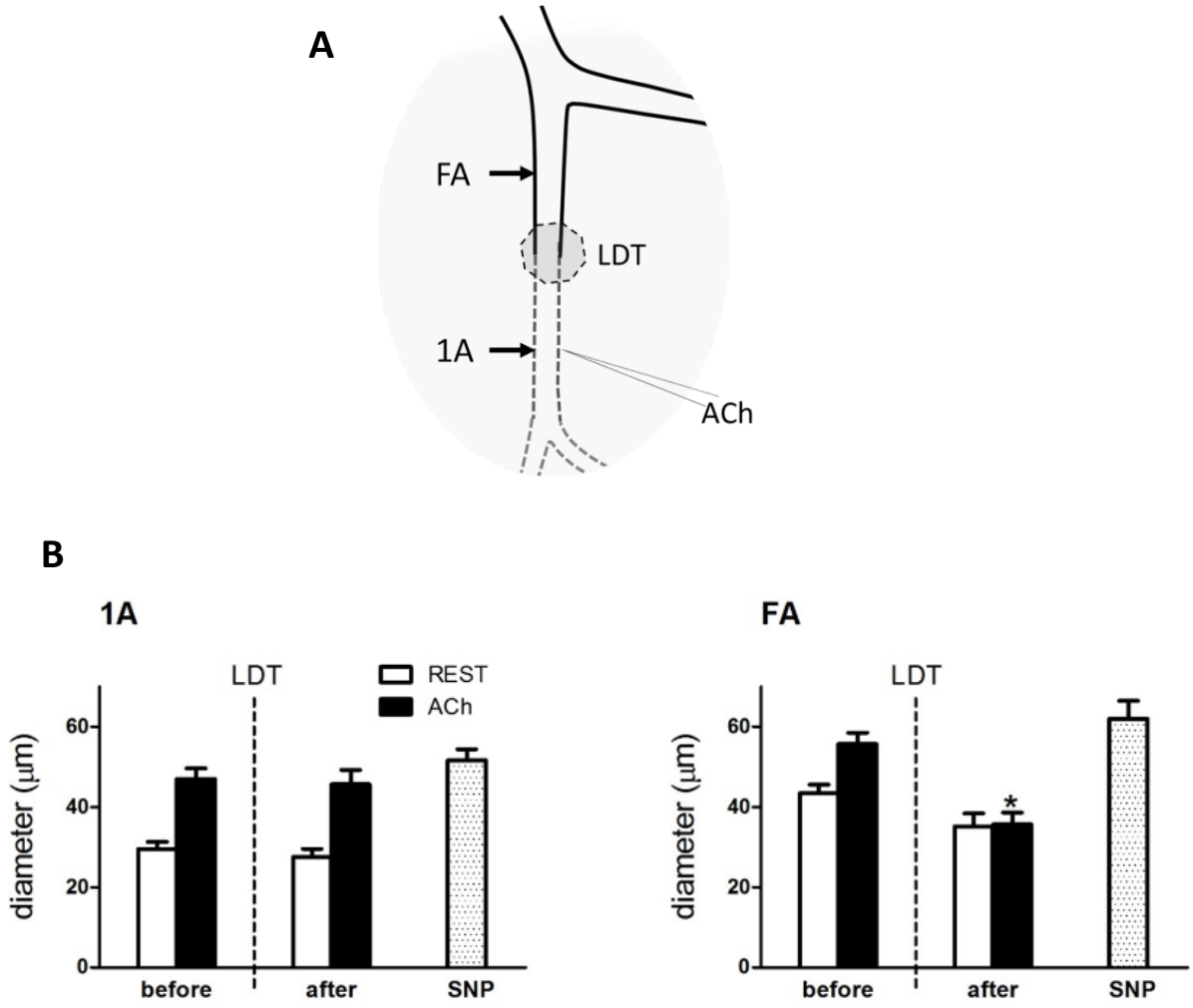

Figure 4.3. Light-Dye Treatment of endothelium blocked conducted vasodilation to ACh.
A. ACh micropipette positioned at 1A located ~500 μm downstream from site of LDT, Arrows indicate local and upstream sites of observation in 1A and FA during microiontophoresis of ACh.
B. Before LDT, ACh triggered local dilation of 1A that conducted upstream into FA. After LDT, local dilation of the 1A was intact while conducted vasodilation of FA was abolished. Both sites dilated to respective maximal diameters during SNP superfusion. Summary data are means ± SE, n=6. **P*<0.05, before vs. after LDT.

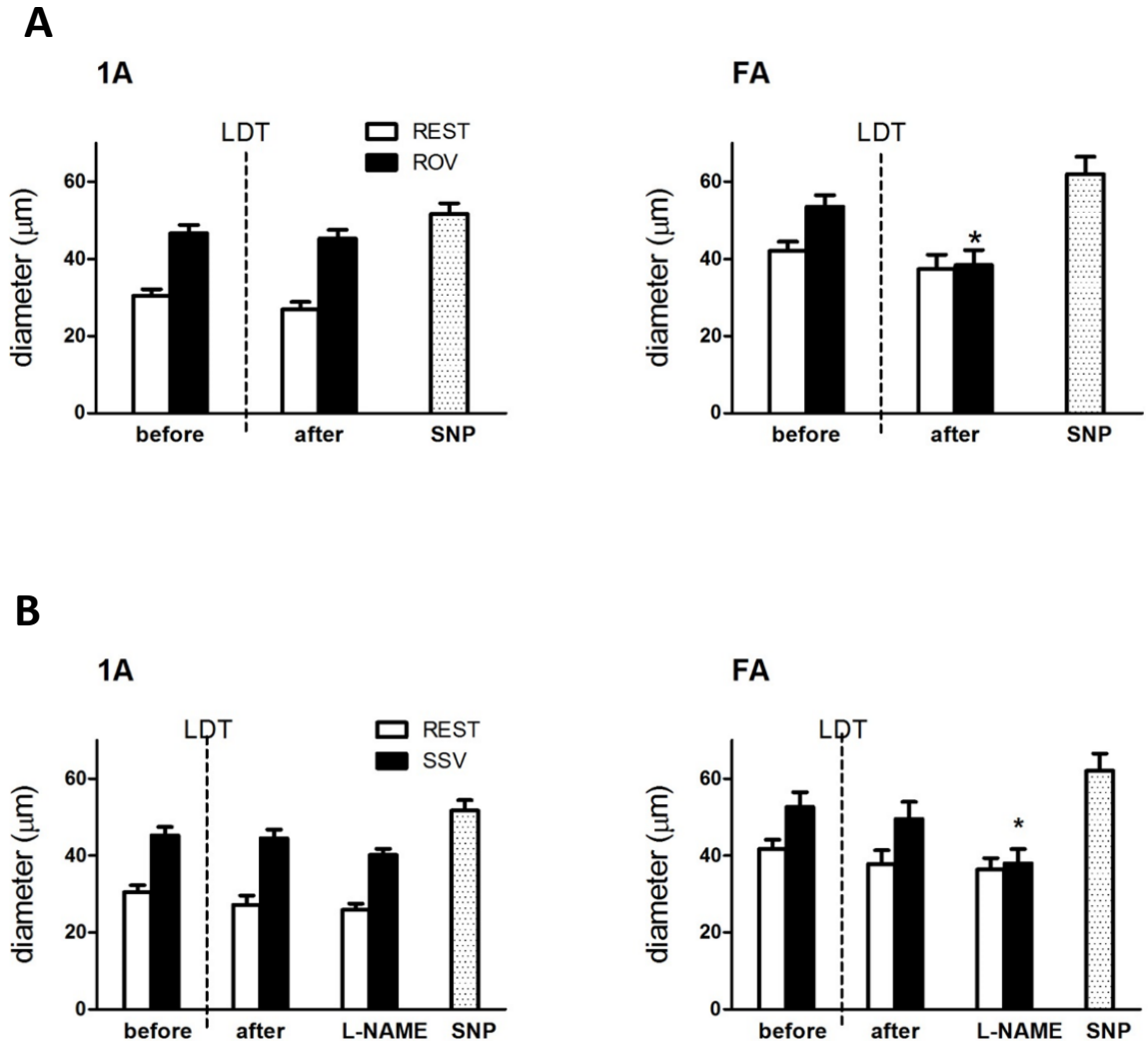

Figure 4.4. Rapid onset vasodilation of FA was blocked by LDT while SSV remained intact until inhibition of NO production. The GM motor nerve was stimulated as in Figure 4.1 to evoke tetanic contraction (100 Hz for 500 ms). **A.** Before LDT: Following contraction, ROV peaked within 4s in 1A and FA (see Figure 4.6). Following LDT, ROV remained intact in 1A but was abolished in FA. **B**. During 4 Hz twitch contractions, SSV remained intact in 1A and FA following LDT. However, ensuing superfusion of L-NAME (10^{-4} M) blocked SSV in FA but not 1A. Summary data are means ± SE, n=6. *P<0.05 vs. before respective interventions.

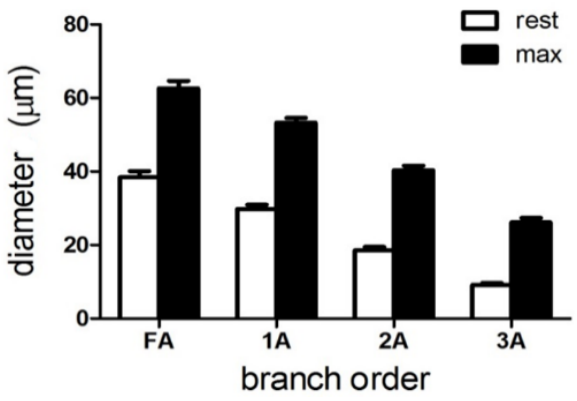

Figure 4.5. **Resting and maximal internal diameters.** Diameters decreased and vasomotor tone increased as vessel branch order increased. Summary data are means ± SE; n=12.

Branch order	Control	I+L	T+U	I+L+T+U
FA	38 ± 2	32 ± 1	29 ± 2*	30 ± 2*
1A	30 ± 1	27 ± 2	30 ± 2	25 ± 2*
2A	19 ± 1	15 ± 1	19 ± 2	19 ± 2
3A	9 ± 1	7 ± 1	10 ± 1	9 ± 1

Table 4.1. Effect of pharmacological agents on resting diameters. Internal vessel diameters at rest decreased significantly from Control in FA during superfusion of I+L, T+U, I+L+T+U and in 1A during superfusion of I+L+T+U. In contrast, downstream 2A and 3A were not significant affected. I+L: indomethacin + L-NAME; T+U: TRAM34 + UCL1684; I+L+T+U: indomethacin + L-NAME + TRAM34 + UCL1684. *P<0.05 vs. control. n=12 for control, n=6 for I+L, n=5 for T+U, n=9 for I+L+T+U.

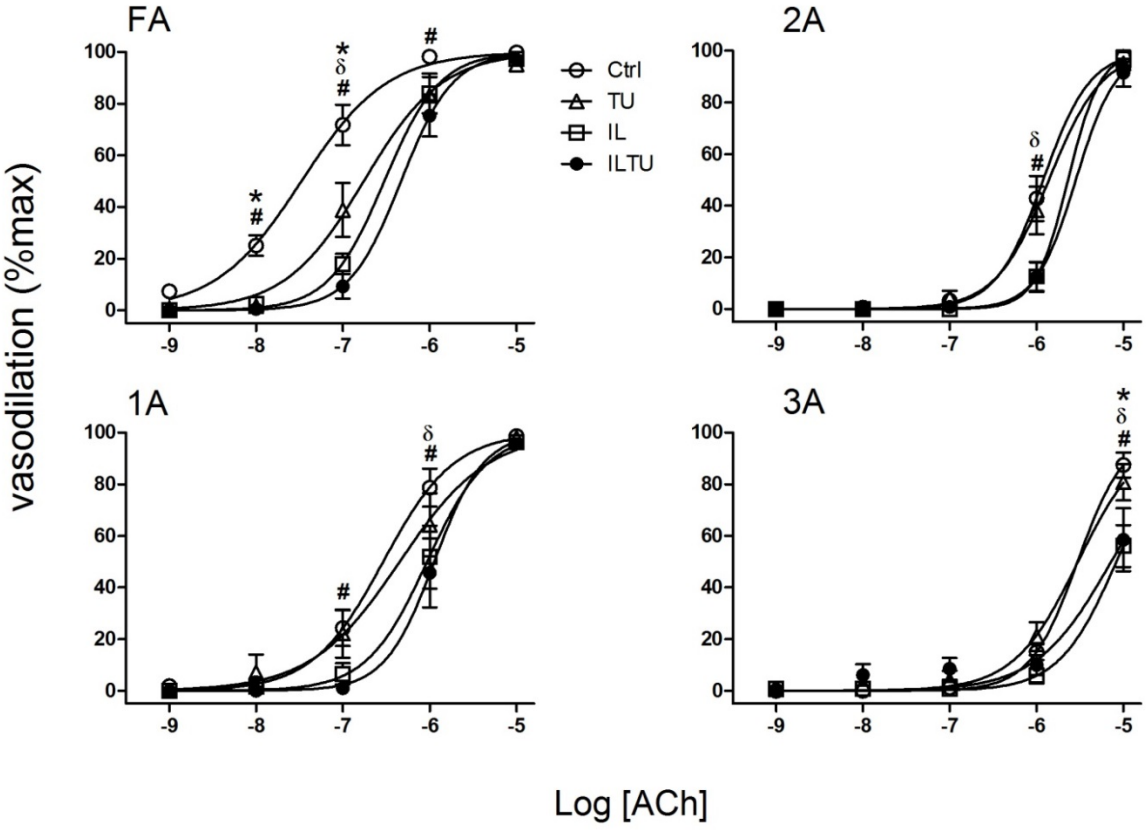

Figure 4.6. Concentration response curves to ACh in FA and arterioles during inhibition of endothelial autacoids and K_{Ca} channels. In FA, superfusion of I+L to inhibit endothelial autacoids (NO + prostacglandins), and superfusion of T+U to inhibit K_{Ca} (EDH) shifted the response curve of FA to the right, with the effect of I+L+T+U > I+L > T+U. Superfusion of I+L also shifted the response curves in 1A and 2A without further effects of I+L+T+U combined. Maximal vasodilation by 10^{-5}M ACh was attenuated only in 3A during I+L+T+U. Ctrl: Control; IL: indomethacin + L-NAME; TU: TRAM34 + UCL1684; ILTU: indomethacin + L-NAME + TRAM34 + UCL1684; TRAM34 + UCL1684; **P*< 0.05, main effect of treatment. Summary data are means ± SE; n=12 for control, n=5 for I+L, n=8 for T+U, n=6 for I+L+T+U.

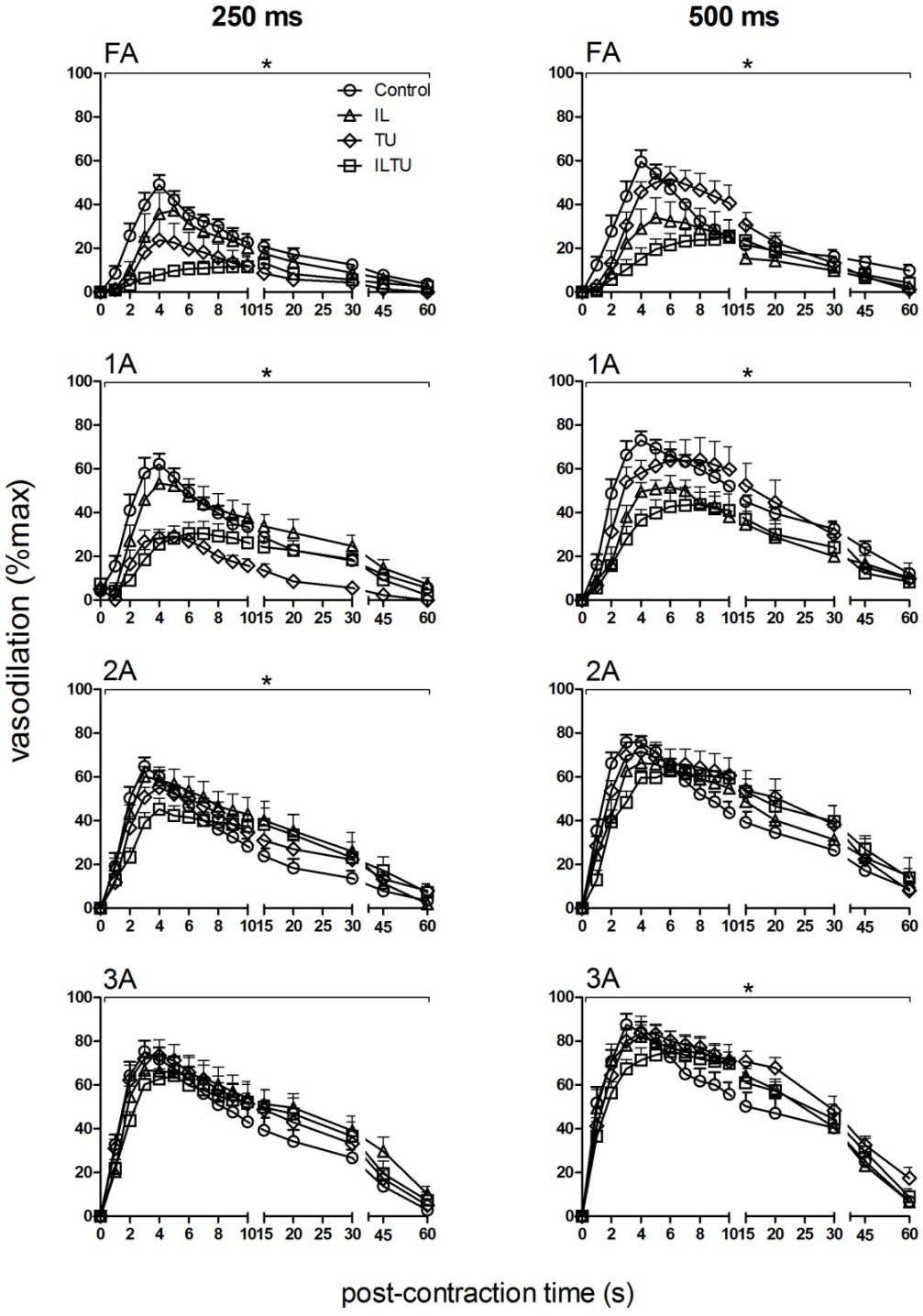

Figure 4.7. Magnitude and time course of ROV: Effect of pharmacological treatments. ROV peaked within 4s for all branches in response to a single 250 ms or 500 ms tetanic contraction. In proximal FA and 1A, superfusion with I+L or T+U decreased ROV and combining I+L+T+U further decreased ROV while slowed initiation and delayed peak response. Respective treatments had more subtle effects on distal 2A and 3A. Abbreviations: Ctrl: Control; IL: indomethacin + L-NAME; TU: TRAM34+UCL1684; ILTU: indomethacin + L-NAME + TRAM34 + UCL1684; *P< 0.05; n=10 for Control, n=5 for I+L and T+U, n=8 for I+L+T+U.

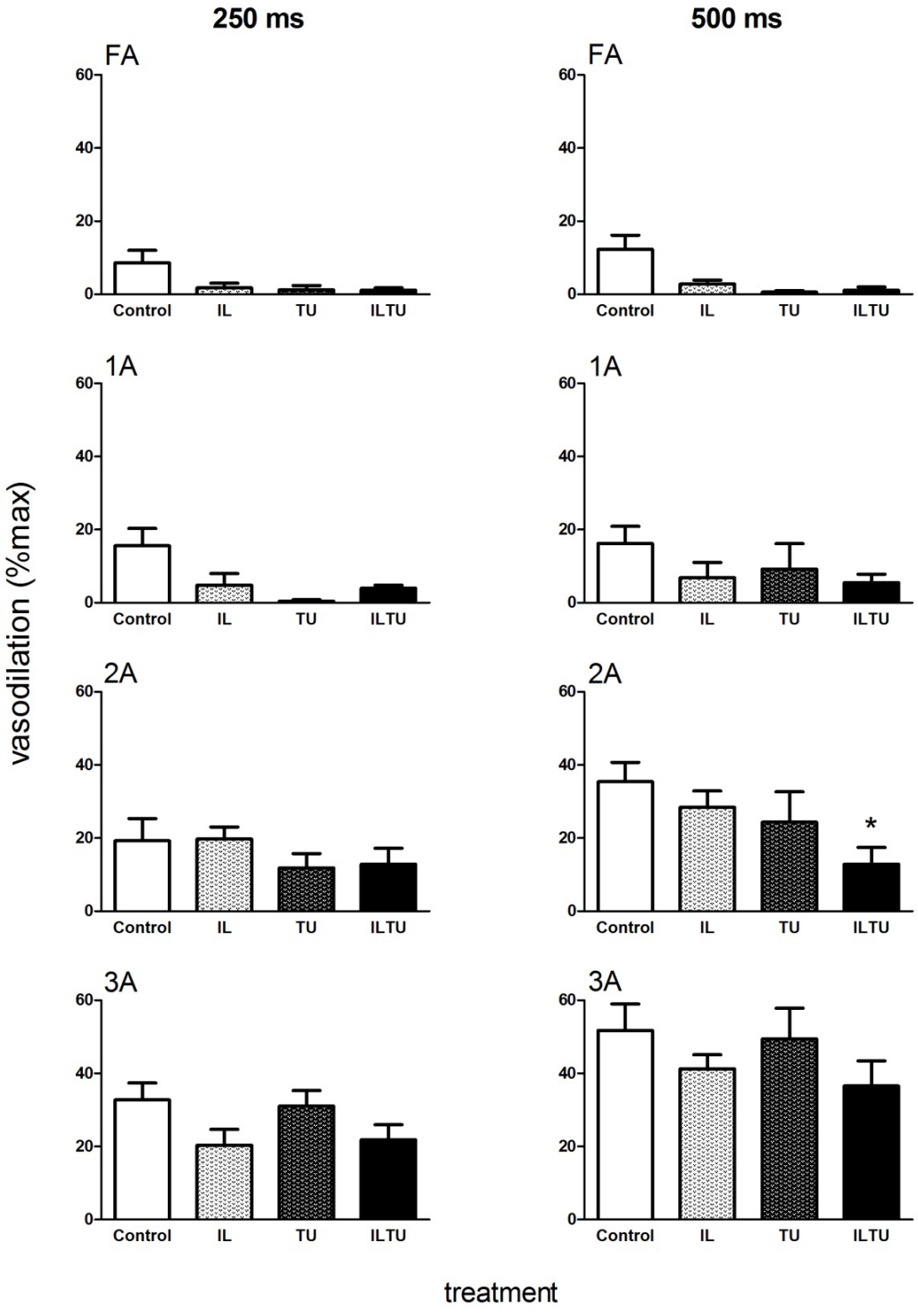

Figure 4.8. Inhibition of autacoids and EDH attenuates the initiation of ROV. Following 250 ms and 500 ms contraction duration, the initiation of ROV at 1s post-contraction increased with branch order (FA<1A<2A<3A, $P< 0.05$). These initial responses were attenuated overall ($P<0.05$), particularly in proximal 1A and 2A, with any combination of inhibitors. Ctrl: Control; IL: indomethacin + L-NAME; TU: TRAM34 + UCL1684; ILTU: indomethacin + L-NAME + TRAM34 + UCL1684. *$P< 0.05$, vs. control within respective branch order. Summary data are means ± S.E.; n=10 for Control, n=5 for I+L and T+U, n=8 for I+L+T+U.

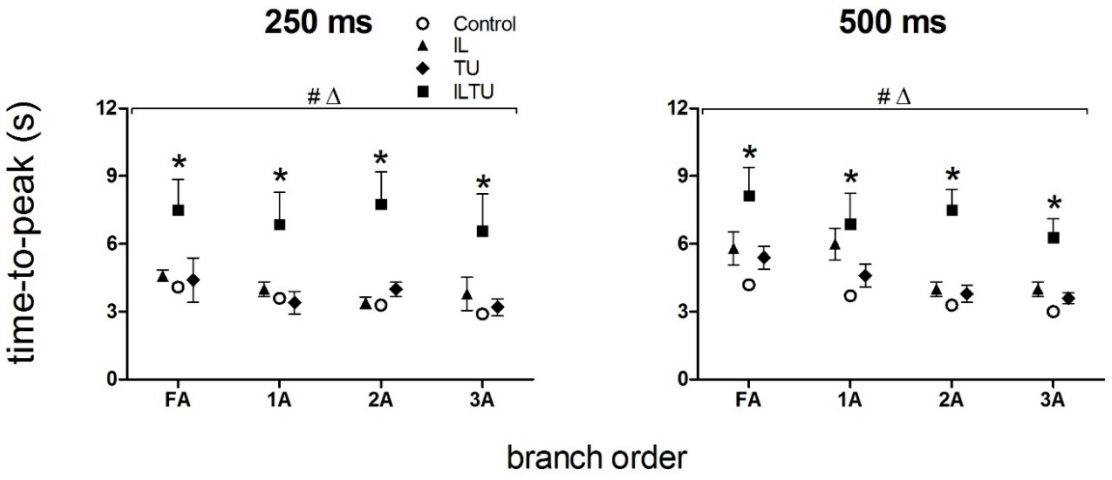

Figure 4.9. Combined inhibition of autacoids and EDH delayed peak ROV. The time-to-peak for ROV decreased as branch order increased (FA>1A>2A>3A, $P<0.05$) following 250 ms and 500 ms GM tetanic contractions, indicating that vasodilation occurred earlier in more distal branches. Combined inhibition of autacoids and EDH doubled the time-to-peak ROV throughout the resistance network. Ctrl: Control; IL: indomethacin + L-NAME; TU: TRAM34 + UCL1684; ILTU: indomethacin + L-NAME + TRAM34 + UCL1684. $^{\#}P< 0.05$, main effects of branch orders; $^{\Delta}P< 0.05$, main effect of treatment; $^{*}P< 0.05$, vs. control within respective branch order. Summary data are means ± S.E.; n=10 for Control, n=5 for I+L and T+U, n=8 for I+L+T+U.

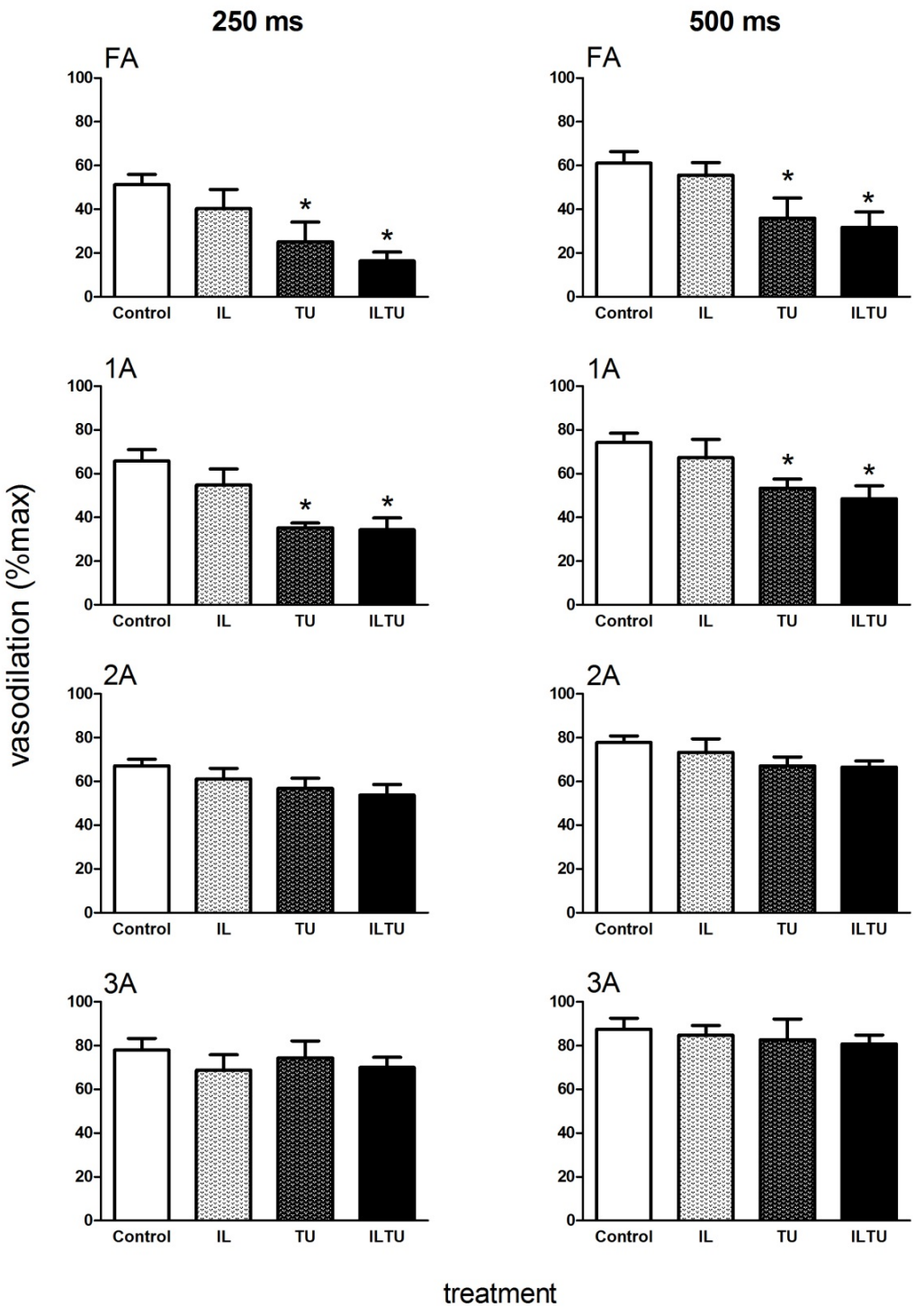

Figure 4.10. Inhibition of EDH decreased Peak ROV in FA and 1A but not 2A or 3A. Peak ROV increased with branch order from FA to 3A ($P<0.05$). Whereas I+L did not change peak ROV throughout the resistance network. Superfusion of TU decreased peak ROV in FA and 1A but not in 2A or 3A for both contraction durations; the addition of I+L to T+U had no further effect. Control; IL: indomethacin + L-NAME; TU: TRAM34+UCL1684; ILTU: indomethacin + L-NAME + TRAM34 + UCL1684. *P<0.05 vs Control. Summary data are means ± SE; n=10 for Control, n=5 for I+L and T+U, n=8 for I+L+T+U.

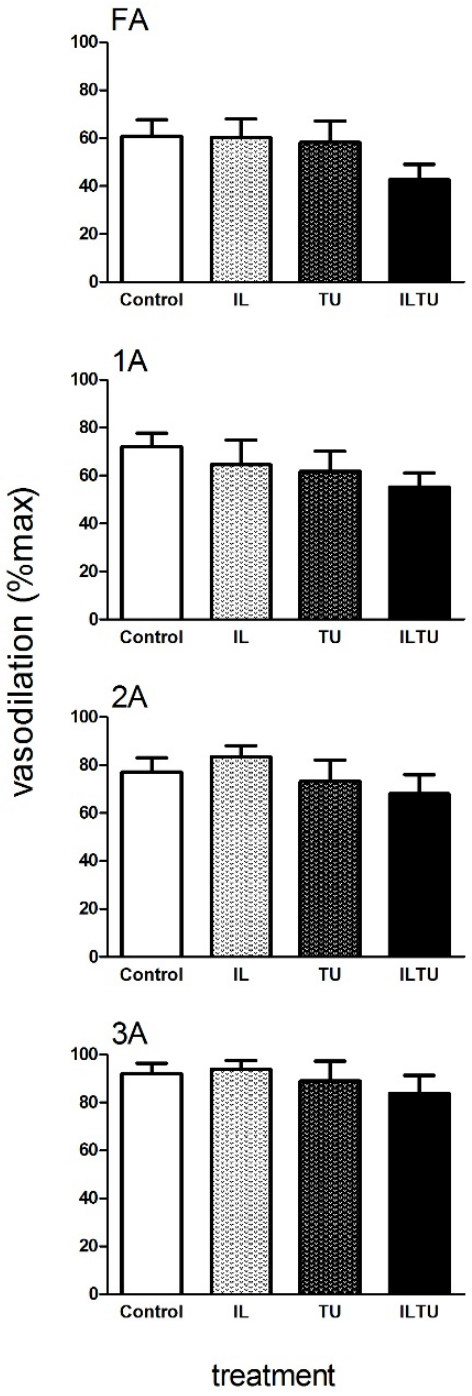

Figure 4.11. Steady state vasodilation was not affected by pharmacological interventions. Steady state vasodilation increased with branch order from FA to 3A ($P<0.05$). Superfusion of I+L or T+U had no effect on SSV in any branch order. Combined superfusion of I+L+T+U tended to decrease SSV in FA and 1A however the effect was not statistically significant. Ctrl: Control; IL: indomethacin+L-NAME; TU:TRAM34+UCL1684; ILTU:indomethacin+L-AME+TRAM34+UCL1684. Summary data are means ± SE, n=10 for Control, n=5 for I+L and T+U, n=8 for I+L+T+U.

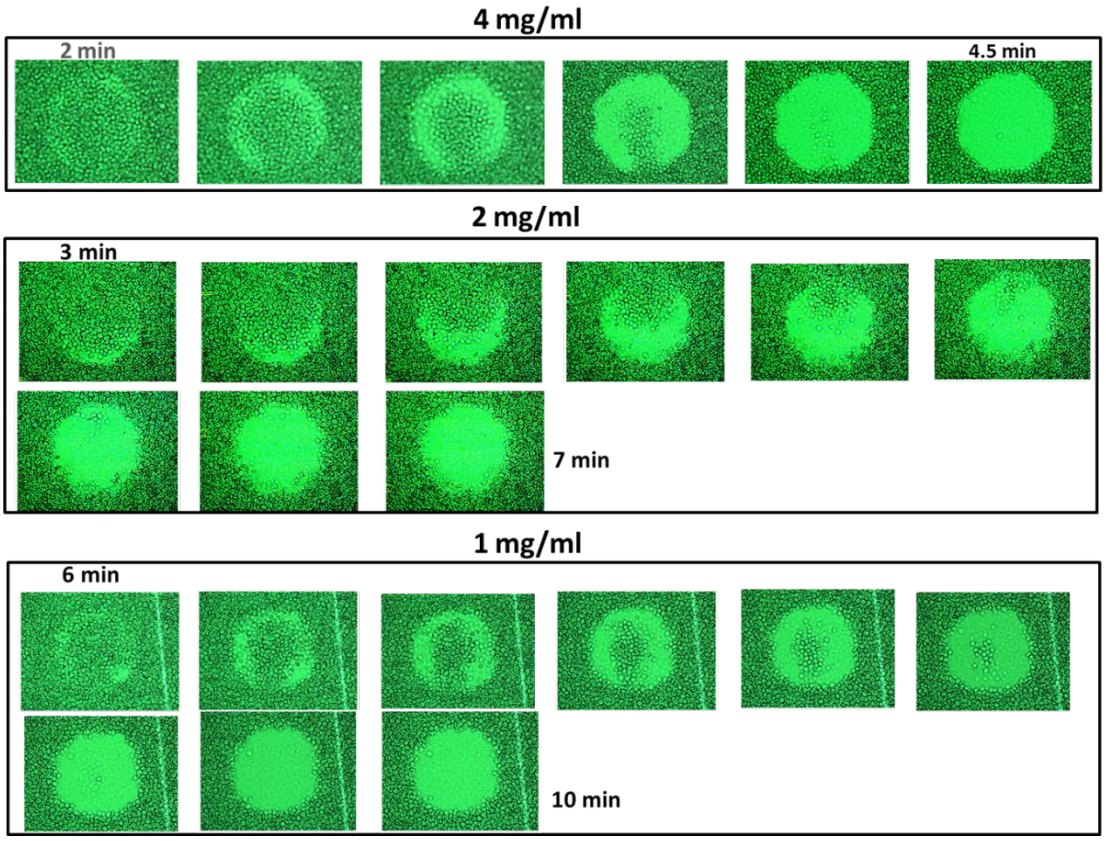

Supplemental Figure 4.1. Time course of erythrocytes photohemolysis. The fresh blood samples were collected from C57BL/6 mice (21, 23 months old) in heparinized tube. After centrifugation and removal of the plasma and buffy coat, erythrocytes were re-suspend in 0.9% NaCl to a hematocrit of 8%. After mixed with FITC-Dextran (70kD), 20 µL of 4% hematocrit of erythrocytes solutions was loaded on the hemocytometer. The time course of the erythrocyte photolysis with the activation of FITC was shown. The final concentration of FITC was 4 mg/ml (top panel), 2 mg/ml (middle panel), and 1 mg/ml (bottom panel) respectively. In each panel, the first image was the onset of hemolysis, the following images were captured at every 30s until the completion of hemolysis shown in the last image. The concentration of LDT at 2 mg/ml was chosen in our final LDT protocol.

CHAPTER 5

CONCLUSIONS

SUMMARY

My dissertation research has investigated the effects of aging on microvascular reactivity in skeletal muscle, from the perspectives of α-adrenergic modulation and endothelial signaling pathways with an emphasis on gaining insight into ROV. By resolving the functional contribution and regulation of respective branch orders of the resistance network governing the regulation of blood flow, my dissertation research encompasses 3 chapters that are based upon intravital microscopy of mouse gluteus maximus muscle.

Chapter 2 has defined microvascular reactivity along resistance networks of skeletal muscle in young and old male C57BL/6 mice, by measuring the internal vessel diameters, vasomotor tone and responses to defined vasoactive stimuli. Under resting conditions, young and old mice exhibited similar diameters for feed arteries and respective arteriolar branches. During maximal dilation, diameters of distal arterioles (i.e., 2A and 3A) tended to be larger in old compared to young mice, reflecting greater spontaneous vasomotor tone. Nevertheless, vasoconstriction in response to elevated O_2 was attenuated throughout the networks of old compared to Young mice. Further, while α_1ARs were twice as effective as α_2ARs in evoking constrictions, advanced age had the effect of attenuating α_2AR-mediated vasoconstriction to the greatest extend. Remarkably, with similar resting diameters, vasodilation to ACh (i.e., EDD) was greater in distal arterioles of old compared to young.

Thus the effect of advanced age on the reactivity of microvessels supplying skeletal muscle varies with branch order and nature of the vasoactive stimulus.

Chapter 3 defined the kinetics and magnitude of ROV along microvascular resistance networks controlling blood flow to the mouse GM, and resolved the differential modulation of ROV through αARs in young versus old male mice. In response to single tetanic contractions, ROV typically began within 1 s of muscle contraction and reached peak dilatation within 4 s post-contraction throughout the networks of young and old mice. The relative magnitude of ROV increased from proximal to distal branches (FA<1A<2A<3A) and increased with contraction duration. ROV was depressed in all vessel branches of old compared to young mice. Subtle manipulation of αARs had significant physiological consequences that vary with age: Subthreshold stimulation of αARs with NE depressed ROV only in young mice, inhibition of αARs with phentolamine improved ROV only in old mice. With pharmacological interventions selective for α_1ARs versus α_2ARs, activating either AR subtype attenuated ROV in young mice, while inhibiting α_2ARs was more effective (versus α_1ARs) in restoring ROV for old mice. Integration of these findings uniquely illustrates differential modulation of ROV by ARs in young versus old skeletal muscle. While manifest throughout resistance networks, the modulation of ROV through αARs is most effective in upstream branches (FA, 1A) that govern the volume of blood flowing into arteriolar networks. In contrast, the downstream 2A and 3A, which control regional distribution of flow to capillary beds, are less susceptible to modulation through αARs, particularly as contraction duration increases.

Chapter 4 has defined the role of endothelium in AVD of ROV in FA and in ROV initiation in downstream arterioles while resolving its differences from SSV, a slower mechanism for vasodilation during sustained exercise. By differing the nature of GM contractions (single tetanic maximal contraction vs. rhythmic twitch contractions) to evoked ROV or SSV in all branch orders, I was able to separate the "fast" and "slow" vascular responses contributing to exercise hyperemia. Using LDT to selectively disrupt the endothelium segment between FA and 1A, I was able to block conducted vasodilation of FA in response to stimulating a downstream 1A with ACh. Importantly, LDT also eliminated ROV in FA following single tetanic contraction, demonstrating for the first time that ROV is conducted along the endothelium as a mechanism of AVD. In contrast, the SSV with rhythmic twitch contractions was not affected by LDT, but was blocked by further inhibition of NO production – thereby identifying a distinct signaling pathway for AVD. In intact GM networks, inhibition of EDH through selective $K_{Ca}2.3$ and $K_{Ca}3.1$ blockers attenuated ROV in upstream FA and 1A with only subtle effects in downstream 2A and 3A. In contrast, blockade of autacoids (NO and prostaglandins) had little effect on peak ROV across all vascular branch orders. Remarkably, simultaneous inhibition of NO, prostaglandins and EDH significantly attenuated the onset vasodilation and delayed peak ROV across the entire network. In contrast, inhibition of autacoids or EDH failed to attenuate SSV, except for a tendency to attenuate SSV when EDH and autacoids were inhibited at the same time. Collectively, these findings have distinguished different signaling pathways for AVD in ROV vs. SSV in accord with different types of contractile activity. Thus, ROV in FA following tetanic muscle contractions reflects conducted vasodilation along the endothelium initiated by EDH in downstream arterioles, while SSV

in FA following rhythmic muscle twitches can also be mediated by NO release. Consistent with findings reported in earlier classic studies, additional vasodilator signaling prevails in downstream arterioles to ensure the muscle oxygen supply meets local metabolic needs.

INTEGRATION OF FINDINGS

Vascular reactivity and vasomotor responses to muscle contraction with advanced age was characterized in the mouse GM. Compared to young mice, EDD was attenuated in feed arteries of the GM but was enhanced in distal arterioles in association with greater vasomotor tone. The α_1AR-mediated vasoconstriction was attenuated only in distal arterioles of the GM in old mice, while the α_2AR-mediated vasoconstriction was attenuated across the entire resistance network. For ROV, the ability of the resistance vasculature to respond rapidly to the onset of muscle contraction was attenuated across the GM network in old vs. young mice and this attenuation was greater in proximal vessels (FA and 1A) compared to distal vessels (2A and 3A). From the perspective of systemic hemodynamic regulation, the chief sites for controlling total blood flow entering the muscle are the proximal resistance vessels. My findings thereby explain why muscle blood flow is attenuated during advanced age. In contrast, the local distribution of blood flow within the muscle is controlled by downstream arterioles that are embedded within the muscle and influenced directly by the surrounding tissue (80, 138). My findings suggest that these smaller branches of the resistance network are less affected by advanced age, thus may still function to distribute blood flow according to local metabolic demand within the muscle.

Sympathetic (adrenergic) modulation of ROV is most strongly manifested at proximal vessel branches of GM, where a subtle level of αAR stimulation attenuates ROV. Both α_1AR and α_2AR activation are able to attenuate ROV. However, while α_1AR activation is nearly twice as effective as α_2AR activation in mediating vasoconstriction, the inhibition of α_2ARs is more effective on rescuing the attenuated ROV during advanced age than is the inhibition of α_1ARs. Aging depressed α_2AR but not α_1AR mediated vasoconstriction with aging. These findings suggest a differential role for α_1ARs and α_2ARs in blood flow regulation. In such manner, the maintenance of α_1AR-mediated constriction serves to ensure the maintenance of peripheral resistance and arterial blood pressure during exercise (152). In contrast, α_2AR signaling involving multiple cellular pathways (40, 58, 115, 167), serves as regulatory mechanism for responding to functional sympatholysis during exercise or more long-term adaptations such as aging. A key finding from my dissertation research is that enhanced constitutive activation of αARs contributes to ROV attenuation with aging and that rescuing such an effect occurs primarily through the inhibition of α_2ARs at proximal vessel branches.

My experiments also provide definitive new insight into endothelial mechanisms underlying ROV (**Figure 5.1**). Selective damage of endothelium between the FA and the downstream arterioles eliminates the ROV, confirming that this response conducts from downstream arterioles into proximal FA. Pharmacological inhibition of EDH attenuated peak ROV by approximately half in FA and 1A while significantly delaying the time to peak dilation. Thus, ROV of feed arteries reflects AVD initiated by hyperpolarization of endothelium in downstream arterioles that is conducted rapidly from cell to cell along the endothelium. In distal arterioles, endothelium is integral to ROV initiation by generating

EDH through activation of $K_{Ca}2.3$ and $K_{Ca}3.1$ channels. However, the actual signal that initiates EDH in response to tetanic muscle contraction was not resolved in my experiments. Nevertheless, I was able to resolve 2 distinct signaling pathways for AVD. The first entails conducted vasodilation along the endothelium and is most effectively initiated by brief intense contraction. I used single maximal tetanic contractions for this purpose. The second involves the release of nitric oxide and was most effectively resolved using sustained repetitive contractions of moderate intensity. In turn, resolving such differences may provide a foundation for developing more specific therapeutic interventions to promote and restore muscle blood flow during advanced age. The ability to engage in physical activity, including daily tasks, will enhance the quality of life of those most affected.

My findings collectively illustrate that ROV of the resistance vasculature supplying skeletal muscle is initiated by EDH and conducted along the vascular wall through the endothelium (Chapter 4). Importantly, ROV is regulated by signaling pathways that involve αARs in a manner that differs with vessel branch order (Chapter 3). Thus, aging may attenuate ROV through (but need not be restricted to) the mechanisms summarized in Figure 5.1. With enhanced SNA, the constitutive activation of α_1ARs and α_2ARs attenuated ROV in FA while activation of α_2ARs attenuated ROV in 1A. In addition to its well-known effect of vasoconstriction, sympathetic activation also decreases endothelium conduction of vasodilation (65, 66, 105). These effects contribute to attenuated ROV in the proximal vessels. With endothelium dysfunction, blunted EDH will attenuate the initiation and conduction of ROV along the resistance network. As EDD was attenuated in proximal vessels, while in distal vessels it was surprisingly enhanced (Chapter 2), it is likely that

additional vasodilator signaling events may compensate for endothelium dysfunction to minimize the attenuation of ROV in distal vs. proximal vessels. By recording frame-by-frame from video recordings, I was able to resolve a temporal gradient in the onset of ROV along the resistance network, thereby illustrating that ROV occurs sooner in the distal branches (Chapter 3), consistent with AVD originating downstream and then encompassing more proximal branches. From the perspective that principal sites for the regulation of peripheral resistance, distribution of cardiac output and tissue blood flow are within the proximal vessels, the concerted effects that impair ROV help to explain the deficiency in functional sympatholysis during advancing age. Indeed, such loss of function causes difficulty in transitioning from rest to physical activity or to increase from moderate to more intense levels of exercise (133).

IMPLICATIONS OF CURRENT FINDINGS

Current understanding of endothelium dysfunction is based primarily on impaired EDD of large conduit arteries or in vitro studies of isolated vessels. Our findings that EDD is actually enhanced in distal arterioles in vivo provides valuable new insight into therapeutic strategies designed to adjust EDD – for example to improve endothelial conduction rather than augment vasodilation through the release of autacoids such as nitric oxide.

The endothelium is integral to both the initiation and conduction of ROV, thus serves as the key signaling pathway for rapidly increasing blood flow with exercise onset and transition to more strenuous activity. I found that ROV - but not SSV - was attenuated with

inhibitors that interfere with EDD. Therefore, for individuals at advanced age or in diseases with endothelium dysfunction, the extended period of “warm up” and moderate intensity exercise is recommended when performing physical activity or exercise training.

Because constitutive activation of α_2ARs contributes to the attenuated ROV at proximal vessels with aging, selective intervention of α_2AR signaling would appear most likely to exhibit better effects in improving muscle blood flow with less effects in arterial pressure and peripheral resistance changes compared to targeting α_1AR signaling. For this purpose, selective and targeting drug delivery system is needed. For example, a local infusion with nanoparticles loaded with selective α_2AR inhibitors could be ideal for safe and convenient application for individuals, who are at advanced age or in other conditions with enhanced SNA, before or during muscular exercise, in order to improve ROV and their ability to transition to activity.

FUTURE DIRECTIONS

In light of evidence supporting the role of endothelium in the rapid vascular response to muscle contraction, and the changes in EDD along with endothelium dysfunction in advanced age, future studies should evaluate the role of endothelial conduction and the respective endothelial vasodilator (NO, prostaglandins and EDH) in old mice to determine whether changes in EDD with aging reflect the attenuated ROV or whether signaling pathways (e.g., reactive oxygen species) may be involved as an adaptation to advanced age. Further, because aging is inevitable in both males and females, the relationships

investigated here in male mice should also be examined in female mice. Unlike the cremaster muscle, which is unique to males, the GM used in my studies is integral to locomotion in both sexes thus is an ideal model to pursue such studies in the future. My current findings have also shed a light on endothelial mechanisms in initiating ROV in downstream arterioles. Nevertheless, the exact signal(s) evoking EDH or the conducted response during muscle contraction is not clear and requires further studies. Thus, molecular and genetic approaches may prove useful to selectively modify the proteins involved in the cellular signaling pathway of K_{Ca} 2.3 and K_{Ca} 3.1 channel opening. Examples include those mediating Ca^{2+} entry through the plasma membrane and those mediating Ca^{2+} release from internal stores. In addition, new experimental approaches are needed to resolve mechanism(s) that activates AVD and endothelial signaling further downstream from the smallest arterioles studied here. Key questions center on what signals may be generated from the active muscle fibers and from within capillary networks to effect vasomotor responses of proximal arterioles that govern their perfusion with red blood cells.

FINAL COMMENTS

The insight gained in this dissertation research is from utilizing a mouse model to directly observe and thereby study microcirculation in skeletal muscle in vivo, thereby overcoming the limitations of human studies. The mouse GM is of mixed fiber type (90, 98) and thereby consistent with the composition of human skeletal muscles (93, 127). Intravital microscopy of the microcirculation in mouse skeletal muscle allows direct observation and evaluation defined branch orders of vascular networks, and acquisition of measurements that cannot

be obtained from human subjects. Thus our understanding where and how advanced age affects vascular reactivity and blood flow control in respective microvascular branch orders of the mouse GM *in vivo* may well be applied towards developing selective therapeutic strategies for promoting muscle blood flow in aging humans.

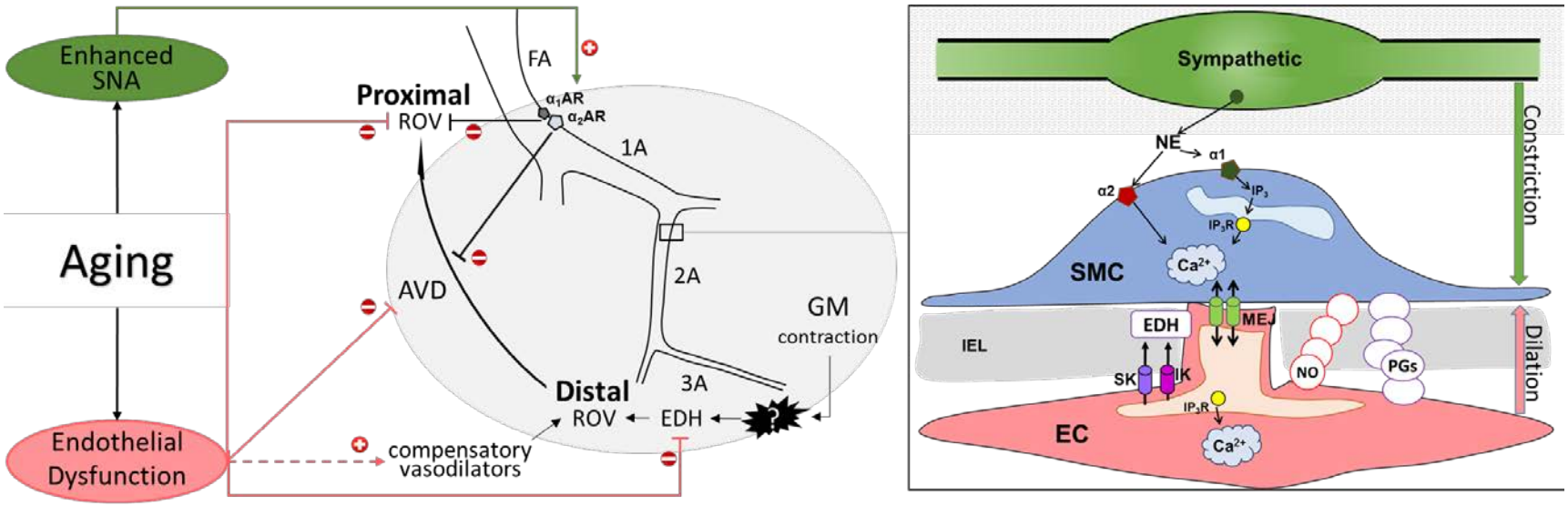

Figure 5.1. Mechanism of ROV attenuation with aging.

ROV reflects the nearly instant relaxation of SMCs in response to muscle contraction. ROV is regulated by both perivascular sympathetic nerves within the adventitia and the endothelium lining the vessel lumen. Sympathetic nerves release NE to activate α_1 and α_2 ARs and thus promote vasoconstriction. Endothelial cells release NO, PGs and generate EDH through activation of Kca2.3 and Kca3.1 channels to promote vasodilation. Following tetanic muscle contraction, ROV reflects conducted vasodilation along the endothelium initiated by EDH in downstream arterioles, however, the exact stimulus that triggers EDH is not known. Activation of post-synaptic α_1AR and α_2AR attenuates ROV in proximal vessels and also blunts conduction of vasodilation along endothelium.

With aging, the enhanced SNA and activation of ARs attenuates ROV in proximal vessels due to impaired conduction along endothelium. Endothelium dysfunction decreases EDD and conduction, thus contributes to attenuation of ROV (and blood flow restriction) in proximal vessels. In distal arterioles, additional vasodilators can compensate for the endothelium dysfunction, thus peak ROV is apparently maintained in these vessel branches.

REFERENCES

1. Armstrong ML, Dua AK, and Murrant CL. Potassium initiates vasodilatation induced by a single skeletal muscle contraction in hamster cremaster muscle. J Physiol 581: 841-852, 2007.

2. Barcroft H and Millen JL. The blood flow through muscle during sustained contraction. J Physiol 97: 17-31, 1939.

3. Bartlett IS and Segal SS. Resolution of smooth muscle and endothelial pathways for conduction along hamster cheek pouch arterioles. Am J Physiol Heart Circ Physiol 278: H604-612, 2000.

4. Bayliss WM. On the local reactions of the arterial wall to changes of internal pressure. J Physiol 28: 220-231, 1902.

5. Beach JM, McGahren ED, and Duling BR. Capillaries and arterioles are electrically coupled in hamster cheek pouch. Am J Physiol 275: H1489-1496, 1998.

6. Bearden SE, Payne GW, Chisty A, and Segal SS. Arteriolar network architecture and vasomotor function with ageing in mouse gluteus maximus muscle. J Physiol 561: 535-545, 2004.

7. Behnke BJ and Delp MD. Aging blunts the dynamics of vasodilation in isolated skeletal muscle resistance vessels. J Appl Physiol 108: 14-20, 2010.

8. Behringer EJ and Segal SS. Spreading the signal for vasodilatation: implications for skeletal muscle blood flow control and the effects of ageing. J Physiol 590: 6277-6284, 2012.

9. Behringer EJ, Shaw RL, Westcott EB, Socha MJ, and Segal SS. Aging impairs electrical conduction along endothelium of resistance arteries through enhanced Ca2+-activated K+ channel activation. Arterioscler Thromb Vasc Biol 33: 1892-1901, 2013.

10. Behringer EJ, Socha MJ, Polo-Parada L, and Segal SS. Electrical conduction along endothelial cell tubes from mouse feed arteries: Confounding actions of glycyrrhetinic acid derivatives. Br J Pharmacol 166: 774-787, 2012.

11. Bender SB and Laughlin MH. Modulation of endothelial cell phenotype by physical activity: impact on obesity-related endothelial dysfunction. Am J Physiol Heart Circ Physiol 309: H1-8, 2015.

12. Berg BR, Cohen KD, and Sarelius IH. Direct coupling between blood flow and metabolism at the capillary level in striated muscle. Am J Physiol 272: H2693-2700, 1997.

13. Berne RM, Knabb RM, Ely SW, and Rubio R. Adenosine in the local regulation of blood flow: a brief overview. Fed Proc 42: 3136-3142, 1983.

14. Boegehold MA and Johnson PC. Response of arteriolar network of skeletal muscle to sympathetic nerve stimulation. Am J Physiol 254: H919-928, 1988.

15. Booth FW and Zwetsloot KA. Basic concepts about genes, inactivity and aging. Scand J Med Sci Sports 20: 1-4, 2010.

16. Boushel R, Langberg H, Gemmer C, Olesen J, Crameri R, Scheede C, Sander M, and Kjaer M. Combined inhibition of nitric oxide and prostaglandins reduces human skeletal muscle blood flow during exercise. J Physiol 543: 691-698, 2002.

17. Brandes RP, Schmitz-Winnenthal FH, Feletou M, Godecke A, Huang PL, Vanhoutte PM, Fleming I, and Busse R. An endothelium-derived hyperpolarizing factor distinct from NO and prostacyclin is a major endothelium-dependent vasodilator in resistance vessels of wild-type and endothelial NO synthase knockout mice. Proc Natl Acad Sci U S A 97: 9747-9752, 2000.

18. Budel S, Bartlett IS, and Segal SS. Homocellular conduction along endothelium and smooth muscle of arterioles in hamster cheek pouch: unmasking an NO wave. Circ Res 93: 61-68, 2003.

19. Busse R, Edwards G, Feletou M, Fleming I, Vanhoutte P, and Weston A. EDHF: bringing the concepts together. Trends Pharmacol Sci 23: 374-380, 2002.

20. Carlson RE, Kirby BS, Voyles WF, and Dinenno FA. Evidence for impaired skeletal muscle contraction-induced rapid vasodilation in aging humans. Am J Physiol Heart Circ Physiol 294: H1963-1970, 2008.

21. Casey DP, Curry TB, and Joyner MJ. Measuring muscle blood flow: a key link between systemic and regional metabolism. Curr Opin Clin Nutr Metab Care 11: 580-586, 2008.

22. Casey DP and Joyner MJ. Influence of alpha-adrenergic vasoconstriction on the blunted skeletal muscle contraction-induced rapid vasodilation with aging. J Appl Physiol 113: 1201-1212, 2012.

23. Casey DP, Mohamed EA, and Joyner MJ. Role of nitric oxide and adenosine in the onset of vasodilation during dynamic forearm exercise. Eur J Appl Physiol 113: 295-303, 2013.

24. Clifford PS and Hellsten Y. Vasodilatory mechanisms in contracting skeletal muscle. J Appl Physiol 97: 393-403, 2004.

25. Clifford PS and Tschakovsky ME. Rapid vascular responses to muscle contraction. Exerc Sport Sci Rev 36: 25-29, 2008.

26. Cohen RA and Vanhoutte PM. Endothelium-dependent hyperpolarization. Beyond nitric oxide and cyclic GMP. Circulation 92: 3337-3349, 1995.

27. Cook JJ, Wailgum TD, Vasthare US, Mayrovitz HN, and Tuma RF. Age-related alterations in the arterial microvasculature of skeletal muscle. J Gerontol 47: B83-88, 1992.

28. Corcondilas A, Koroxenidis GT, and Shepherd JT. Effect of a brief contraction of forearm muscles on forearm blood flow. J Appl Physiol 19: 142-146, 1964.

29. Crecelius AR, Kirby BS, Luckasen GJ, Larson DG, and Dinenno FA. Mechanisms of rapid vasodilation after a brief contraction in human skeletal muscle. Am J Physiol Heart Circ Physiol 305: H29-40, 2013.

30. Credeur DP, Holwerda SW, Restaino RM, King PM, Crutcher KL, Laughlin MH, Padilla J, and Fadel PJ. Characterizing rapid-onset vasodilation to single muscle contractions in the human leg. J Appl Physiol 118: 455-464, 2015.

31. Davies PF. Flow-mediated endothelial mechanotransduction. Physiol Rev 75: 519-560, 1995.

32. de Wit C, Esser N, Lehr HA, Bolz SS, and Pohl U. Pentobarbital-sensitive EDHF comediates ACh-induced arteriolar dilation in the hamster microcirculation. Am J Physiol 276: H1527-1534, 1999.

33. Delp MD. Control of skeletal muscle perfusion at the onset of dynamic exercise. Med Sci Sports Exerc 31: 1011-1018, 1999.

34. Delp MD, Behnke BJ, Spier SA, Wu G, and Muller-Delp JM. Ageing diminishes endothelium-dependent vasodilatation and tetrahydrobiopterin content in rat skeletal muscle arterioles. J Physiol 586: 1161-1168, 2008.

35. Di Francescomarino S, Sciartilli A, Di Valerio V, Di Baldassarre A, and Gallina S. The effect of physical exercise on endothelial function. Sports Med 39: 797-812, 2009.

36. Diep HK, Vigmond EJ, Segal SS, and Welsh DG. Defining electrical communication in skeletal muscle resistance arteries: a computational approach. J Physiol 568: 267-281, 2005.

37. Dinenno FA, Dietz NM, and Joyner MJ. Aging and forearm postjunctional alpha-adrenergic vasoconstriction in healthy men. Circulation 106: 1349-1354, 2002.

38. Dinenno FA, Jones PP, Seals DR, and Tanaka H. Limb blood flow and vascular conductance are reduced with age in healthy humans: relation to elevations in sympathetic nerve activity and declines in oxygen demand. Circulation 100: 164-170, 1999.

39. Dinenno FA, Masuki S, and Joyner MJ. Impaired modulation of sympathetic alpha-adrenergic vasoconstriction in contracting forearm muscle of ageing men. J Physiol 567: 311-321, 2005.

40. Docherty JR. Subtypes of functional alpha1- and alpha2-adrenoceptors. Eur J Pharmacol 361: 1-15, 1998.

41. Dodd LR and Johnson PC. Antagonism of vasoconstriction by muscle contraction differs with alpha-adrenergic subtype. Am J Physiol 264: H892-900, 1993.

42. Domeier TL and Segal SS. Electromechanical and pharmacomechanical signalling pathways for conducted vasodilatation along endothelium of hamster feed arteries. J Physiol 579: 175-186, 2007.

43. Donato AJ, Gano LB, Eskurza I, Silver AE, Gates PE, Jablonski K, and Seals DR. Vascular endothelial dysfunction with aging: endothelin-1 and endothelial nitric oxide synthase. Am J Physiol Heart Circ Physiol 297: H425-432, 2009.

44. Donato AJ, Uberoi A, Wray DW, Nishiyama S, Lawrenson L, and Richardson RS. Differential effects of aging on limb blood flow in humans. Am J Physiol Heart Circ Physiol 290: H272-278, 2006.

45. Duling BR and Berne RM. Longitudinal gradients in periarteriolar oxygen tension. A possible mechanism for the participation of oxygen in local regulation of blood flow. Circ Res 27: 669-678, 1970.

46. Egashira K, Inou T, Hirooka Y, Kai H, Sugimachi M, Suzuki S, Kuga T, Urabe Y, and Takeshita A. Effects of age on endothelium-dependent vasodilation of resistance coronary artery by acetylcholine in humans. Circulation 88: 77-81, 1993.

47. Emerson GG and Segal SS. Electrical coupling between endothelial cells and smooth muscle cells in hamster feed arteries: role in vasomotor control. Circ Res 87: 474-479, 2000.

48. Emerson GG and Segal SS. Endothelial cell pathway for conduction of hyperpolarization and vasodilation along hamster feed artery. Circ Res 86: 94-100, 2000.

49. Faber JE. In situ analysis of alpha-adrenoceptors on arteriolar and venular smooth muscle in rat skeletal muscle microcirculation. Circ Res 62: 37-50, 1988.

50. Feletou M and Vanhoutte PM. Endothelial dysfunction: a multifaceted disorder (The Wiggers Award Lecture). Am J Physiol Heart Circ Physiol 291: H985-1002, 2006.

51. Figueroa XF, Isakson BE, and Duling BR. Connexins: gaps in our knowledge of vascular function. Physiology (Bethesda) 19: 277-284, 2004.

52. Fisher JP and Paton JF. The sympathetic nervous system and blood pressure in humans: implications for hypertension. J Hum Hypertens 26: 463-475, 2012.

53. Flurkey K, Currer J, and Harrison D. The Mouse in Aging Research. In: The Mouse in Biomedical Research, edited by Fox JG, Davisson MT, Quimby FW, Barthold SW, Newcomer CE and Smith AL. Burlington: American College of Laboratory Animal Medicine (Elsevier), 2007, p. 637–672.

54. Folkow B, Sonnenschein RR, and Wright DL. Loci of neurogenic and metabolic effects on precapillary vessels of skeletal muscle. Acta Physiol Scand 81: 459-471, 1971.

55. Fuglevand AJ and Segal SS. Simulation of motor unit recruitment and microvascular unit perfusion: spatial considerations. J Appl Physiol 83: 1223-1234, 1997.

56. Garland CJ, Hiley CR, and Dora KA. EDHF: spreading the influence of the endothelium. Br J Pharmacol 164: 839-852, 2011.

57. Gaskell WH. The Changes of the Blood-stream in Muscles through Stimulation of their Nerves. J Anat Physiol 11: 360-402 363, 1877.

58. Gesek FA. Alpha 2-adrenergic receptors activate phospholipase C in renal epithelial cells. Mol Pharmacol 50: 407-414, 1996.

59. Giles RW and Wilcken EL. Reactive hyperaemia in the dog heart: evidence for a myogenic contribution. Cardiovasc Res 11: 64-73, 1977.

60. Goodman AH, Einstein R, and Granger HJ. Effect of changing metabolic rate on local blood flow control in the canine hindlimb. Circ Res 43: 769-776, 1978.

61. Granger HJ, Goodman AH, and Granger DN. Role of resistance and exchange vessels in local microvascular control of skeletal muscle oxygenation in the dog. Circ Res 38: 379-385, 1976.

62. Haas TL and Duling BR. Morphology favors an endothelial cell pathway for longitudinal conduction within arterioles. Microvasc Res 53: 113-120, 1997.

63. Hakim CH, Jackson WF, and Segal SS. Connexin Isoform Expression in Smooth Muscle Cells and Endothelial Cells of Hamster Cheek Pouch Arterioles and Retractor Feed Arteries. Microcirculation 15: 503-514, 2008.

64. Hamann JJ, Buckwalter JB, and Clifford PS. Vasodilatation is obligatory for contraction-induced hyperaemia in canine skeletal muscle. J Physiol 557: 1013-1020, 2004.

65. Haug SJ and Segal SS. Sympathetic neural inhibition of conducted vasodilatation along hamster feed arteries: complementary effects of alpha1- and alpha2-adrenoreceptor activation. J Physiol 563: 541-555, 2005.

66. Haug SJ, Welsh DG, and Segal SS. Sympathetic nerves inhibit conducted vasodilatation along feed arteries during passive stretch of hamster skeletal muscle. J Physiol 552: 273-282, 2003.

67. Hellsten Y, Nyberg M, Jensen LG, and Mortensen SP. Vasodilator interactions in skeletal muscle blood flow regulation. J Physiol 590: 6297-6305, 2012.

68. Higashi Y, Sasaki S, Nakagawa K, Kimura M, Noma K, Hara K, Jitsuiki D, Goto C, Oshima T, Chayama K, and Yoshizumi M. Tetrahydrobiopterin improves aging-related impairment of endothelium-dependent vasodilation through increase in nitric oxide production. Atherosclerosis 186: 390-395, 2006.

69. Hilton SM. A peripheral arterial conducting mechanism underlying dilatation of the femoral artery and concerned in functional vasodilatation in skeletal muscle. J Physiol 149: 93-111, 1959.

70. Hutchins PM. Arteriolar rarefaction in hypertension. Bibl Anat: 166-168, 1979.

71. Hutchins PM, Lynch CD, Cooney PT, and Curseen KA. The microcirculation in experimental hypertension and aging. Cardiovasc Res 32: 772-780, 1996.

72. Ignarro LJ, Buga GM, Wood KS, Byrns RE, and Chaudhuri G. Endothelium-derived relaxing factor produced and released from artery and vein is nitric oxide. Proc Natl Acad Sci U S A 84: 9265-9269, 1987.

73. Irion GL, Vasthare US, and Tuma RF. Age-related change in skeletal muscle blood flow in the rat. J Gerontol 42: 660-665, 1987.

74. Ishii K, Liang N, Oue A, Hirasawa A, Sato K, Sadamoto T, and Matsukawa K. Central command contributes to increased blood flow in the noncontracting muscle at the start of one-legged dynamic exercise in humans. J Appl Physiol

112: 1961-1974, 2012.

75. Jackson DN, Moore AW, and Segal SS. Blunting of rapid onset vasodilatation and blood flow restriction in arterioles of exercising skeletal muscle with ageing in male mice. J Physiol 588: 2269-2282, 2010.

76. Jackson WF. Arteriolar oxygen reactivity: where is the sensor? Am J Physiol 253: H1120-1126, 1987.

77. Jackson WF and Duling BR. The oxygen sensitivity of hamster cheek pouch arterioles. In vitro and in situ studies. Circ Res 53: 515-525, 1983.

78. Jantzi MC, Brett SE, Jackson WF, Corteling R, Vigmond EJ, and Welsh DG. Inward rectifying potassium channels facilitate cell-to-cell communication in hamster retractor muscle feed arteries. Am J Physiol Heart Circ Physiol 291: H1319-1328, 2006.

79. Joannides R, Haefeli WE, Linder L, Richard V, Bakkali EH, Thuillez C, and Luscher TF. Nitric oxide is responsible for flow-dependent dilatation of human peripheral conduit arteries in vivo. Circulation 91: 1314-1319, 1995.

80. Joyner MJ and Casey DP. Regulation of increased blood flow (hyperemia) to muscles during exercise: a hierarchy of competing physiological needs. Physiol Rev 95: 549-601, 2015.

81. Joyner MJ and Halliwill JR. Neurogenic vasodilation in human skeletal muscle: possible role in contraction-induced hyperaemia. Acta Physiol Scand 168: 481-488, 2000.

82. Kirby BS, Crecelius AR, Voyles WF, and Dinenno FA. Modulation of postjunctional α-adrenergic vasoconstriction during exercise and exogenous ATP infusions in ageing humans. J Physiol 589: 2641-2653, 2011.

83. Koller A and Kaley G. Endothelium regulates skeletal muscle microcirculation by a blood flow velocity-sensing mechanism. Am J Physiol 258: H916-920, 1990.

84. Koller A, Sun D, Huang A, and Kaley G. Corelease of nitric oxide and prostaglandins mediates flow-dependent dilation of rat gracilis muscle arterioles. Am J Physiol 267: H326-332, 1994.

85. Kraemer-Aguiar LG, de Miranda ML, Bottino DA, Lima Rde A, de Souza M, Balarini Mde M, Villela NR, and Bouskela E. Increment of body mass index is positively correlated with worsening of endothelium-dependent and independent changes in forearm blood flow. Front Physiol 6: 223, 2015.

86. Kuo L, Davis MJ, and Chilian WM. Longitudinal gradients for endothelium-dependent and -independent vascular responses in the coronary microcirculation. Circulation 92: 518-525, 1995.

87. Kurjiaka DT and Segal SS. Conducted vasodilation elevates flow in arteriole networks of hamster striated muscle. Am J Physiol 269: H1723-1728, 1995.

88. Lacolley P, Regnault V, Nicoletti A, Li Z, and Michel JB. The vascular smooth muscle cell in arterial pathology: a cell that can take on multiple roles. Cardiovasc Res 95: 194-204, 2012.

89. Lakatta EG and Levy D. Arterial and cardiac aging: major shareholders in cardiovascular disease enterprises: Part I: aging arteries: a "set up" for vascular disease. Circulation 107: 139-146, 2003.

90. Lampa SJ, Potluri S, Norton AS, and Laskowski MB. A morphological technique for exploring neuromuscular topography expressed in the mouse gluteus maximus muscle. J Neurosci Methods 138: 51-56, 2004.

91. Laughlin MH. Physical activity-induced remodeling of vasculature in skeletal muscle: role in treatment of type 2 diabetes. J Appl Physiol 120: 1-16, 2016.

92. Laurent S, Boutouyrie P, and Lacolley P. Structural and genetic bases of arterial stiffness. Hypertension 45: 1050-1055, 2005.

93. Lexell J. Human aging, muscle mass, and fiber type composition. J Gerontol A Biol Sci Med Sci 50 Spec No: 11-16, 1995.

94. Lindbom L, Tuma RF, and Arfors KE. Influence of oxygen on perfused capillary density and capillary red cell velocity in rabbit skeletal muscle. Microvasc Res 19: 197-208, 1980.

95. Lombard JH and Duling BR. Multiple mechanisms of reactive hyperemia in arterioles of the hamster cheek pouch. Am J Physiol 241: H748-755, 1981.

96. Looft-Wilson RC, Haug SJ, Neufer PD, and Segal SS. Independence of Connexin Expression and Vasomotor Conduction from Sympathetic Innervation in Hamster Feed Arteries. Microcirculation 11: 397-408, 2004.

97. Looft-Wilson RC, Payne GW, and Segal SS. Connexin expression and conducted vasodilation along arteriolar endothelium in mouse skeletal muscle. J Appl Physiol 97: 1152-1158, 2004.

98. Manttari S and Jarvilehto M. Comparative analysis of mouse skeletal muscle fibre type composition and contractile responses to calcium channel blocker. BMC Physiol 5: 4, 2005.

99. Marshall JM. The influence of the sympathetic nervous system on individual vessels of the microcirculation of skeletal muscle of the rat. J Physiol 332: 169-186, 1982.

100. McCarty R, Pacak K, Goldstein DS, and Eisenhofer G. Regulation of Peripheral Catecholamine Responses to Acute Stress in Young Adult and Aged F-344 Rats. Stress 2: 113-122, 1997.

101. Messina EJ, Weiner R, and Kaley G. Arteriolar reactive hyperemia: modification by inhibitors of prostaglandin synthesis. Am J Physiol 232: H571-575, 1977.

102. Mihok ML and Murrant CL. Rapid biphasic arteriolar dilations induced by skeletal muscle contraction are dependent on stimulation characteristics. Can J Physiol Pharmacol 82: 282-287, 2004.

103. Milkau M, Kohler R, and de Wit C. Crucial importance of the endothelial K+ channel SK3 and connexin40 in arteriolar dilations during skeletal muscle contraction. FASEB J 24: 3572-3579, 2010.

104. Mohrman DE and Sparks HV. Myogenic hyperemia following brief tetanus of canine skeletal muscle. Am J Physiol 227: 531-535, 1974.

105. Moore AW, Bearden SE, and Segal SS. Regional activation of rapid onset vasodilatation in mouse skeletal muscle: regulation through alpha-adrenoreceptors. J Physiol 588: 3321-3331, 2010.

106. Moore AW, Jackson WF, and Segal SS. Regional heterogeneity of alpha-adrenoreceptor subtypes in arteriolar networks of mouse skeletal muscle. J Physiol 588: 4261-4274, 2010.

107. Muller-Delp JM, Gurovich AN, Christou DD, and Leeuwenburgh C. Redox balance in the aging microcirculation: new friends, new foes, and new clinical directions. Microcirculation 19: 19-28, 2012.

108. Muller-Delp JM, Spier SA, Ramsey MW, and Delp MD. Aging impairs endothelium-dependent vasodilation in rat skeletal muscle arterioles. Am J Physiol Heart Circ Physiol 283: H1662-1672, 2002.

109. Naik JS, Valic Z, Buckwalter JB, and Clifford PS. Rapid vasodilation in response to a brief tetanic muscle contraction. J Appl Physiol 87: 1741-1746, 1999.

110. Najjar SS, Scuteri A, and Lakatta EG. Arterial aging: is it an immutable cardiovascular risk factor? Hypertension 46: 454-462, 2005.

111. Nelson MT, Patlak JB, Worley JF, and Standen NB. Calcium channels, potassium channels, and voltage dependence of arterial smooth muscle tone. Am J Physiol 259: C3-18, 1990.

112. North BJ and Sinclair DA. The intersection between aging and cardiovascular disease. Circ Res 110: 1097-1108, 2012.

113. Novielli NM and Jackson DN. Contraction-evoked vasodilation and functional hyperaemia are compromised in branching skeletal muscle arterioles of young pre-diabetic mice. Acta Physiol (Oxf) 211: 371-384, 2014.

114. Ohyanagi M, Faber JE, and Nishigaki K. Differential activation of alpha 1- and alpha 2-adrenoceptors on microvascular smooth muscle during sympathetic nerve stimulation. Circ Res 68: 232-244, 1991.

115. Parkinson NA and Hughes AD. The mechanism of action of alpha 2-adrenoceptors in human isolated subcutaneous resistance arteries. Br J Pharmacol 115: 1463-1468, 1995.

116. Pohl U, De Wit C, and Gloe T. Large arterioles in the control of blood flow: role of endothelium-dependent dilation. Acta Physiol Scand 168: 505-510, 2000.

117. Pohl U, Holtz J, Busse R, and Bassenge E. Crucial role of endothelium in the vasodilator response to increased flow in vivo. Hypertension 8: 37-44, 1986.

118. Potocnik SJ, McSherry I, Ding H, Murphy TV, Kotecha N, Dora KA, Yuill KH, Triggle CR, and Hill MA. Endothelium-dependent vasodilation in myogenically active mouse skeletal muscle arterioles: role of EDH and K(+) channels. Microcirculation 16: 377-390; 371 p following 390, 2009.

119. Proctor DN, Le KU, and Ridout SJ. Age and regional specificity of peak limb vascular conductance in men. J Appl Physiol 98: 193-202, 2005.

120. Reis DJ, Ross RA, and Joh TH. Changes in the activity and amounts of enzymes synthesizing catecholamines and acetylcholine in brain, adrenal medulla, and sympathetic ganglia of aged rat and mouse. Brain Res 136: 465-474, 1977.

121. Remensnyder JP, Mitchell JH, and Sarnoff SJ. Functional sympatholysis during muscular activity. Observations on influence of carotid sinus on oxygen uptake. Circ Res 11: 370-380, 1962.

122. Riches AC, Sharp JG, Thomas DB, and Smith SV. Blood volume determination in the mouse. J Physiol 228: 279-284, 1973.

123. Rizzoni D and Agabiti-Rosei E. Structural abnormalities of small resistance arteries in essential hypertension. Intern Emerg Med 7: 205-212, 2012.

124. Rizzoni D and Rosei EA. Small artery remodeling in diabetes mellitus. Nutr Metab Cardiovasc Dis 19: 587-592, 2009.

125. Roseguini BT, Davis MJ, and Harold Laughlin M. Rapid vasodilation in isolated skeletal muscle arterioles: impact of branch order. Microcirculation 17: 83-93, 2010.

126. Rowell LB. Human cardiovascular adjustments to exercise and thermal stress. Physiol Rev 54: 75-159, 1974.

127. Saltin B, Henriksson J, Nygaard E, Andersen P, and Jansson E. Fiber types and metabolic potentials of skeletal muscles in sedentary man and endurance runners. Ann N Y Acad Sci 301: 3-29, 1977.

128. Saltin B and Mortensen SP. Inefficient functional sympatholysis is an overlooked cause of malperfusion in contracting skeletal muscle. J Physiol 590: 6269-6275, 2012.

129. Saltin B, Radegran G, Koskolou MD, and Roach RC. Skeletal muscle blood flow in humans and its regulation during exercise. Acta Physiol Scand 162: 421-436, 1998.

130. Sandow SL and Hill CE. Incidence of myoendothelial gap junctions in the proximal and distal mesenteric arteries of the rat is suggestive of a role in endothelium-derived hyperpolarizing factor-mediated responses. Circ Res 86: 341-346, 2000.

131. Sandow SL, Looft-Wilson R, Doran B, Grayson TH, Segal SS, and Hill CE. Expression of homocellular and heterocellular gap junctions in hamster arterioles and feed arteries. Cardiovasc Res 60: 643-653, 2003.

132. Sarelius I and Pohl U. Control of muscle blood flow during exercise: local factors and integrative mechanisms. Acta Physiol (Oxf) 199: 349-365, 2010.

133. Saunders NR and Tschakovsky ME. Evidence for a rapid vasodilatory contribution to immediate hyperemia in rest-to-mild and mild-to-moderate forearm exercise transitions in humans. J Appl Physiol 97: 1143-1151, 2004.

134. Seals DR. Influence of muscle mass on sympathetic neural activation during isometric exercise. J Appl Physiol 67: 1801-1806, 1989.

135. Seals DR. Sympathetic neural discharge and vascular resistance during exercise in humans. J Appl Physiol 66: 2472-2478, 1989.

136. Seals DR, Jablonski KL, and Donato AJ. Aging and vascular endothelial function in humans. Clin Sci (Lond) 120: 357-375, 2011.

137. Segal SS. Microvascular recruitment in hamster striated muscle: role for conducted vasodilation. Am J Physiol 261: H181-189, 1991.

138. Segal SS. Regulation of blood flow in the microcirculation. Microcirculation 12: 33-45, 2005.

139. Segal SS and Duling BR. Communication between feed arteries and microvessels in hamster striated muscle: segmental vascular responses are functionally coordinated. Circ Res 59: 283-290, 1986.

140. Segal SS and Duling BR. Flow control among microvessels coordinated by intercellular conduction. Science 234: 868-870, 1986.

141. Segal SS and Jacobs TL. Role for endothelial cell conduction in ascending vasodilatation and exercise hyperaemia in hamster skeletal muscle. J Physiol 536: 937-946, 2001.

142. Sejersted OM, Hargens AR, Kardel KR, Blom P, Jensen O, and Hermansen L. Intramuscular fluid pressure during isometric contraction of human skeletal muscle. J Appl Physiol Respir Environ Exerc Physiol 56: 287-295, 1984.

143. Shimokawa H, Yasutake H, Fujii K, Owada MK, Nakaike R, Fukumoto Y, Takayanagi T, Nagao T, Egashira K, Fujishima M, and Takeshita A. The importance of the hyperpolarizing mechanism increases as the vessel size decreases in endothelium-dependent relaxations in rat mesenteric circulation. J Cardiovasc Pharmacol 28: 703-711, 1996.

144. Shoemaker JK, Tschakovsky ME, and Hughson RL. Vasodilation contributes to the rapid hyperemia with rhythmic contractions in humans. Can J Physiol Pharmacol 76: 418-427, 1998.

145. Sinkler SY and Segal SS. Aging alters reactivity of microvascular resistance networks in mouse gluteus maximus muscle. Am J Physiol Heart Circ Physiol 307: H830-839, 2014.

146. Smiesko V, Lang DJ, and Johnson PC. Dilator response of rat mesenteric arcading arterioles to increased blood flow velocity. Am J Physiol 257: H1958-1965, 1989.

147. Smith EG, Voyles WF, Kirby BS, Markwald RR, and Dinenno FA. Ageing and leg postjunctional alpha-adrenergic vasoconstrictor responsiveness in healthy men. J Physiol 582: 63-71, 2007.

148. Song H and Tyml K. Evidence for sensing and integration of biological signals by the capillary network. Am J Physiol 265: H1235-1242, 1993.

149. Stowe DF, Owen TL, Anderson DK, Haddy FJ, and Scott JB. Interaction of O2 and CO2 in sustained exercise hyperemia of canine skeletal muscle. Am J Physiol 229: 28-33, 1975.

150. Tevald MA, Lowman JD, and Pittman RN. Skeletal muscle arteriolar function following myocardial infarction: Analysis of branch-order effects. Microvasc Res 81: 337-343, 2011.

151. Thomas GD. Functional sympatholysis in hypertension. Auton Neurosci 188: 64-68, 2015.

152. Thomas GD and Segal SS. Neural control of muscle blood flow during exercise. J Appl Physiol 97: 731-738, 2004.

153. Thompson RJ, Doran JF, Jackson P, Dhillon AP, and Rode J. PGP 9.5--a new marker for vertebrate neurons and neuroendocrine cells. Brain Res 278: 224-228, 1983.

154. Toth P, Tucsek Z, Sosnowska D, Gautam T, Mitschelen M, Tarantini S, Deak F, Koller A, Sonntag WE, Csiszar A, and Ungvari Z. Age-related autoregulatory dysfunction and cerebromicrovascular injury in mice with angiotensin II-induced hypertension. J Cereb Blood Flow Metab 33: 1732-1742, 2013.

155. Trott DW, Luttrell MJ, Seawright JW, and Woodman CR. Aging impairs PI3K/Akt signaling and NO-mediated dilation in soleus muscle feed arteries. Eur J Appl Physiol 113: 2039-2046, 2013.

156. Tschakovsky ME and Sheriff DD. Immediate exercise hyperemia: contributions of the muscle pump vs. rapid vasodilation. J Appl Physiol 97: 739-747, 2004.

157. Tschakovsky ME, Shoemaker JK, and Hughson RL. Vasodilation and muscle pump contribution to immediate exercise hyperemia. Am J Physiol 271: H1697-1701, 1996.

158. Tuma RF, Lindbom L, and Arfors KE. Dependence of reactive hyperemia in skeletal muscle on oxygen tension. Am J Physiol 233: H289-294, 1977.

159. VanTeeffelen JW and Segal SS. Effect of motor unit recruitment on functional vasodilatation in hamster retractor muscle. J Physiol 524 Pt 1: 267-278, 2000.

160. VanTeeffelen JW and Segal SS. Interaction between sympathetic nerve activation and muscle fibre contraction in resistance vessels of hamster retractor muscle. J Physiol 550: 563-574, 2003.

161. VanTeeffelen JW and Segal SS. Rapid dilation of arterioles with single contraction of hamster skeletal muscle. Am J Physiol Heart Circ Physiol 290: H119-127, 2006.

162. Vargas F, Osuna A, and Fernandez-Rivas A. Abnormal renal vascular reactivity to acetylcholine and nitroprusside in aging rats. Gen Pharmacol 28: 133-137, 1997.

163. Welsh DG, Jackson WF, and Segal SS. Oxygen induces electromechanical coupling in arteriolar smooth muscle cells: a role for L-type Ca2+ channels. Am J Physiol 274: H2018-2024, 1998.

164. Welsh DG and Segal SS. Coactivation of resistance vessels and muscle fibers with acetylcholine release from motor nerves. Am J Physiol 273: H156-163, 1997.

165. Woodman CR, Price EM, and Laughlin MH. Aging induces muscle-specific impairment of endothelium-dependent dilation in skeletal muscle feed arteries. J Appl Physiol 93: 1685-1690, 2002.

166. Woodman CR, Price EM, and Laughlin MH. Selected Contribution: Aging impairs nitric oxide and prostacyclin mediation of endothelium-dependent dilation in soleus feed arteries. J Appl Physiol 95: 2164-2170, 2003.

167. Yamboliev IA and Mutafova-Yambolieva VN. PI3K and PKC contribute to membrane depolarization mediated by alpha2-adrenoceptors in the canine isolated mesenteric vein. BMC Physiol 5: 9, 2005.

168. Yardeni T, Eckhaus M, Morris HD, Huizing M, and Hoogstraten-Miller S. Retro-orbital injections in mice. Lab Anim (NY) 40: 155-160, 2011.

169. Yildiz O. Vascular smooth muscle and endothelial functions in aging. Ann N Y Acad Sci 1100: 353-360, 2007.

VITA

Shenghua is originally from Guizhou, China. She attended China Pharmaceutical University where she majored in Business Administration and minored in Pharmacy. Later she received her master degree in Pharmacology under Prof. Dezai Dai from the same university. She had been a pharmacist in Clinical Pharmacy Division at Drum Tower Hospital, Nanjing, China for 4 years before coming to the University of Missouri to work in Steven Segal's lab. While at Missouri, she was supported by a Graduate Research Assistantship and an AHA MWA Pre-Doctoral Fellowship.